Journal of Research of the National Bureau of Standards Vol. 50, No. 6, June 1953 Research Paper 2419

# Electron Microscopy of Synthetic Elastomer Latices

Robert R. Stromberg, Max Swerdlow, and John Mandel

The effects on the apparent particle size and its frequency distribution arising from the method of specimen preparation, shadowcasting, distortion of shape, and other artifacts inherent in the electron microscopy of synthetic elastomer latices are described. The possibility of applying a single, reproducible method of examination to four latices involving three copolymers (butadiene-styrene, butadiene-acrylonitrile, and butadiene-styrene-acrylonitrile) is statistically evaluated. These copolymers contain particles ranging in size from approximately 100 to 2100 A, and their average particle diameters are about 600, 800, and 1700 A, respectively.

## 1. Introduction

### 1.1. Purpose and Problem

The purpose of this investigation is to determine the shape and size of the particles found in a variety of commercial and experimental elastomer latices in order to relate the findings with the use of such latices for the impregnation of leather as a substitute for impregnation by means of polymer solutions [1][1] or by means of in situ polymerization [2].

For a comparison of the behavior of different latices in the impregnation of leather and for a comparison of their particle-size distributions, it was thought that a single, reproducible method common to all of them would be necessary in order to discount the errors and artifacts inherent in any one method. Furthermore, it would be necessary to evaluate the advantages and limitations of the method selected as a means for determining the shape, size, and frequency distribution of these synthetic elastomer latices.

Particle-size studies may be made by the methods of radiation diffraction and scattering, surface adsorption, fractionation, and microscopy. Because of the necessity for data on the shape and mode of flocculation, as well as the particle-size distributions of impure synthetic elastomer suspensions, microscopy was chosen. Inasmuch as the size of material lies in the colloidal range, the electron microscope was needed to provide the direct means for observation.

The available methods of specimen preparation impose severe limitations on the accuracy of electron microscopical measurements. An inherent difficulty of such methods lies in the nature of the material being examined. With synthetic elastomer latices, the problem is threefold. 1. To maintain the dispersed material as individual particles. 2. To fix the nonrigid particles in their original, presumably spherical, shape without changing their size. 3. To separate the polymer particles from other material in the suspension.

If one applies the usual method of specimen preparation involving direct dilution with water and drying onto a collodion substrate, the particles flatten and merge into a hazy layer in which one particle cannot be distinguished from another. With further dilution, layers of elastomer of smaller area are formed, but still no particulate structure is exhibited.

### 1.2. Evaluation of Existing Methods

Two approaches have been used to overcome some of these difficulties. In one, the latex was dispersed in an aqueous solution of polyvinyl alcohol; and upon drying, the particles became embedded in the resulting plastic film [3]. It was found that the tendency of the particles to flatten and coalesce was reduced. However, this technique impairs image sharpness and contrast because of additional scattering and reduced transmission of the electron beam. Shadowcasting such a specimen is not effective and, therefore, observations of the third dimension and the extent of flattening of the particles are precluded. Also, any extraneous matter, such as emulsifying agent, catalyst, inhibitor, etc., in the original latex suspension will contaminate and partially obscure the elastomer particles in the preparation.

In the other approach, the latex suspension was brominated [4]. This served to diminish the amount of flattening by hardening the soft particles. Application of bromine by itself may fix the particles as spheres, but severe flocculation prevents accurate particle-size counts. The use of a commercial wetting agent, Daxad-11 [5] or Aerosol OT [6], as a dispersing agent in addition to bromination has been described. Although the dispersing agent reduces flocculation, the excessive amount required encases and obscures the individual elastomer particles. To remove the excess dispersant a thorough washing of the final specimen preparation is necessary.

Neither the exact washing technique nor the effect of washing on the particle-size distribution have been described. Regarding the shape of the particles, assumptions have been made that the particles are either perfect spheres [4] or ellipsoids [5] resting entirely on top of the sagging substrate. The effect of bromination on the size of the particle has been estimated to be about a 9-percent increase in diameter [4]. A 9.6-percent increase, calculated from an indirect measurement, has also been reported [7]. No correction has been made, however, for partial embedding in the softened substrate. This could be a considerable factor in the case of particle diameters nearly equal to the thickness of the substrate.

[1] Figures in brackets indicate the literature references at the end of this paper.

| Sample | Source | Ratio of monomer charge | Emulsifier | pH | Total solids |
|---|---|---|---|---|---|
| A | University of Akron Master-stock No. 1277 | {Butadiene} / {Styrene} = {71.5} / {28.5} | Office of Rubber Reserve soap flakes | 11.0 | 21 |
| B | University of Akron Master-stock No. 1295 | {Butadiene} / {Styrene} = {71.5} / {28.5} | Dodecylamine | 11.0 | 18 |
| C | B. F. Goodrich Chemical Co. Hycar 1502x392 | {Butadiene} / {Acrylonitrile} = (*) | (*) | 4.3 | 32.0 |
| D | University of Akron | {Butadiene} / {Styrene} / {Acrylonitrile} = {50} / {45} / {5} | None | 2.5 | 17.0 |

* Information unavailable.

## 2. Materials Used

The identification and composition of the four latices investigated are contained in the above tabulation [8, 9, 10].

## 3. Specimen Preparation

### 3.1. Exploratory Methods

Various methods were investigated in attempts to eliminate swelling the particles by bromination and using a dispersing agent, yet fixing their original shape and size and retaining discrete separations between particles. A freeze-drying method was tried, in which a drop of a dilute aqueous suspension of latex was placed upon a collodion-covered specimen screen, supported by a glass microscope slide. The glass slide was immediately placed on a brass block, previously chilled to about minus 100° C, freezing the drop. The entire block of frozen specimens was placed in the chamber of an RCA type EMV–1 vacuum unit where the ice sublimed during evacuation, leaving the particles on the collodion film.

Another method was tried with latices A and B, in which the pH of the diluent was matched by addition of ammonia to that of the latex suspension and the diluted suspension was dried onto the collodion substrate.

In a third approach, diluted suspensions were sprayed by means of an ordinary nasal atomizer onto collodion-covered specimen screens. Three or four "shots" of the diluted latex were applied to each screen from a distance of about 1 m.

Each of these methods of specimen preparation frequently gave well-dispersed, round particles with some of the latices, but not consistently with all. Because one reproducible method that was equally good for all the latices was desired, these approaches to the problem of specimen preparation were set aside, even though each method tried showed promise of producing a good specimen for particle-size studies with the electron microscope.

### 3.2. Method Used

In order to arrive at a single, reproducible method suitable for a statistical determination of the particle-size distributions of the four synthetic elastomer latices it was, therefore, decided to apply a combination of various methods already reported. Because such a large quantity of dispersing agent is required to prevent flocculation of the particles and such a thorough washing of the dried specimens is necessary in order to expose the particles as individual units, concern was felt about the preferential removal of certain size ranges. Consequently, it was necessary to devise several specific washing techniques and to evaluate not only the comparative effects of the washing techniques on the particle-size distribution but also the inherent limitations of electron microscopy as a means for determining the size and shape of these latex particles.

A sample of each of the four latices was diluted with an aqueous solution of 0.2 percent of dispersing agent (Daxad–11) to make a rubber concentration of approximately 0.01 percent by weight. A few drops of this diluted suspension were placed in a watch glass and exposed to bromine vapors poured from a bottle of liquid bromine for 15 sec. The brominated suspension was further diluted with distilled water to give a rubber concentration of about 0.0001 percent. Drops of the final suspension were placed upon collodion-covered specimen screens, supported by glass microscope slides, and dried for an hour longer than the time required for the drops to evaporate in an air-conditioned room kept at about 22° C and 50-percent relative humidity. Immediately thereafter, each of the following washing techniques was applied to eight separate specimens of each sample of latex. The washing was performed either with distilled water at about 80° C or with steam at atmospheric pressure.

#### a. Jet Washing

A fine stream of hot water from a wash bottle was played over the prepared specimen screens on the glass slides. The slides were held, specimens up, at an angle of about 45° from the vertical, and the jet of water was applied at a near-grazing angle. This washing was repeated 3 or 4 times for periods of about 15-sec duration.

#### b. Immersion Washing

The prepared specimen screens supported by the glass microscope slide were immersed edgewise at an angle of about 45° into a dish of hot water for about 15 sec. Successive immersions and withdrawals were repeated 3 or 4 times in the same dish of water.

#### c. Pipette Washing

Drops of hot water were placed upon the prepared specimen screens and removed after 15-sec contact by means of a medicine dropper. This process was immediately repeated 3 or 4 times with fresh drops of water.

#### d. Steam Washing

The prepared screens on their supporting glass slides were placed at an angle of about 15° from the vertical in a wire basket in the upper part of an insulated glass column about 40 cm long. Steam was passed continuously through the column and around the specimens for a period of about 15 min.

#### e. No Washing

One group of specimens from latex sample A was prepared with Daxad–11 and fixed with bromine in the manner described above, except that a slightly lower concentration of rubber was used. Even though no washing technique was applied, an acceptable preparation was obtained (fig. 1, A). Although this unwashed preparation was not reproducible, the micrographs can be used for comparison with the other washing procedures used in the specimen preparations for latex sample A.

### 3.3. Shadowcasting

The specimens were washed and then dried overnight. Those specimens selected for shadowcasting were evacuated to a pressure of about $10^{-5}$ mm of mercury or less. Pure electrolytic chromium metal pieces were slowly evaporated from a conical tungsten wire basket placed in such a manner as to create radiation shadows whose lengths were 4 and 5 times the altitude of the particle causing them.

## 4. Interpretation of Electron Micrographs

Figure 1, B, illustrates the appearance and shape of the latex particles when the latex (sample A) is merely diluted with water and allowed to dry out on the collodion substrate. This particular field offers more information than the usual micrograph obtained from such a preparation. The rubber latex is generally coagulated into large flattened masses showing no particulate detail at all. Figure 1, C, is an example of the same latex in which the diluted sample was given additional treatment by exposure to bromine and allowed to dry. Instead of formless masses, round particles are observed. However, the poor dispersion of these discrete particles prevents an accurate measure of their size and number.

Figure 2 represents electron micrographs of latex sample B prepared as described in section 3.2. For figure 2, A, the specimen was given a jet washing; 2, B, immersion; 2, C, pipette; and 2, D, steam. The presence of residual material in the background of these micrographs indicates that the specimens were not overwashed, and that only a minimum number of particles was removed. Excessive washing will remove not only the extraneous material but also a much greater number of particles. The delicacy of the steam washing is shown in figures 1, D, and 2, D, where the covering of dispersing agent has not been completely removed. The existence of such an envelope around the particles is borne out by their diffuse outline and by the shortened lengths of the shadows, which would have been five times the diameter for unembedded hard spheres. The envelope of dispersant provides an advantage in that it reduces the free energy of the surface of the water helping to prevent the particles from coagulating during the drying-out process and, in addition, cements them to the collodion substrate. Originally it was believed that steam as a method of washing would prove to be the best, in that it would dissolve away the dispersant leaving all the particles behind. In practice, however, in order to accomplish adequate washing, it was found necessary to allow the steam to condense so that the actual washing was done in part by vapor and in part by hot water. Attempts to prevent condensation of droplets on the specimen preparation by employing additional insulation around the glass column and infrared radiation for the time required for effective washing destroyed the collodion film.

The electron micrographs seen in figure 3 represent the results obtained when the four different latices were given the same washing technique, that is, pipette. The conspicuous differences in the number and the sizes of particles should not be taken to mean that these differences result from preferential removal of particles in the washing process. Rather, they are most likely due to variations in the original concentrations, pH, surface charges, rate of drying, the ratio of the substrate area to the volume of the drop of latex suspension, and other factors that influence the settling out of the particles onto the collodion substrate. No single selected view is necessarily typical of the over-all observations, and a statistical analysis is required before any conclusions can be made with respect to particle-size distributions.

Prior to determinations of the particle size for these latices, a consideration of the actual shape has to be made. The large sphere seen in figure 4 (presumably a mass of molten chromium that fell on the dried collodion substrate and subsequently shadowed) demonstrates what a rigid sphere lying on top of the film would look like when shadowcast in such a way that the length of the shadow is four times that of the height of the particle. Actual measurement gives a value of 9000 A for the transverse diameter of the "sphere."

(The transverse diameter is that distance measured across the particle and normal to the direction of shadowing.) This value is about 5 percent less than the height determined from the geometry of the shadowcasting technique. This discrepancy can can result from sagging of the supporting substrate under load and a very slight embedding of the particle in the film, as shown schematically in figure 5. Furthermore, the inherent approximations

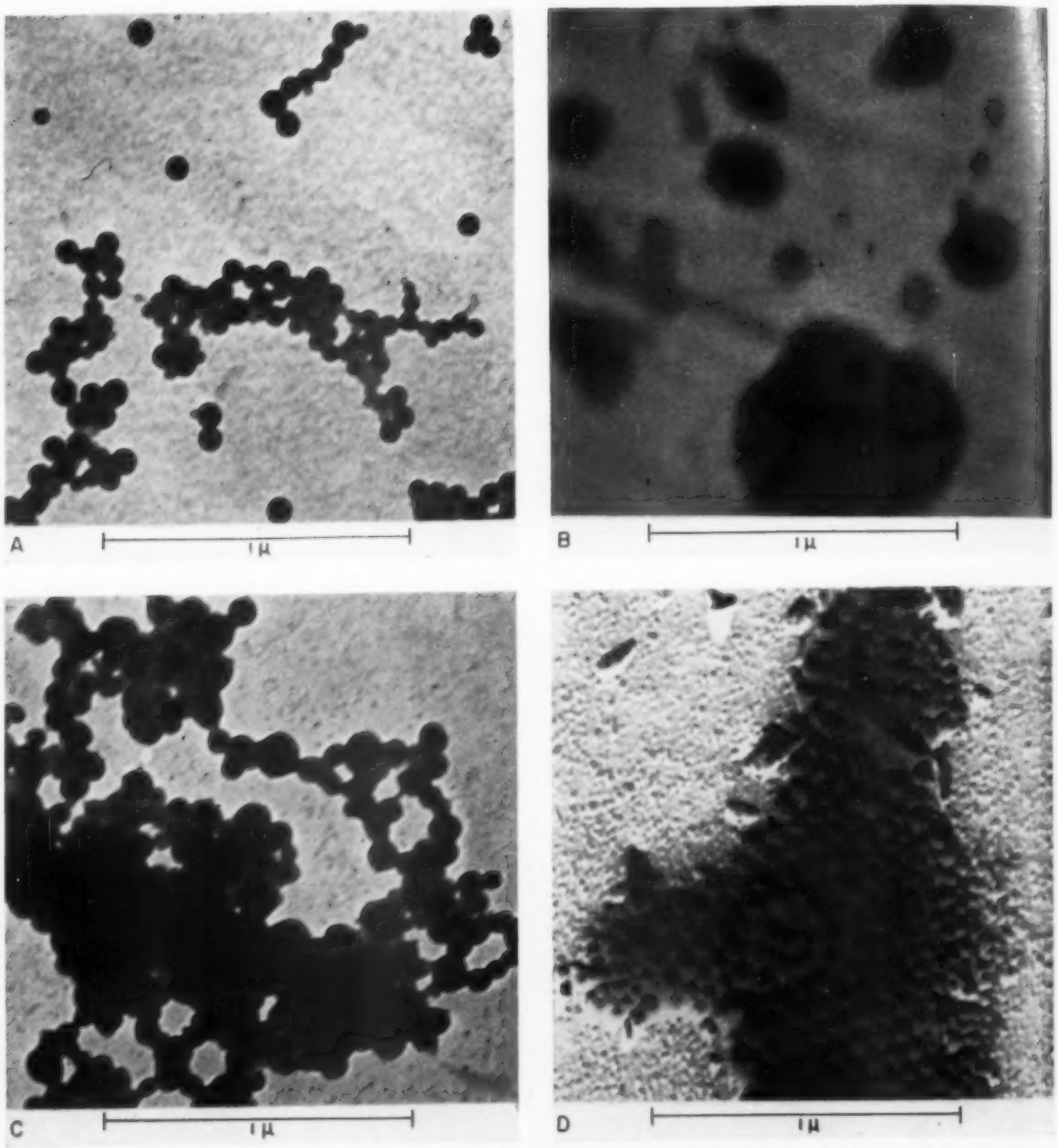


FIGURE 1. *Effect of various techniques of specimen preparation on shape and dispersion of latex particles.*

A, sample A (butadiene-styrene), treated with dispersing agent and bromine but unwashed.
B, sample A (butadiene-styrene), untreated except for dilution.
C, sample A (butadiene-styrene), treated with bromine only.
D, sample C (butadiene-acrylonitrile), treated with dispersing agent and bromine, steam washed, shadowed 4:1.

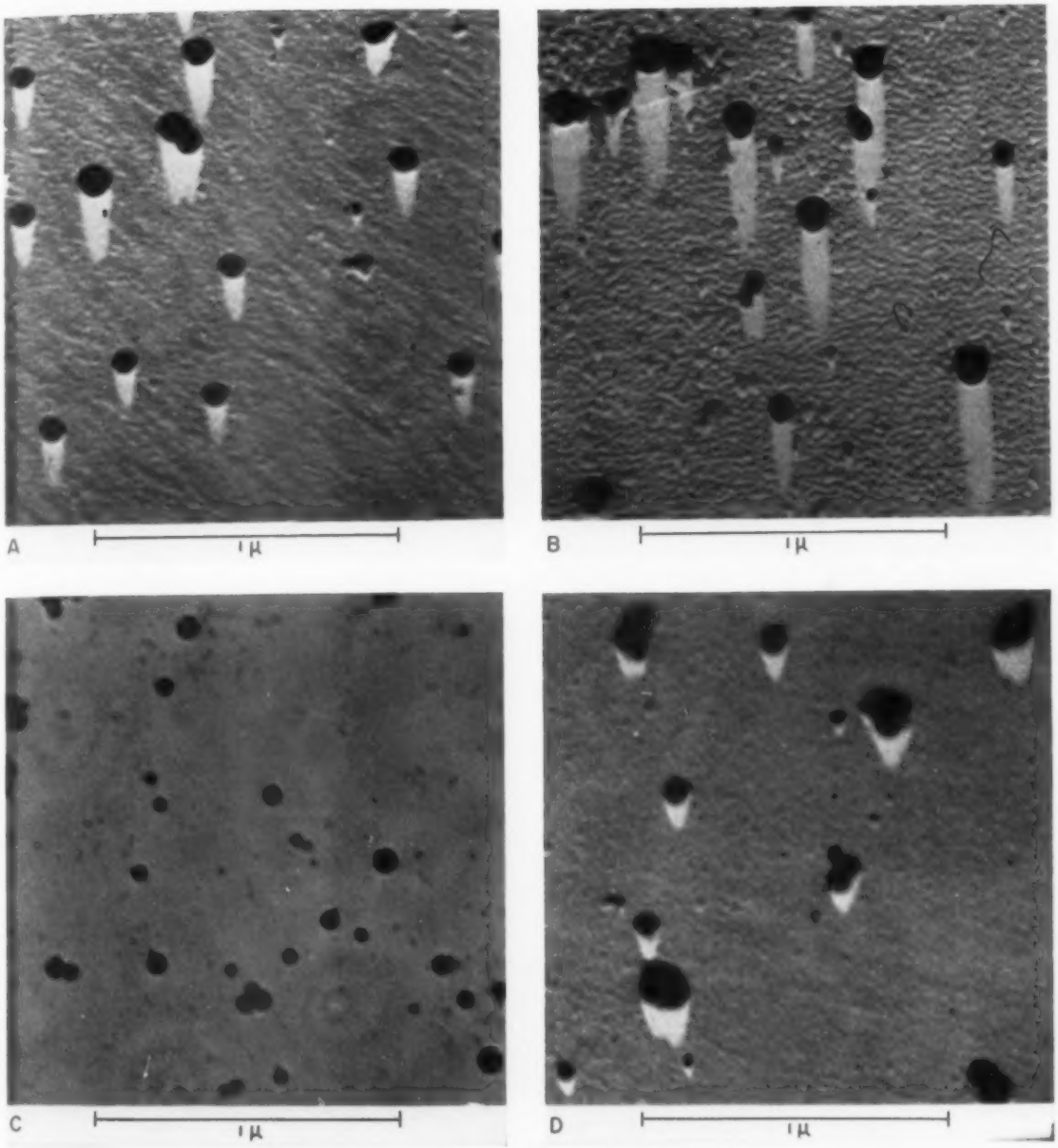


FIGURE 2. *Four washing techniques applied to one latex.*

A, sample B (butadiene-styrene), jet washed, shadowed 5:1.
B, sample B, immersion washed, shadowed 5:1.
C, sample B, pipette washed.
D, sample B, steam washed, shadowed 5:1.

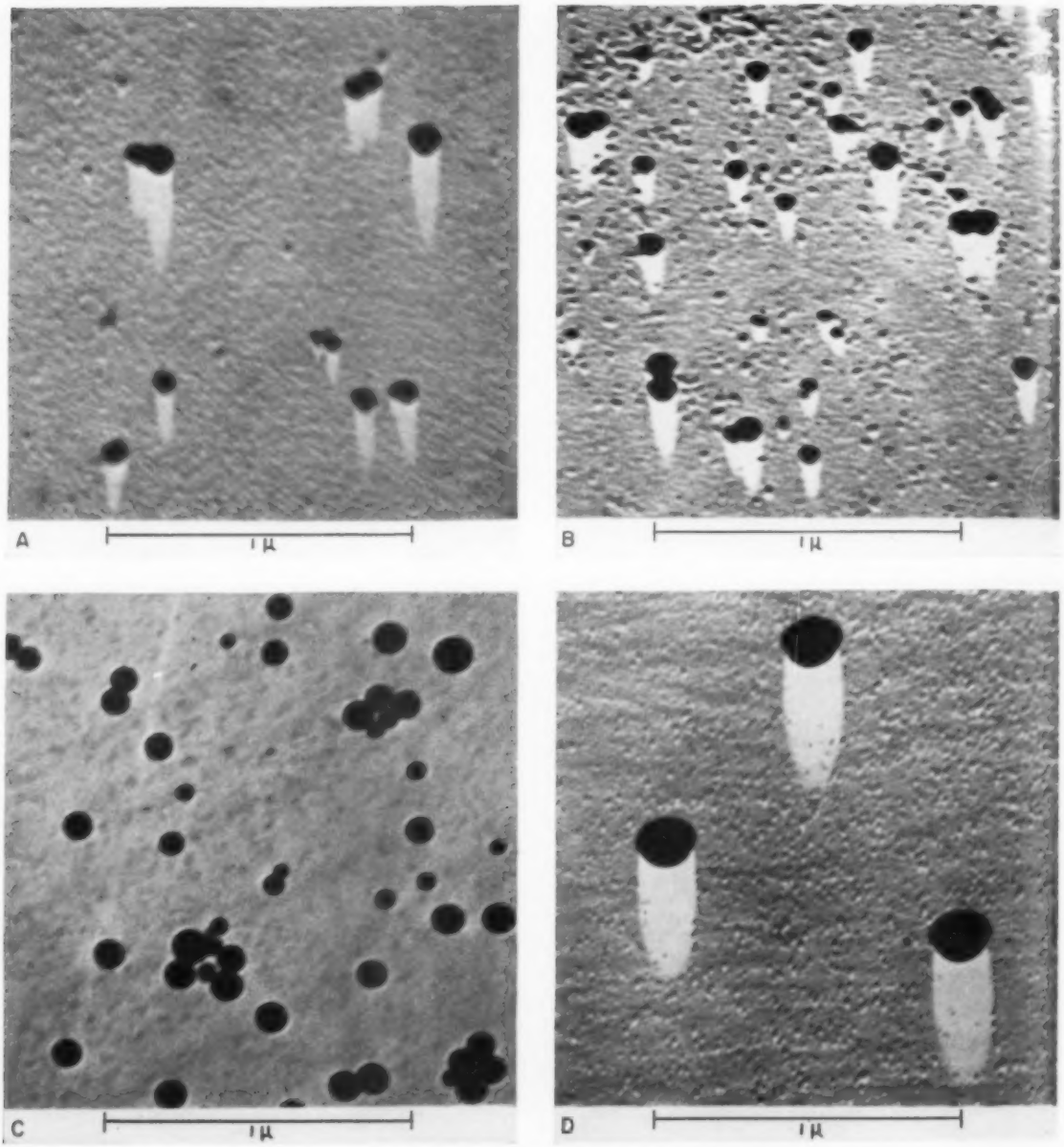


FIGURE 3. *One washing technique applied to four latices.*

A, sample A (butadiene-styrene), pipette washed, shadowed 5:1.
B, sample B (butadiene-styrene), pipette washed, shadowed 5:1.
C, sample C (butadiene-acrylonitrile), pipette washed.
D, sample D (butadiene-styrene-acrylonitrile), pipette washed, shadowed 4:1.

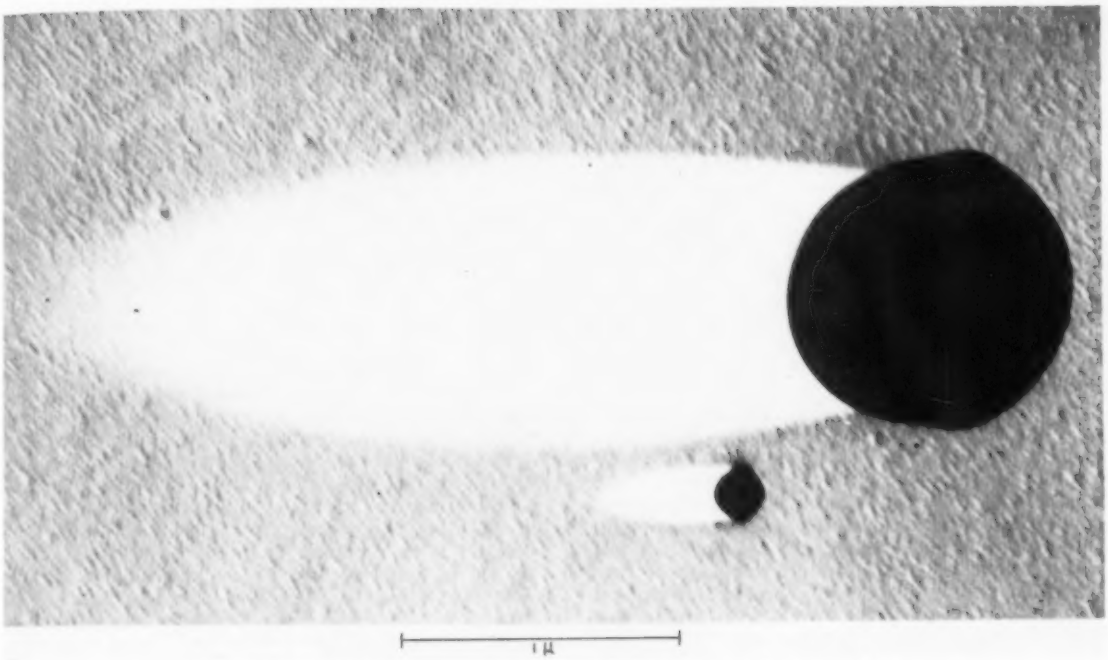


FIGURE 4. *Sample D (butadiene-styrene-acrylonitrile), jet washed, shadowed 4:1.*

The large particle is probably a "sphere" of chromium metal produced at the beginning of the shadowcasting process and subsequently shadowed.

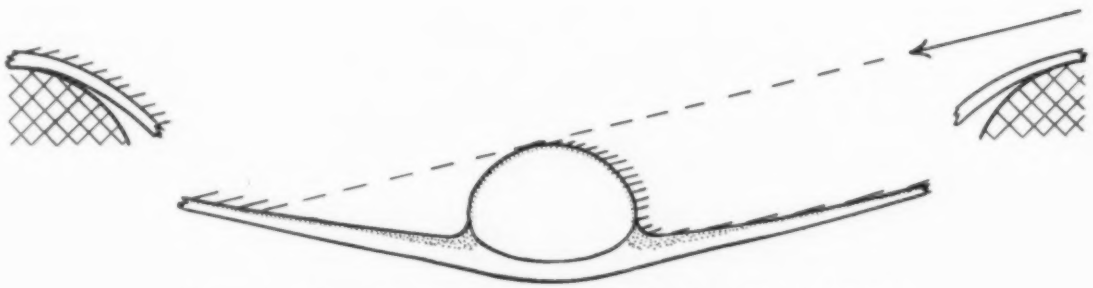

FIGURE 5. *Schematic representation of the acquired shape of an elastomer particle.*

This shows a cross-sectional view of a single elastomer particle and its probable geometry after treatment with bromine and dispersing agent, and after application of washing and shadowcasting techniques. The collodion film is shown to sag between the supporting wires of the 200-mesh screen. The particle showning the center produces additional sag and embeds itself into the softened substrate. The dotted area surrounding the particle represents a residual layer of dispersing agent and other material in the latex suspension. Bromination does not harden the particle sufficiently, and the subsequent slumping of the sphere gives it a flattened ovoid shape. Although the shadowcasting, indicated by the arrow and dashes, produces a three-dimensional aspect, these artifacts, in general, make the use of shadowcasting geometry inaccurate as a means for calculating the diameter of the particle. The observed diameter used in this study is that distance measured across the particle and normal to the direction of shadowing.

and assumptions made in the setup required for shadowcasting also contribute to this error. If this kind of precision could, nevertheless, be attained on measurements made on the small particles, determination of the diameters derived from the lengths of the shadows would be perfectly valid and well within the experimental errors of the method. Such measurements, however, can be grossly in error because during the removal of the matrix of extraneous material surrounding the particles the hot water softens the collodion substrate, not only causing the film to sag between the wires of the 200-mesh supporting screen but also allowing the particles to sink in and partially embed themselves into the gelatinous collodion membrane. In addition, as was seen in the case of steam washing, some of the matrix of extraneous material remains, thereby partially obscuring the particle. A residual film of dispersing agent and other material in the latex suspension remains to form a layer of varying thicknesses on all the preparations. This adsorbed layer of additional material can be seen not only on the collodion substrate but on the latex particles as well. In figure 4 compare the smooth profile of the large sphere produced by a molten mass of chromium, which never was in the latex suspension, with the rougher surfaces of the small latex particles to which a layer of extraneous material dispersed in the latex suspension has been added during the drying-out process.

There is also a flattening of the particles themselves, because exposure of the latex suspension to bromine vapors does not completely fix the particle in its original spherical form. (It is assumed that the particle is a true sphere while in the undisturbed elastomer suspension.) This change in shape results from flow of polymer during the drying-out process when the forces of surface tension of the water and interfacial tensions act upon the nonrigid particle. These forces all act in the same direction, reducing the vertical and increasing the horizontal "diameter". The resultant shape of the particle is probably the flattened ovoid form indicated in figure 5. No direct measurements were made of the distortion of the spherical shape, of the thickness of the adhering layer of extraneous material, or of the amount of sag in the collodion substrate.

All of these factors contribute to a foreshortening of the shadow lengths on the substrate. Thus, calculations to determine the true diameter of these latex particles based upon geometrical relationships between shadow length and altitude can lead to serious errors. On the other hand, the widest portion of the shadow can be used as a criterion for measuring the diameter of these particles only if the metal radiates in effect from a point source. For the distances used, the conical tungsten basket that serves as a crucible and source for the chromium atoms is relatively large. The "polar cap" of metal built up during the deposition of the chromium goes beyond the equatorial diameter of the particle. (The thickness of the "polar cap" may be reduced by the use of suitable metals with higher atomic number, producing adequate lectron scattering with thinner deposits.) In the case of the much larger 9000-A "sphere", this is not as serious an error. The effect of the "polar caps" on relatively small and large particles can be compared in figure 4. Moreover, comparison of the shapes of the shadows caused by the small particles seen in figures 2 and 3 with that of the large particle of figure 4 makes it clear that the almost triangular shadows associated with the small particles are not characteristic of an exposed sphere in contact with a flat surface.

These cumulative errors preclude the measurement of shadows as a precise means for determining particle diameters of these latices. Although the shadowcasting technique does not perfectly reflect the true shape and size of these elastomer particles, it does, nevertheless, provide a three-dimensional aspect to the electron micrographs and creates sufficient contrast to aid the observer in measuring the transverse (horizontal) diameters of the particles.

From the above considerations regarding swelling of the particle upon exposure to bromine and distortion from the spherical shape during the drying-out process in the specimen preparation, a correction of the observed diameters should be applied. Both of these factors operate to make the apparent diameters too large. Contamination-growth of the particles by electron-beam bombardment was kept to a minimum by the avoidance of long exposures. In the opposite sense, because of the vacuum conditions required for shadowcasting and the actual examination of the specimen in the electron microscope, the particles may undergo a shrinkage through loss of monomer. In view of the indeterminate nature of these errors, no quantitative correction could be applied to the observed data.

## 5. Measurement of Particles

At least 10 micrographs of representative fields of each of the samples for each washing technique were taken at 10,000 diameters. The RCA type EMU–2 (50 kv.) electron microscope was used for this work. Calibration of the instrument was obtained by means of a shadowcast Formvar (polyvinyl formal) replica of a planar 4-in. speculum metal diffraction grating having 20,000 rulings per inch. This method of calibration was reliable within 2 percent. The original negatives of the electron micrographs were projected on a screen to provide further linear enlargement of about 30 times. A 10-cm scale in 0.5-mm graduations on a glass plate was simultaneously projected with the electron micrograph. At the magnifications used, the smallest scale division represented 500 A. A pair of dividers was used to compare the diameters of the particles with the superimposed scale. Some of the extraneous material appeared in the final preparation as discrete particles less than 100 A in size. In order to avoid confusion with elastomer particles, an arbitrary lower limit was set. Consequently, no particles under 100 A were counted. The diameters were measured to the nearest 100 A. The values reported here are the apparent diameters of the particles as observed in the projected electron micrographs.

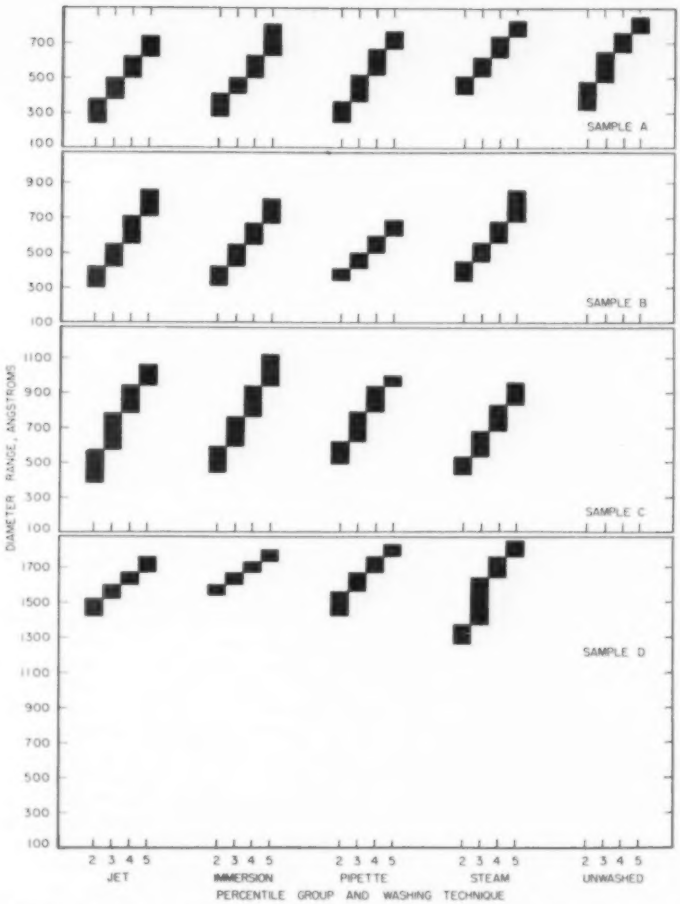


FIGURE 6. *Effect of washing techniques on particle-size distribution of synthetic elastomer latices.*

Percentile group: 2=10 to 25, 3=25 to 50, 4=50 to 75, and 5=75 to 90.

## 6. Statistical Data and Their Physical Significance

A comparison of average particle diameters obtained from individual micrographs of unshadowed and shadowed preparations showed no significant differences. No distinction was made, therefore, regarding this particular feature of the specimen preparation. A statistical analysis [11] was made from the viewpoint of determining what effects, if any, the washing techniques have on the particle size distribution. The results are indicated in figure 6. The frequency distribution of particle sizes corresponding to each washing technique is summarized for each sample in the following manner. The particles of each size, as observed in the various micrographs corresponding to a particular sample and washing technique, were counted and arranged according to size into six groups. The first group consisted of the smallest particles comprising 10 percent of the total count; the second group of the next larger 15 percent; the third and fourth groups of 25 percent each; the fifth group of the next larger 15 percent; and the sixth group consisted of the largest particles making up the final 10 percent of the total count. The range of particle sizes covered by each of these percentile groups is plotted versus the corresponding group number. The median value occurs at the boundary of the third and fourth percentile groups. Following the usual procedure, it was considered advisable to omit from figure 6 the smallest and highest percentile groups, because of the considerable variability that exists at the extremes for samples of moderate size. The distribution corresponding to the unwashed specimen of sample A is plotted in the same manner in order to provide a comparison with the washed specimens of sample A.

TABLE 1. *Diameters and related data of synthetic rubber latex particles*

| Hot-water washing technique | Sample A.—Butadiene-styrene | | | | | | Sample B.—Butadiene-styrene | | | | | |
|---|---|---|---|---|---|---|---|---|---|---|---|---|
| | $m$ | $\bar{x}$ | $s_{\bar{x}}$ | $s_m$ | $n$ | $k$ | $m$ | $\bar{x}$ | $s_{\bar{x}}$ | $s_m$ | $n$ | $k$ |
| | A | A | A | A | | | A | A | A | A | | |
| Jet | 500 | 550 | 7 | 60 | 672 | 9 | 550 | 620 | 12 | 104 | 329 | 9 |
| Immersion | 500 | 580 | 17 | 38 | 137 | 5 | 550 | 610 | 11 | 116 | 266 | 10 |
| Pipette | 520 | 570 | 12 | 63 | 283 | 5 | 500 | 560 | 5 | 51 | 739 | 10 |
| Steam | 620 | 680 | 15 | 27 | 129 | 5 | 560 | 630 | 10 | 110 | 355 | 9 |
| Unwashed | * 650 | * 660 | 8 | 88 | 680 | 10 | ..... | ..... | ..... | ..... | ..... | ..... |
| Sample mean | 540 | 600 | ..... | ..... | ..... | ..... | 540 | 600 | ..... | ..... | ..... | ..... |
| | Sample C.—Butadiene-acrylonitrile | | | | | | Sample D.—Butadiene-styrene-acrylonitrile | | | | | |
| Jet | 780 | 800 | 14 | 214 | 314 | 10 | 1600 | 1650 | 16 | 101 | 78 | 10 |
| Immersion | 760 | 820 | 15 | 76 | 284 | 10 | 1670 | 1710 | 18 | 91 | 90 | 10 |
| Pipette | 790 | 820 | 8 | 57 | 725 | 10 | 1670 | 1690 | 25 | 112 | 70 | 10 |
| Steam | 680 | 740 | 9 | 141 | 618 | 10 | 1640 | 1610 | 44 | 272 | 49 | 10 |
| Sample mean | 750 | 800 | ..... | ..... | ..... | ..... | 1640 | 1660 | ..... | ..... | ..... | ..... |

* Excluded from sample mean.

*Symbol:* $m$ = median of particle diameters observed in all micrographs *combined*,
$\bar{x}$ = average of particle diameters observed in all micrographs *combined*,
$s_{\bar{x}}$ = standard deviation of $\bar{x}$,
$s_m$ = standard deviation of averages of particle diameters observed in *single* micrographs,
$n$ = total number of particles measured,
$k$ = number of micrographs.

The graphical presentation of these data shows no consistent systematic differences among the four washing techniques with regard to particle-size distribution. A more detailed statistical analysis does uncover some significant variation among the distributions corresponding to any one sample, but the lack of consistency of these effects from sample to sample and the smallness of their variations renders them unimportant from a practical point of view. For sample A, the effect of washing can be evaluated with reference to the unwashed sample. Figure 6 shows that this effect, regardless of the washing technique employed, is slight.

Table 1 lists the essential statistical information relating to the particle-size measurements described in this paper. The medians and averages are based on measurements obtained from all the elastomer particles counted. The average values obtained by the various techniques for any given latex do not differ from each other by more than 11 percent for sample B, 9 percent for sample C, and 6 percent for sample D. In the case of sample A, the discrepancies are somewhat larger (approximately 20 percent) because of errors of an accidental nature that occurred during the preparation. (During the steam washing of this sample the specimens were prematurely removed from the steam bath and insufficiently washed, making the measurement of the particles difficult because of uncertainties regarding their edges.) Judged on the basis of their standard deviations, denoted by the symbol $s_{\bar{x}}$, the averages listed show that any of the four washing techniques could be used to distinguish latices A and B from latex C or D, and latex C from D.

It is interesting to note that in almost all cases, the median particle size is smaller than the corresponding average value. This would indicate an apparent skewness in the particle-size distribution. Very probably this effect was brought about by the fact that no particles smaller than 100 A in diameter were recorded. Therefore, the distributions are, in reality, truncated at the lower end, rather than skewed.

An indication of the reproducibility of the experimental procedure may be obtained from the magnitude of the fluctuations of average particle sizes calculated from individual micrographs. For this purpose the values $s_m$ were computed. These are standard deviations characterizing the variability of the averages obtained from the single micrographs corresponding to a given latex and washing technique. Thus, the standard deviations $s_m$ express the fluctuations of averages of *single* micrographs, whereas the standard deviations $s_{\bar{x}}$ express the fluctuations of averages based on all particles from the combined total of *all* micrographs. Accordingly, every $s_m$ should be larger than the corresponding standard deviation $s_{\bar{x}}$ by a factor depending on the ratio of the number of particles in a single micrograph to that of all micrographs combined. A statistical examination based on an analysis of the variances shows, however, that in each case the difference between the two standard deviations is larger than can be accounted for by this ratio. This suggests that more variability exists among micrographs than would be inferred from the average range of particle sizes within a single micrograph. (These findings are in line with the observation made in section 4 about the conspicuous differences observed among the individual micrographs of figs. 2 and 3.) Consequently, the advantage gained from the examination of a greater number of micrographs is larger than that due to the mere increase in the number of particles. From the viewpoint of a comparison of washing techniques, it is significant that the additional variability among micrographs is approximately the same for all washing techniques.

On the basis of the foregoing analysis of the data, it appears that each of the four washing techniques is equally suitable and there is little reason for

selecting any single technique as being the most suitable for all the latices studied here. These latices contained particles ranging in size from approximately 100 to 2100 A. The use of any of the 4 washing techniques resulted in the same classification of the 4 latices into 3 separate groups, with average particle diameters of about 600, 800, and 1700 A, corresponding to the 3 copolymers of butadiene-styrene, butadiene-acrylonitrile, and butadiene-styrene-acrylonitrile, respectively. All the washing techniques yielded results that agreed within approximately 15 percent and had approximately the same order of reproducibility. Consequently, the selection of a single washing technique might be based on practical considerations. Inasmuch as the pipette procedure is experimentally easier to carry out and to control, this technique may tentatively be considered as preferable.

In view of the fact that absolute values for the particle size and frequency distribution of these synthetic latices are not available for comparison, the absolute accuracy of the results obtained by electron microscopy cannot be ascertained. These results do, however, provide the only data available at present and are adequate for reliable intercomparisons among latices.

The practical conclusion that one can draw from this analysis is that although the data do not permit one to make exact quantitative recommendations, they nevertheless provide substantial qualitative and even semiquantitative information regarding the effect of the various techniques of specimen preparation upon the distribution of particle sizes for the electron microscopical examination of the four synthetic latices. With a knowledge of the pore-size distribution of a given leather, the data shown in figure 6 would enable the leather technologist to estimate the number of particles of a given latex that could possibly penetrate the pore structure.

The authors welcome this opportunity to express their indebtedness to several members of the National Bureau of Standards: to Mary N. Steel for assistance with the calculations of the statistical data; and to René Oehler, Samuel G. Weissberg, Chares E. Weir, Norman P. Bekkedahl, and Lawrence A. Wood for their suggestions concerning these problems.

## 7. References

[1] R. Oehler, T. J. Kilduff, and S. Dahl, Treatment of leather with castilloa and hevea rubbers, J. Am. Leather Chem. Assoc. **45,** 349–77 (1950).

[2] R. Oehler and T. J. Kilduff, Treatment of Leather with synthetic resins, J. Research NBS **42,** 63–73 (1949) RP1951.

[3] R. H. Kelsey and E. E. Hanson, A method for preparing rubber latex specimens for the electron microscope, J. Appl. Phys. **17,** 675–77 (1946).

[4] W. E. Brown, Procedure for preparing latex samples for electron micrographs, Proceedings of the Electron Microscope Society of America, Abstract 33, J. Appl. Phys. **18,** 273 (1947).

[5] S. H. Maron, C. Moore, and A. S. Powell, Electron microscopy of synthetic latices, J. Appl. Phys. 23. 900–5 (1952).

[6] E. Schmidt and R. H. Kelsey, Creaming latex with ammonium alginate, Ind. Eng. Chem **43,** 406–12 (1951).

[7] E. A. Willson, J. R. Miller, and E. H. Rowe, Adsorption areas in the soap titration of latex for particle-size measurement, J. Phys. & Colloid Chem **53,** 357–74 (1949).

[8] W. K. Taft, University of Akron, private communication, August 8, 1951. (Samples A and B).

[9] G. A. Daum, B. F. Goodrich Chemical Co., private communication, February 27, 1951. (Sample C).

[10] G. S. Whitby, University of Akron, private communication, February 9, 1951). (Sample D).

[11] S. S. Wilks, Elementary Statistical Analysis, Chapter 2, (Princeton University Press, Princeton, N. J., 1949).

Washington, March 31, 1953.

Journal of Research of the National Bureau of Standards Vol. 50, No. 6, June 1953 Research Paper 2420

# Second-Order Transitions of Rubbers at High Pressures[1]

Charles E. Weir

Pressure-volume-temperature data on rubber-sulfur vulcanizates are analyzed in connection with their bearing on the second-order, or glass, transition in rubber. The results show no measurable change in transition temperature with increasing pressure nor any noticeable discontinuity in compressibility at the transition. No evidence is found for an isothermal transition produced by pressure. Possible explanations for the absence of the pressure transition are discussed.

## 1. Introduction

In a previous report [1][2] experimental pressure-volume-temperature (PVT) data were presented for rubber-sulfur vulcanizates in the ranges 10 to 28 percent of sulfur, 10° to 80° C, and 1,000 to 10,000 atm. No interpretations of these data were made in that report. In this study the significance of the data with respect to unresolved questions concerning the second-order, or glass, transition in rubbers are considered.

The glass transition (denoted here as $T_g$) defines a temperature or temperature interval in which marked changes in properties occur in high polymers, glasses, and other materials that may manifest a glassy state. There is considerable doubt as to whether the phenomena observed are representative of a true thermodynamic transition or merely of a very slow rate process in which attainment of equilibrium may be considered temporally impractical [2]. Resolution of these problems is of great theoretical importance, particularly with respect to the third law of thermodynamics [3] but is beyond the scope of this report. The widespread interest in the glass transition comes from its practical importance in commercial applications, and there is considerable literature on the subject, such as the extensive reviews by Boyer and Spencer [4], Berger [5], Morey [6], Kauzmann [7], and others.

There is no established isothermal volume change that takes place at $T_g$ and similarly no latent heat, although $C_p$ (and presumably $C_v$) change markedly. To a first approximation, therefore, it would appear that $T_g$ should be independent of pressure. The interest in the effect of $P$ on $T_g$ is indicated by the numerous recent attempts to deduce this relationship from data given by Scott [8].

Scott [8] previously reported $PVT$ data on rubber-sulfur vulcanizates over essentially the same temperature interval but to a maximum pressure of only 800 bars. These have heretofore represented the only available data on high polymers with a direct bearing on the relationship between $P$, $V$, and $T_g$. However, at the time the measurements were made the future significance of the discontinuities in slopes of isobars was not apparent, and the data are given only by means of graphs and empirical equations that are somewhat difficult to use. With subsequent increasing interest in the nature of the processes responsible for the changes observed at $T_g$, the data of Scott have received major attention from recent workers. It would appear, in view of the way the results are presented and the fact that their future significance could not be anticipated, that several questionable conclusions have been derived recently from these data. The unsoundness of such conclusions is confirmed in most instances by the original numerical experimental data that have been made available through the cooperation of A. H. Scott [9]. The previously reported data at high pressures [1] are designed to cover essentially the same sulfur and temperature ranges studied by Scott [8] and to give an unequivocal answer to the interdependence of $T_g$ and $P$, as well as other matters of interest here.

Rubber-sulfur vulcanizates were selected so that several specimens were expected to pass through $T_g$ in the temperature interval used, although studies were made of specimens exhibiting no $T_g$ in this temperature interval. These were added to round out the picture in so far as possible. However, very low sulfur contents could not be conveniently studied because of the action of the confining liquid—a light petroleum distillate—on such specimens. The numerical data obtained, and the empirical equations derived to fit the data, have been given previously [1].

It must be emphasized that subsequent interpretations of these data can be considered to apply only to the pressure interval studied (1,000 to 10,000 atm) and to the rubber-sulfur vulcanizate system of high sulfur content.

## 2. Results and Discussion

### 2.1. Isobaric Transition, $T_g$

Isobars calculated from the numerical data are shown for six vulcanizates in figures 1 to 6, in which specific volumes are plotted as ordinates. Each isobar is labelled with the corresponding pressure in units of thousands of atmospheres. In these figures the isobars are drawn as linear above and below $T_g$, which is taken to correspond to the intersection of these lines. In figures 1 and 2 no transition is observed, and they are included to illustrate other matters to be pointed out later. In figures 4 and 6, the transition temperature is not well defined; in the

[1] This work was sponsored by the Office of Naval Research.
[2] Numbers in brackets refer to the literature references at the end of this paper.

former because of scatter of points, and in the latter because only a single point occurs at temperatures above $T_g$. In figures 3 and 5, $T_g$ is considered to be sufficiently well defined to conclude, with due consideration of the experimental errors [1], that there is no evidence for any measureable change in $T_g$ with changing pressure. It is suggested, therefore, that for these materials in this pressure range, $T_g$ is not a function of pressure to a rather good degree of approximation.

It will be noted that some discrepancy exists between the values of $T_g$ given here and those of Scott [8], from which these data were essentially derived. These discrepancies are to be attributed to uncertainties in deriving the specific volumes from the graphical data of Scott [8] and inherent variations to be expected in lines drawn through experimental points. Therefore, no significance may be attached to the actual values of $T_g$ shown here. It is of the utmost importance to recognize that no factor appears to act on compression to produce any measurable change in $T_g$.

Specimens used in these studies will ultimately be analyzed and studied dilatometrically at 1 atm. No significant change in any conclusion presented here is to be expected as a result of any measurements at 1 atm. Slight revisions of specific volumes or values of $T_g$ may be expected and these will be reported in due course.

From the fact that the isobars represent a family of divergent lines, shown best in figures 1 and 2, it is possible to deduce qualitatively the effects of pressure on expansivity and of pressure and temperature on compressibility. Such effects are interrelated by the geometry of the family of isobaric lines and the fact that the expansivity is proportional to the slope of the isobars and the isothermal compressibility to the separation of the isobars at a given temperature. Qualitatively, the expansivities and compressibilities behave in a manner similar to that pointed out by Bridgman for solids and liquids [10].

From the empirical equations derived previously, the compressibility may be written as

$$-\frac{1}{V_0}\frac{\partial V}{\partial P}=\frac{1}{V_0}\left[a-bP+cP^2+(a'-b'P+c'P^2)t+(-a''+b''P-c''P^2)t^2\right], \quad (1)$$

where the coefficients are essentially positive. In all empirical equations it is noted that $b'$ and $c'$ may change signs rarely; but $a''$, $b''$, and $c''$ are found to reverse in sign somewhat more frequently. The change in compressibility with temperature is then

$$-\frac{1}{V_0}\frac{\partial^2 V}{\partial P \partial T}=\frac{1}{V_0}\left[a'-b'P+c'P^2+2(-a''+b''P-c''P^2t\right] \quad (2)$$

with similar considerations regarding the signs of the coefficients. At a given pressure it is apparent from eq (1) that the compressibility increases with increasing temperature, since $|a'|\gg|a''|,|b'|\gg|b''|,|c'|\gg|c''|$. From eq (2) it appears that at a given pressure, the rate of increase of compressibility with temperature is less at higher temperatures (that is, above $T_g$) than at lower temperatures (that is, below $T_g$).

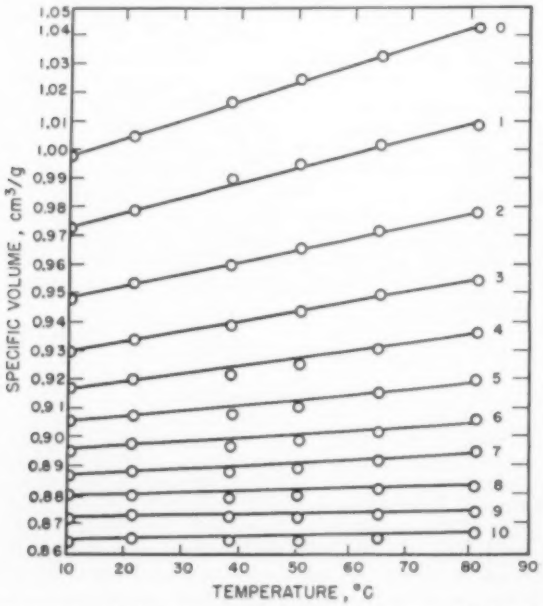


FIGURE 1. *Isobars for rubber-sulfur vulcanizate containing 10 percent of sulfur.*

The number opposite each isobar denotes the pressure in units of thousands of atmospheres.

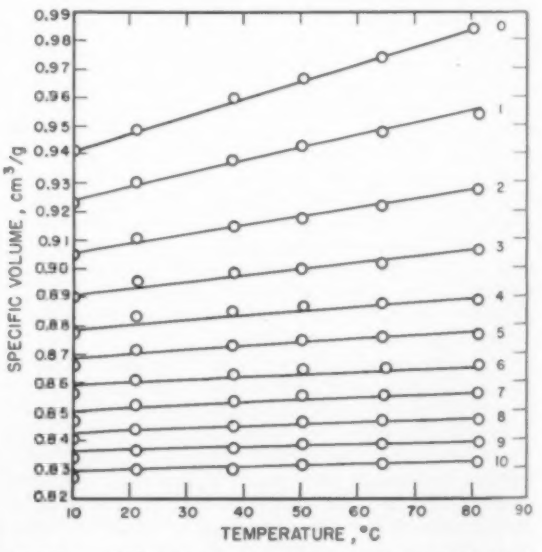


FIGURE 2. *Isobars for rubber-sulfur vulcanizate containing 16 percent of sulfur.*

The number opposite each isobar denotes the pressure in units of thousands of atmospheres.

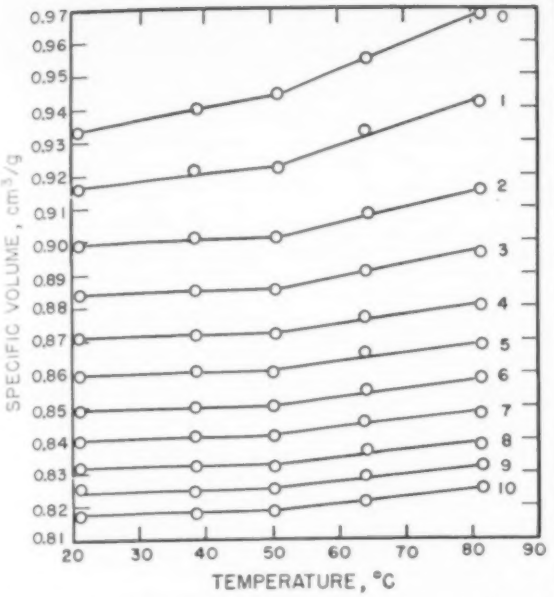


FIGURE 3. *Isobars for rubber-sulfur vulcanizate containing 18 percent of sulfur.*

The number opposite each isobar denotes the pressure in units of thousands of atmospheres.

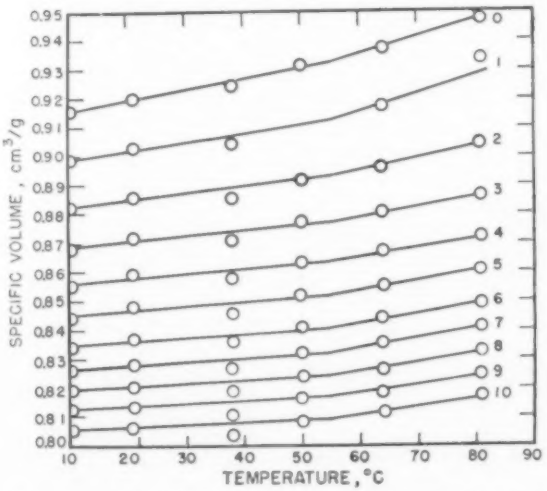


FIGURE 4. *Isobars for rubber-sulfur vulcanizate containing 20 percent of sulfur.*

The number opposite each isobar denotes the pressure in units of thousands of atmospheres.

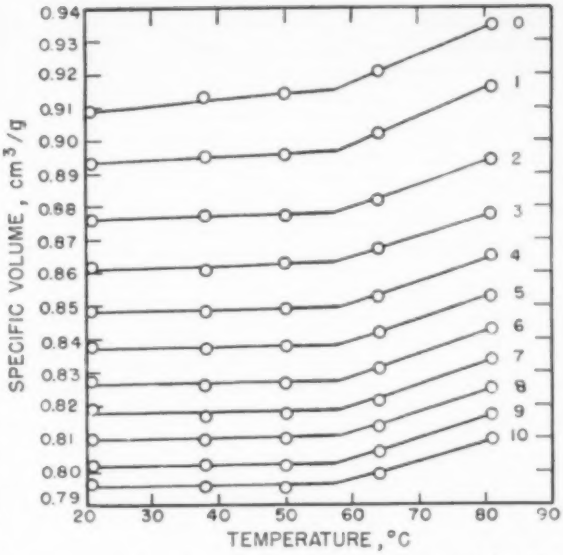


FIGURE 5. *Isobars for rubber-sulfur vulcanizate containing 22 percent of sulfur.*

The number opposite each isobar denotes the pressure in units of thousands of atmospheres.

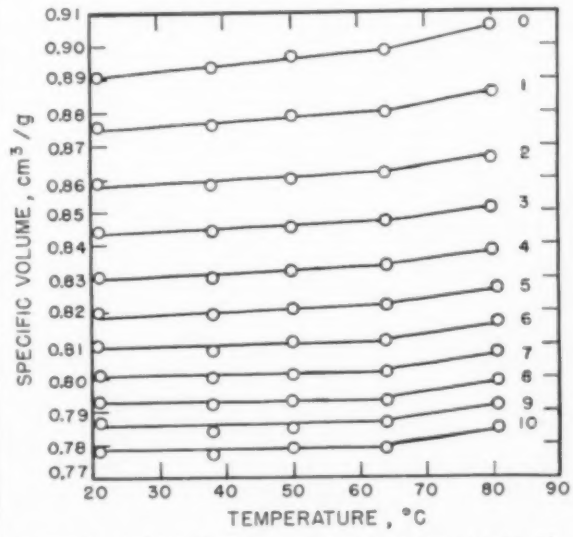


FIGURE 6. *Isobars for rubber-sulfur vulcanizate containing 25 percent of sulfur.*

The number opposite each isobar denotes the pressure in units of thousands of atmospheres.

However, for some specimens exhibiting $T_g$ in this temperature interval, $a''$ is negative so that the reverse is true. This fact, together with the errors inherent in defining the smaller coefficients, renders a decision on the variation of compressibility with temperature somewhat uncertain. From the equations, however, it may be stated with confidence that any change in compressibility on passing through $T_g$ is not large. From figures 3 to 6, it can be concluded that such an increase in compressibility would probably decrease with increasing pressure and that such an effect, if it exists, is larger at low pressures. Consideration of the experimental data furnished by Scott [9] yields the conclusion that existence of a change in compressibility on passing through $T_g$ is very doubtful, and if present is certainly rather small. Because compressibility is generally not determined with the precision of expansivity and is a strong function of pressure and temperature, any conclusions involving small changes in such a property are subject to some uncertainty. There is little doubt that a change in compressibility of the order of 2 or 3 to 1 is not shown by these data.

Inasmuch as eq (1) and (2) do not readily permit an unequivocal general analysis, it is of interest to show the compressibility-temperature behavior numerically. Such calculations have been made for several vulcanizates with results similar to those shown for a flexible rubber (13 percent of S) and a rigid rubber (22 percent of S) which shows the marked isobaric transition of figure 5. The results of these calculations are shown graphically in figures 7 and 8, in which compressibility is plotted against temperature, the pressure being denoted on each curve in units of thousands of atmospheres. It will be noted that a discontinuity in compressibility at $T_g$ is absent at all pressures in figure 8, the compressibility isobars being essentially as smooth as those for the 13-percent vulcanizate shown in figure 7 for comparison. Differences between the shapes of the curves in these figures are not of interest here, the principal point of interest being the essential smoothness of the curves. It is to be noted that any assumptions involved in calculations of the original data [1] have negligible effect on these curves, which are defined essentially by the *shapes* of the compression isotherms and not by their absolute magnitudes. Discontinuities in compressibility must show up as irregularities in the original experimental data irrespective of any extensive properties of the material. No such irregularities have ever been observed within the experimental errors of the measurements.

It is of interest to calculate the change of $T_g$ with increasing pressure on the assumption that the phenomenon is representative of a true thermodynamic transition of second order. The equations defining this variation are

$$dP/dT=(Cp_1-Cp_2)/Tv(\alpha_1-\alpha_2), \tag{3}$$

and

$$dP/dT=(\alpha_1-\alpha_2)/(\beta_1-\beta_2), \tag{4}$$

where the terms have the usual significance [10]. Equation (3) has been evaluated by Gee [11], who found $dT/dP \approx 0.016$ deg/bar. Sufficient data are available here to evaluate eq (4). From eq (1), $\beta_1-\beta_2=\Delta\beta$ is found to be

$$\Delta\beta=(a'-b'P+c'P^2)(t_1-t_2)+(-a''+b''P-c''P^2)(t_1^2-t_2^2), \tag{5}$$

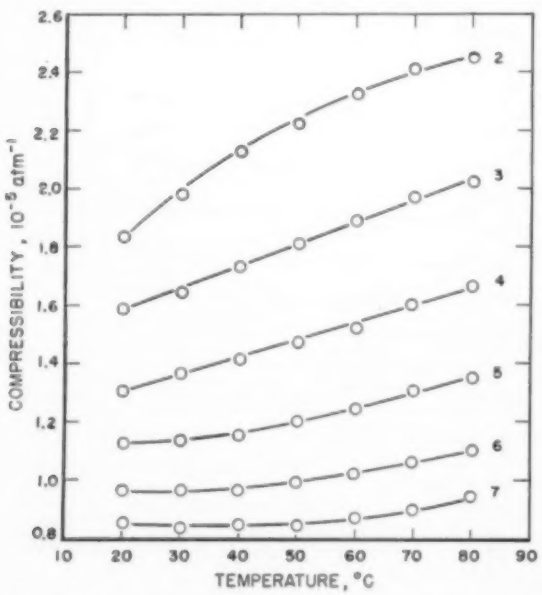


FIGURE 7. *Compressibility isobars for rubber-sulfur vulcanizate containing 13 percent of sulfur.*

The number opposite each isobar denotes the pressure in units of thousands of atmospheres.

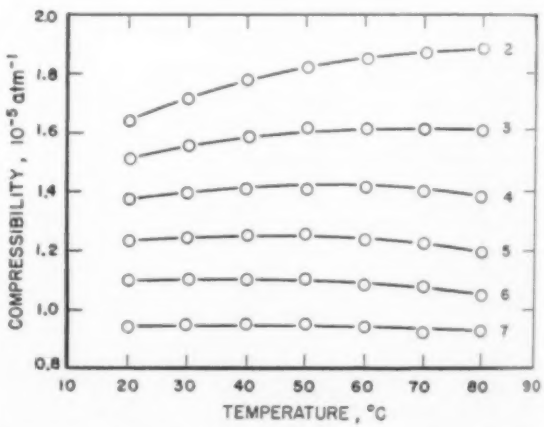


FIGURE 8. *Compressibility isobars for rubber-sulfur vulcanizate containing 22 percent of sulfur.*

The number opposite each isobar denotes the pressure in units of thousands of atmospheres.

where $t_1$ and $t_2$ refer to temperatures slightly below and slightly above $T_g$. From the empirical equation [1], $\alpha_1 - \alpha_2 = \Delta\alpha$ is found to be

$$\Delta\alpha = 2(a_0'' + a''P - b''P^2 + c''P^3)(t_1 - t_2) \qquad (6)$$

whence, by substituting, eq (4) may be shown to be

$$dT/dP = (a' - b'P + c'P^2) + (-a'' + b''P - c''P^2)(t_1 + t_2)/2(a_0'' + a''P - b''P^2 + c''P^3), \qquad (7)$$

which reduces at low pressures to

$$dT/dP \approx a' - a''(t_1 + t_2)/2a_0''. \qquad (8)$$

Considering the 22-percent-rubber-sulfur vulcanizate in particular, although all other rubbers are quite comparable, $t_1 + t_2$ may be taken to be approximately $1 \times 10^2$, while $a''$ is $+3.6 \times 10^{-10}$, $a'$ is $1.3 \times 10^{-7}$ and $2a_0''$ is $1.4 \times 10^{-5}$. The value of $dT/dP$ is then of the order of $7 \times 10^{-3}$ deg/atm. This corresponds to a change of $T_g$ of the order of 7 deg C/1,000 atm at low pressures. It is not apparant that the orders of magnitude of numerator and denominator of eq (7) do not change with increasing pressure. However, simple numerical computations, using the coefficients of the empirical equations, show that such is the case. On the basis of these data, a change of $T_g$ of the order of 70 deg C is predicted from eq (4); and from the value given by Gee [11] for eq (3), the corresponding change would be approximately 160 deg C/10,000 atm. It is obvious that no such change occurs in figures 3 to 6; and indeed, any change in $T_g$ with pressure, if present at all, would appear to be less than 1 deg C/10,000 atm. The discrepancy between predicted and observed change in $T_g$ with varying $P$ would appear to lend support to the suggestions that the phenomena occurring at $T_g$ are not representative of a true thermodynamic transition of second order [2, 4].

### 2.2. Isothermal Compression

Typical isotherms are shown in figure 9, and because all other isotherms are essentially similar, there seems no reason for their reproduction here. All isotherms are inherently smooth, and it must be concluded that a second-order, or glass, transition pressure, $P_g$, does not exist in these data. The existence of $P_g$ would appear to be of importance from both theoretical and practical viewpoints and possible reasons for failure to observe such a phenomenon must be considered.

First, occurrence of such a transition at low pressures, that is, below 1,000 atm, may be essentially ruled out, since Scott [8] observed no such transition up to 800 bars.

Second, the effect of the confining liquid on the transition may be discarded as measurements of the amount of such liquid absorbed yielded results of such small magnitude as to invalidate this possibility.

Third, the small magnitude of any change of compressibility occurring on traversing $P_g$ might render observation of such a phenomenon most difficult, particularly since the compressibility is strongly pressure dependent. The difficulties arising from this possibility cannot be minimized and are very real. However, it would appear from the very real similarity of the compression curves of all polymers studied to date without regard to $T_g$ or the chemical structure of the polymer that it is very improbable that any such $P_g$ exists.

All previous studies of this nature have reported smooth $PV$ relationships. Adams and Gibson [12] used essentially the same experimental apparatus applied here; Bridgman [13] however, has evolved a different method requiring no confining liquid and has reported some irregularities. Tammann and Jellinghaus [14] studied glasses at various temperatures through the transition range at pressures as high as 2,000 kg/cm$^2$ and likewise reported data showing no isothermal irregularities.

The report of Bridgman deserves special consideration. The data from which this report originated were made available through the cooperation of P. W. Bridgman [15]. From these data it would appear that the isotherms themselves are also smooth, but irregularities appear in the differences of the experimental data. Because all rubbers studied which had

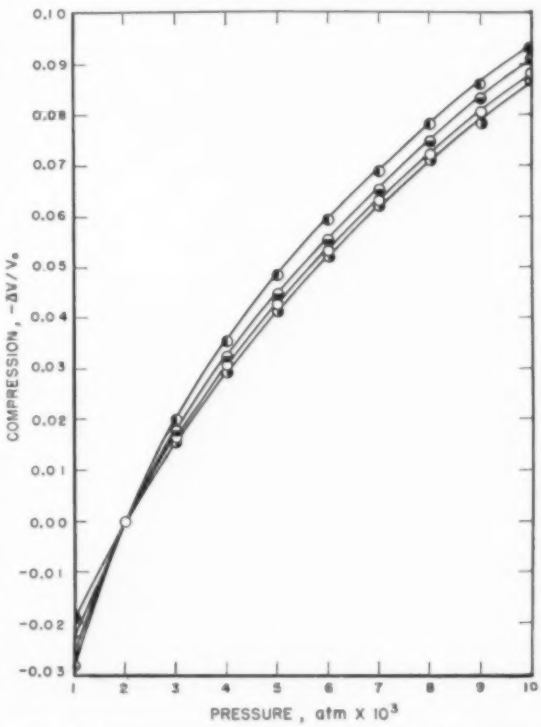


FIGURE 9. *Compression isotherms of rubber-sulfur vulcanizate containing 18 percent sulfur.*

◗, 21.0° C; ○, 50.2° C; ◒, 64.0° C; ◐, 81.5° C.

similar rubber content did not exhibit similar behavior, it appears most probable that the irregularities did not arise from the polymer alone. This is not believed to be typical of the transitions considered here.

It is concluded therefore, that there is no good evidence for a $P_g$ comparable to $T_g$. No absolute requirement for such a $P_g$ exists because $P$ and $T$ are independent and observed behavior in the $V$-$T$ plane does not imply a definite behavior in the $P$-$V$ plane. However, since $V$ is considered to be of great importance in determining the behavior of condensed phases, and values of $V$ smaller than those expected at $T=0°$ K by thermal contraction alone can be produced by these pressures, it is of interest to evaluate internal-energy changes due to isothermal compression over this pressure range and by isobaric expansion over a temperature interval that includes $T_g$. These energy changes may be evaluated by the easily derivable relationships

$$(\Delta E)_T = -TV_0\int_{P_1}^{P_2}\alpha dP + V_0\int_{P_1}^{P_2}\beta PdP \qquad (9)$$

$$(\Delta E)_P = \int_{T_1}^{T_2} C_p dT - PV_0\int_{T_1}^{T_2}\alpha dT \qquad (10)$$

where the quantities have the usual thermodynamic significance. These equations were evaluated for natural rubber in which $T_g \approx 200°$ K. The temperature limits were 300° and 175° K, which include $T_g$, and the corresponding pressure limits were 1 and 10,000 atm, respectively. The following assumptions were required in evaluating eq (9) and (10):

1. $\beta$ for natural rubber was assumed to have the same pressure dependence found for the 10-percent-sulfur vulcanizate studied.

2. $\alpha$ was assumed to be a linear function of pressure, with a pressure dependence similar to that found for liquids by Bridgman [16].

3. Quasi-equilibrium was assumed at $T_g$ so that eq (10) could be applied. This assumption is borne out by experimental data [17].

4. $\alpha$ was assumed to be continuous in a mathematical sense at $T_g$.

Using Bekkedahl's data for specific heats [18] and expansivities [19], together with the above assumptions, the following values are obtained:

$$(\Delta E)_T = -103 \text{ j/g}$$

$$(\Delta E)_P = -200 \text{ j/g}.$$

These values are of the same order of magnitude for natural rubber where $T_g$ is far below room temperature. If harder rubbers are considered, the lower limit of temperature required on the integrals of eq (10) to encompass $T_g$ becomes higher, and for very hard rubbers the value of $(\Delta E)_P$ reverses in sign as $T_g$ becomes greater than room temperature. The value of $(\Delta E)_T$, however, will remain relatively unchanged. It is clear therefore that for the rubbers studied here that $|(\Delta E)_T|$ is certainly not necessarily smaller than $|(\Delta E)_P|$. Therefore, a quantitative difference in internal energy changes cannot be used to account for the absence of $P_g$ on isothermal compression. It must be emphasized that the source of the respective internal-energy changes has not been considered. On isothermal compression, it is most probable that the decrease in internal energy arises principally from change in potential energy [16], whereas in isobaric contraction, the decrease is to be attributed principally to kinetic sources. It appears reasonable to suppose that the transition is not caused by potential effects, particularly because recent theories of the causes of the transition in polymers [4, 17] emphasize the retarded viscous-response concept. The latter of these, however, deduces the viscous-response concept from an hypothesis of critical free volume. The free-volume concept would appear to require some modification because free volumes attained in the present studies, although considerably less than those expected at 0° K by thermal contraction alone, produce no isothermal transition and appear to have no effect on the isobaric transition. In the light of the present evidence no extension of such concepts appears justified.

Important quantitative conclusions differing from those of this report have been deduced from the data obtained in previous studies at elevated pressures. Although the measurements were made by Scott [8] and Tamman and Jellinghaus [14], pertinent conclusions of interest here have been reached by later workers from a study of the reported data. Such conclusions are frequently erroneously attributed to the original authors, and, in most instances, appear to be highly questionable. It is necessary, therefore, to examine those previous data critically and to evaluate such conclusions drawn therefrom that differ from those of this report.

The frequently quoted results of Scott [8], who studied rubbers to a maximum pressure of 800 bars, are cited chiefly with respect to the behavior of the 19.5-percent-rubber-sulfur vulcanizate that undergoes a glass transition in the temperature interval

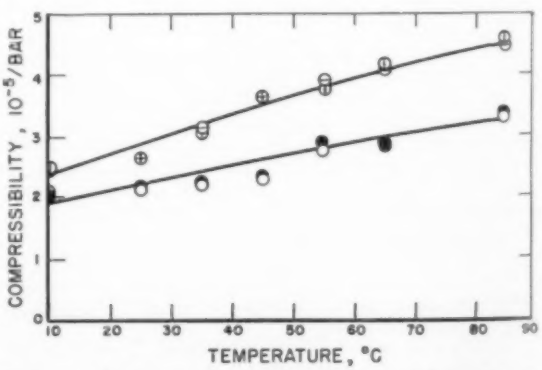


FIGURE 10. *Compressibility isobars calculated from data of Scott [8] for rubber-sulfur vulcanizate containing 19.5 percent of sulfur.*

⊖, 100 bars, decreasing pressure; ⊕, 100 bars, increasing pressure; ○, 700 bars decreasing pressure; ●, 700 bars, increasing pressure.

TABLE 1. *Pressure-volume-temperature data for natural rubber-sulfur vulcanizate containing 19.5 percent of sulfur [9]*

| 10° C | | 25° C | |
|---|---|---|---|
| Pressure | Relative volume | Pressure | Relative volume |
| *Bars* | *ml* | *Bars* | *ml* |
| 1 | 1.00000 | 1 | 1.00000 |
| 198 | .99503 | 191 | .99509 |
| 394 | .99055 | 391 | .99034 |
| 600 | .98597 | 597 | .98567 |
| 813 | .98154 | 808 | .98119 |
| 641 | .98513 | 637 | .98478 |
| 432 | .98936 | 419 | .98966 |
| 214 | .99461 | 216 | .99455 |
| 1 | .99982 | 1 | 1.00005 |
| 25° C | | 35° C | |
| 1 | 1.00000 | 1 | 1.00000 |
| 189 | .99504 | 188 | .99438 |
| 394 | .99007 | 373 | .98938 |
| 601 | .98528 | 587 | .98421 |
| 813 | .98072 | 809 | .97927 |
| 630 | .98457 | 630 | .98318 |
| 424 | .98918 | 422 | .98809 |
| 227 | .99404 | 218 | .99336 |
| 1 | .99992 | 1 | 1.00008 |
| 45° C | | 55° C | |
| 1 | 1.00000 | 1 | 1.00000 |
| 193 | .99300 | 188 | .99208 |
| 389 | .98670 | 386 | .98629 |
| 580 | .98125 | 588 | .97997 |
| 818 | .97557 | 803 | .97377 |
| 630 | .97987 | 622 | .97809 |
| 418 | .98558 | 418 | .98517 |
| 230 | .99169 | 219 | .99149 |
| 1 | .99991 | 1 | .99986 |
| 65° C | | 85° C | |
| 1 | 1.00000 | 1 | 1.00000 |
| 193 | .99194 | 189 | .99131 |
| 388 | .98499 | 386 | .98329 |
| 589 | .97820 | 591 | .97544 |
| 818 | .97162 | 821 | .96794 |
| 622 | .97712 | 629 | .97410 |
| 429 | .98351 | 416 | .98173 |
| 227 | .99084 | 209 | .99000 |
| 1 | .99997 | 1 | .99929 |
| ..... | ..... | 812 | .96789 |

TABLE 2. *Compressibilities of natural-rubber-sulfur vulcanizate containing 19.5 percent of sulfur*

| 10° C | | 25° C | |
|---|---|---|---|
| Pressure | Compressibility | Pressure | Compressibility |
| *Bars* | *1/Bar* | *Bars* | *1/Bar* |
| 99 | $2.52\times10^{-4}$ | 95 | $2.64\times10^{-4}$ |
| 296 | 2.28 | 292 | 2.43 |
| 497 | 2.21 | 497 | 2.31 |
| 707 | 2.08 | 707 | 2.15 |
| 727 | 2.09 | 722 | 2.11 |
| 536 | 2.02 | 527 | 2.24 |
| 323 | 2.40 | 325 | 2.47 |
| 108 | 2.45 | 114 | 2.60 |
| 25° C | | 35° C | |
| 96 | $2.59\times10^{-4}$ | 94 | $3.01\times10^{-4}$ |
| 291 | 2.37 | 280 | 2.70 |
| 494 | 2.27 | 480 | 2.41 |
| 703 | 2.12 | 698 | 2.28 |
| 723 | 2.10 | 720 | 2.18 |
| 528 | 2.19 | 526 | 2.36 |
| 317 | 2.41 | 320 | 2.58 |
| 108 | 2.56 | 110 | 3.10 |
| 45° C | | 55° C | |
| 96 | $3.64\times10^{-4}$ | 94 | $3.75\times10^{-4}$ |
| 291 | 3.21 | 287 | 3.37 |
| 487 | 2.85 | 487 | 3.13 |
| 699 | 2.38 | 696 | 2.88 |
| 724 | 2.27 | 712 | 2.72 |
| 524 | 2.69 | 520 | 3.17 |
| 324 | 3.25 | 319 | 3.18 |
| 116 | 3.59 | 110 | 3.84 |
| 65° C | | 85° C | |
| 97 | $4.20\times10^{-4}$ | 95 | $4.61\times10^{-4}$ |
| 290 | 3.56 | 287 | 4.07 |
| 488 | 3.37 | 488 | 3.83 |
| 704 | 2.87 | 706 | 3.26 |
| 720 | 2.81 | 725 | 3.21 |
| 526 | 3.31 | 523 | 3.58 |
| 328 | 3.63 | 212 | 3.99 |
| 114 | 4.04 | 105 | 4.44 |

reported. The original experimental data on this vulcanizate were made available by A. H. Scott [9], and are reproduced in table 1. From these data the compressibilities ($-\Delta V/V_0\Delta P$) were calculated by first differences. These compressibilities are given in table 2, and a plot of compressibility versus temperature is shown in figure 10 for interpolated pressures of 100 and 700 bars. No appreciable discontinuity in compressibility is manifest at either pressure, and similar results will be obtained at other pressures as is evident by an inspection of the data of table 2.

The generally accepted conclusion that Scott's data show an increase in $T_g$ with increasing pressure is also subject to question. The isobars given by Scott [8] are insufficiently detailed to warrant definite conclusions. *It must be emphasized that if the widely quoted 15 deg C rise in $T_g$ at 800 bars for the 19.5-percent vulcanizate is literally accepted, one must be prepared to ignore completely similar data for the 18.8-percent vulcanizate, which by similar rigorous interpretation, show no change in $T_g$ in the same pressure interval.*

Numerous qualitative and quantitative deductions have also been drawn from the data of Tammann and Jellinghaus [14], who investigated glasses at 100-kg/cm² pressure intervals to a maximum pressure of 2,000 kg/cm². Isothermal measurements were made at approximately 10-deg-C intervals covering a range that included $T_g$. These data have been widely quoted as showing a pronounced change in compressibility on passing through $T_g$. The authors estimated their experimental error through a measurement on water that was compared with the early (1893) data of Amagat [20]. By such a comparison they report an average error of $3\times10^{-4}$ ml/g and a maximum error of $1.1\times10^{-3}$ ml/g in *specific volume*.

Cursory examination of the specific-volume data does lead to indications of a marked change in compressibility at $T_g$ as widely accepted. However, study of the isothermal first differences of the experimental data reported discloses a considerable scatter.

The first differences correspond to the $\Delta V$ values experimentally measured, and it is these values which determine compressibility. The estimated average error of $3\times10^{-4}$ ml/g in specific volume now amounts to a large proportion of the $\Delta V$ value. These considerations apply to the isothermal data; and if it is no x required to estimate the temperature coefficient of compressibility, it is necessary to compare the $\Delta V$ values for a given pressure at the various temperatures. The change in compressibility at $T_g$ is precisely this temperature coefficient of compressibility that is clearly subject to considerably more uncertainty than the compressibility itself. To illustrate the problem, the first differences of the reported data on salicin glass [14], which represent $\Delta V$ values for each 100 kg/cm², are plotted against pressure for four temperatures in figure 11. The vertical dimension of each point is taken as $3\times10^{-4}$ ml/g in accordance with the author's estimated average error in specific volume and is indicated by the barred line. In a statistical sense this estimate for error in the differences is probably considerably too low, but all pertinent conclusions are obvious, even with the underestimated error.

The vertical separation of the points at a given pressure will be a measure of the effect of temperature on compressibility. It is to be anticipated that compressibility will increase with increasing temperature. However, in only 8 of the 20 pressures shown is the order of the points in the order of increasing temperature. The other 12 cases contain at least one instance of an inversion indicating at least one instance of greater compressibility at a lower temperature. In any event, inspection of the amount and degree of overlapping and inversion in figure 11 indicates the questionable nature of any conclusions concerning compressibility as related to

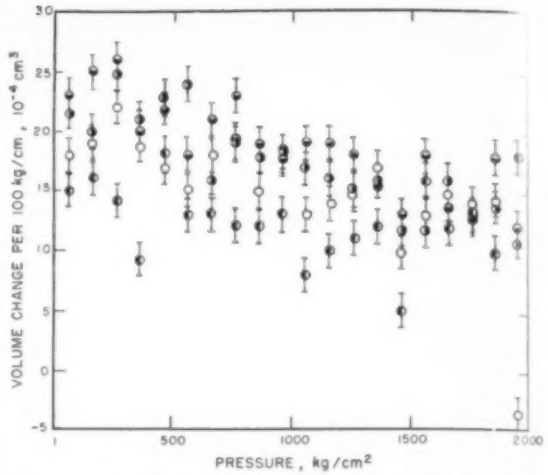


FIG. 11. *Volume changes for salicin glass calculated from data of Tammann and Tellinghaus [14]*

The uncertainties indicated are the errors estimated by the authors in the *specific volume*. ◐, 20° C; ○, 40° C; ◑ 50° C; ◒, 60° C.

temperature. It may be noted that instances of inversion of compressibility with temperature also occur in the data shown in figure 8. The amounts of such inversions are of a much smaller order than most of those indicated in figure 11 and are within the experimental errors of the present measurements.

A tabulation of compression values ($\Delta V/V_0$) for three intervals (1 to 1,000; 1,000 to 2,000; and 1 to 2,000 kg/cm²) is given in table 3 as calculated from the reported specific volumes of the three glasses

TABLE 3. *Compression values for glasses*

| Pressure interval | Compression, $-\Delta V/V_0$ | | | | | | |
|---|---|---|---|---|---|---|---|
| | Selenium glass. $t_g=29.8°$ C | | | | | | |
| | 10° C | 20° C | 30° C | 40° C | 50° C | 60° C | 70° C |
| *kg/cm²* | | | | | | | |
| 1 to 1,000 | 0.002120 | 0.002155 | 0.002550 | 0.002756 | 0.002783 | 0.002839 | 0.002866 |
| 1,000 to 2,000 | .001600 | .001726 | .001654 | .001606 | .002003 | .002122 | .002015 |
| 1 to 2,000 | .003720 | .003881 | .004004 | .004362 | .004786 | .004961 | .004881 |
| | Salicin glass. $t_g=43$ to 44° C | | | | | | |
| | 20° C | 30° C | 40° C | 50° C | 60° C | 70° C | |
| 1 to 1,000 | 0.001350 | 0.001548 | 0.001795 | 0.002068 | 0.002137 | 0.002187 | |
| 1,000 to 2,000 | .001250 | .001318 | .001196 | .001412 | .001593 | .001733 | |
| 1 to 2,000 | .002600 | .002866 | .002991 | .003480 | .003730 | .003920 | |
| | Colophony glass. $t_g=29.5°$ C | | | | | | |
| | 10° C | 18° C | 28° C | 40° C | 50° C | 60° C | |
| 1 to 1,000 | 0.002250 | 0.002343 | 0.002366 | 0.003205 | 0.003499 | 0.005907 | |
| 1,000 to 2,000 | .001900 | .001874 | .001865 | .001883 | .002116 | .002299 | |
| 1 to 2,000 | .004150 | .004217 | .004231 | .005088 | .005615 | .006206 | |

studied [14]. These data show that any conclusions regarding the change in compressibility at $T_g$ must be qualified at least as to the pressure range and in view of the results of figure 11 should be drawn with extreme caution.

It can be concluded solely from a detailed examination of the data of these investigations that the interpretations, which have been subsequently advanced in connection with questions concerning the effect of pressure on the glass transition, are not unequivocally established by these data. It is therefore suggested that as a result of this and the previous studies that there is no valid evidence for a discontinuity of compressibility at $T_g$ nor for any appreciable effect of pressure on $T_g$ in the rubber-sulfur system of high polymers.

## 3. References


[1] C. E. Weir, J. Research NBS **50,** 3 (1953) RP2403.
[2] T. Alfrey, G. Goldfinger, and H. Mark, J. Appl. Phys. **14,** 700 (1943).
[3] G. E. Gibson, G. S. Parks, and W. M. Latimer, J. Am. Chem. Soc. **42,** 1548 (1920).
A. G. Oblad and R. F. Newton, J. Am. Chem. Soc. **59,** 2494 (1937).
[4] R. F. Boyer and R. S. Spencer, Advances in colloid science II, chapter 1, edited by H. Mark and G. S. Whitby (Interscience Publishers, Inc., New York, N. Y., 1946).
[5] E. Berger, J. Am. Ceramic Soc. **15,** 647 (1932).
[6] G. W. Morey, J. Am. Ceramic Soc. **17,** 315 (1934).
[7] W. Kaufmann, Chem. Rev. **43,** 219 (1948).
[8] A. H. Scott, J. Research NBS **14,** 100 (1935) RP760.
[9] A. H. Scott, private communication.
[10] M. W. Zemansky, Heat and thermodynamics (McGraw-Hill Book Co. Inc., New York, N. Y., 1943).
[11] G. Gee, Rev. Chem. Soc. **1,** 265 (1947).
[12] L. H. Adams and R. E. Gibson, J. Wash. Acad. Sci. **20,** 213 (1930).
[13] P. W. Bridgman, Pro. Am. Acad. Arts Sci. **76,** 9 (1945).
[14] G. Tamman and E. Jellinghaus, Ann. Physik **2,** 264 (1929).
[15] P. W. Bridgman, private communication.
[16] P. W. Bridgman, The physics of high pressure (G. Bell & Sons Ltd., London 1949).
[17] T. G. Fox and P. J. Flory, J. Appl. Phys. **21,** 581 (1950).
[18] N. Bekkedahl and H. Matheson, J. Research NBS **15,** 503 (1935) RP844.
[19] N. Bekkedahl, J. Research NBS **13,** 410 (1934) RP717.
[20] E. H. Amagat, Ann. Chim. et Phys. [6] **29,** 543 (1893).



Washington, March 27, 1953.

Journal of Research of the National Bureau of Standards Vol. 50, No. 6, June 1953 Research Paper 2421

# Thermodynamics of the Rubber-Sulfur System at High Pressures[1]

Charles E. Weir

From previously reported $PVT$ data on rubber-sulfur vulcanizates in the ranges 10° to 80° C, 1,000 to 10,000 atm, and 10 to 28 percent of sulfur, calculated values are given for work, heat, internal-energy change, and difference in specific heats. These values are given at 10-deg-C and 1,000-atm intervals for three representative rubbers containing 10, 18, and 28 percent of sulfur. Implications of the results are discussed.

## 1. Introduction

In two previous reports data have been presented on $PVT$ measurements on rubber-sulfur vulcanizates in the ranges 10 to 28 percent of sulfur, 10° to 80° C, and 1 to 10,000 atm [1];[2] the empirical isobaric, isothermal, and $PVT$ equations that represented the data [1]; and some interpretations of the data with regard to the isobaric glass transition temperature ($T_g$) and the isothermal glass transition pressure ($P_g$) [2]. The present report describes additional treatment of the experimental data [1] in calculation of thermodynamic quantities of interest. These calculations are patterned after those carried out by Bridgman in many studies on liquids. A résumé of data so obtained has been given by Bridgman [3]. Data are presented here for the following quantities as functions of pressure and temperature over the ranges referred to above for three rubber-sulfur vulcanizates: 1, work of compression; 2, heat of compression; 3, change in internal energy on compression; and 4, difference between specific heats at constant pressure and constant volume.

## 2. General Considerations

The following considerations are pertinent to the calculations carried out: All measurements carried out earlier [1] were conducted isothermally and represented measurements of relative changes of volume at various pressures. The volume was measured at one temperature (21° C), initial volumes at all other temperatures being derived from the measured volume at 21° C and independent expansivity data. This procedure has been described in detail [1]. Theoretically, such measurements conducted isothermally at various temperatures combined with a measurement of expansitity at a single pressure are sufficient to define all states of interest here. In practice, however, the quantities required for calculation are the derivatives of the volume with respect to temperature or pressure. By virtue of the method of measurement, derivatives of volume with respect to pressure are believed to be known to a satisfactory degree of accuracy at all temperatures. It is clear, however, that the derivatives of volume with respect to temperature are specifically known only at one pressure, atmospheric pressure. At all elevated pressures expansivities must be deduced from compression measurements and are therefore subject to all the errors included in the compression measurements. The expansivities are consequently subject to some uncertainty and any calculations dependent on the expansivities must not be considered as numerically much more significant than for order of magnitude.

It was hoped that the empirical PVT equations derived [1] would suffice for the calculations described here and thereby reduce the calculations to ordinary mathematical manipulations. This expectation was not realized and all data to be presented were obtained by graphical methods. The fact that the empirical equations may not be used in such calculations does not reflect doubt on the validity of the equations because they were derived to reproduce only the volume at various pressures and temperatures. There is no a priori reasoning that predicts that such empirical equations should also reproduce the slopes of the isobars or isotherms.

From the tabulated volume changes and volumes at 21° C given earlier [1] and the expansivities derived from the data of Scott [4], the specific volume was calculated at every pressure and temperature measured. From the tabular data, isobars were drawn to a large scale at every 1,000 atm. Typical isobars of this nature have been given earlier [2]. The isobars may be considered as linear within the experimental error of the measurements and from the straight lines drawn through the experimental points, the specific volume was tabulated at 10-deg intervals.

Calculations are given here for three rubbers containing 10, 18, and 28 percent of sulfur. The sulfur contents indicated correspond to the amounts added in the milling operation [1]. Vulcanization was effected at 140° C for 17 hr. The first of these compounds is soft and the last one is hard at all temperatures studied; the 18-percent-sulfur vulcanizate exhibits a glass transition at approximately 48° C. For the 10- and 28-percent-sulfur vulcanizates, therefore, the linear isobars are well defined

[1] The work described in this report was sponsored by the Office of Naval Research.

[2] Figures in brackets indicate the literature references at the end of this paper.

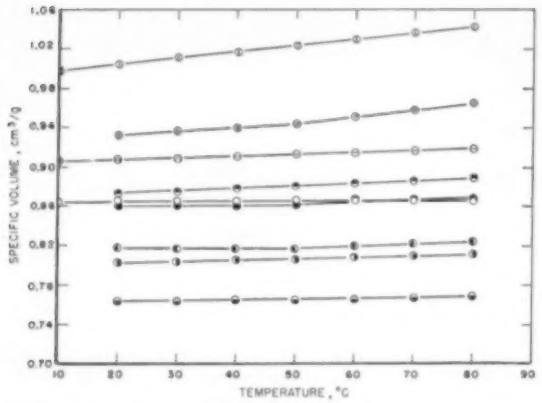


FIGURE 1. *Typical isobars of rubber-sulfur vulcanizates.*

10 percent of sulfur: ⊖, 1 atm; ⊖, 5,000 atm; ○, 10,000 atm.
18 percent of sulfur: ⊖, 1 atm; ●, 5,000 atm; ◐, 10,000 atm.
28 percent of sulfur: ◓, 1 atm; ◑, 5,000 atm; ◒, 10,000 atm.

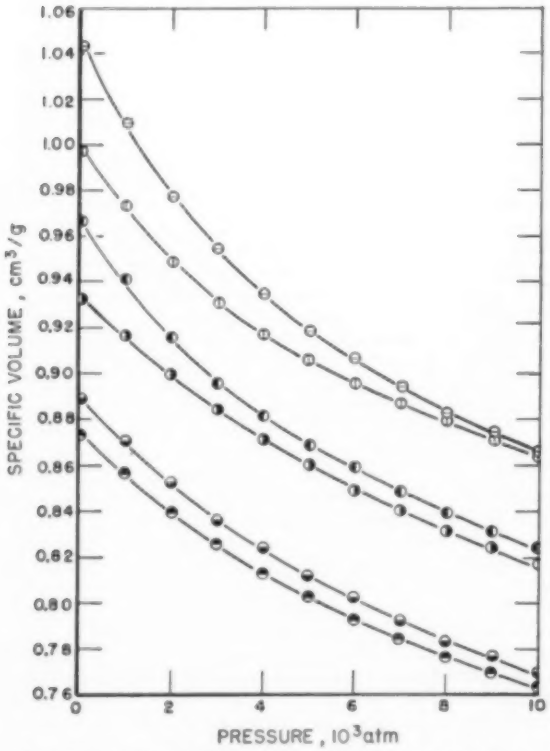


FIGURE 2. *Typical isotherms of rubber-sulfur vulcanizates.*

10 percent of sulfur: ⊖, 80° C; ⊖, 10° C.
18 percent of sulfur: ◐, 80° C; ◑, 20° C.
28 percent of sulfur: ◒, 80° C; ◓, 20° C.

because all experimental points may be considered in drawing the isobars. For the 18-percent-sulfur vulcanizate, two intersecting lines were drawn; the slopes of these lines are not as well defined because fewer experimental points determine each line. The glass transition temperature, $T_g$, is taken to be the temperature at which these lines intersect. The tabular specific volumes obtained in this manner are given in tables 1 to 3, inclusive. All subsequent calculated values are derived directly from the data of these tables.

The expansivities indicated in table 3 are observed to vary with pressure in accordance with the findings of Bridgman [3] on liquids. In tables 1 and 2, it is very probable that the pressure dependence of expansivity is somewhat too large. This conclusion results directly from the experimental data, which if taken literally indicate a *negative* expansivity in some instances at high pressures at the lower temperatures. This negative expansivity may be real (see Bridgman [3]); but since the experimental errors are such as to cause doubt as to its validity, the linear isobars were drawn so as to always show a positive expansivity. However, the value of expansivity thus obtained is lowered by the influence of the points contributing the negative expansivity. In this connection, it may be pointed out that the empirical equations previously derived [1] will also yield negative expansivities in certain ranges of pressure and temperature because they fit the experimental data quite well. This factor represents the principal reason why the equations were not considered suited for these calculations.

Typical specific volume-temperature and specific volume-pressure relationships are shown in figures 1 and 2.

Compressibilities to be used were also calculated directly from the data of tables 1 to 3 by means of first differences. The values so obtained appear as accurate and consistent as two graphical methods that were attempted.

All calculations were performed in experimental units of cm³-atm. The final results were then converted into joules, using the conversion relationship 1j = 9.869 cm³-atm.

TABLE 1. *Specific volumes of rubber-sulfur vulcanizate containing 10 percent of sulfur*

| Pressure | Specific volume at— | | | | | | | |
|---|---|---|---|---|---|---|---|---|
| | 10° C | 20° C | 30° C | 40° C | 50° C | 60° C | 70° C | 80° C |
| *atm* | *cm³/g* | *cm³/g* | *cm³/g* | *cm³/g* | *cm³/g* | *cm³/g* | *cm³/g* | *cm³/g* |
| 1 | 0.9975 | 1.0041 | 1.0106 | 1.0172 | 1.0237 | 1.0300 | 1.0365 | 1.0430 |
| 1,000 | .9732 | .9785 | .9836 | .9890 | .9940 | .9992 | 1.0043 | 1.0094 |
| 2,000 | .9485 | .9527 | .9570 | .9611 | .9652 | .9694 | .9735 | .9775 |
| 3,000 | .9303 | .9338 | .9373 | .9407 | .9442 | .9477 | .9511 | .9545 |
| 4,000 | .9170 | .9196 | .9221 | .9246 | .9270 | .9295 | .9320 | .9345 |
| 5,000 | .9060 | .9078 | .9096 | .9114 | .9132 | .9150 | .9166 | .9184 |
| 6,000 | .8960 | .8975 | .8990 | .9006 | .9021 | .9035 | .9050 | .9065 |
| 7,000 | .8875 | .8886 | .8896 | .8906 | .8916 | .8925 | .8934 | .8943 |
| 8,000 | .8797 | .8802 | .8806 | .8810 | .8814 | .8818 | .8822 | .8826 |
| 9,000 | .8725 | .8727 | .8730 | .8733 | .8736 | .8738 | .8740 | .8743 |
| 10,000 | .8648 | .8649 | .8650 | .8651 | .8652 | .8653 | .8654 | .8655 |

TABLE 2. *Specific volumes of rubber-sulfur vulcanizate containing 18 percent of sulfur*

| Pressure | Specific volume at— | | | | | | |
|---|---|---|---|---|---|---|---|
| | 20° C | 30° C | 40° C | 50° C | 60° C | 70° C | 80° C |
| *atm* | *cm³/g* | *cm³/g* | *cm³/g* | *cm³/g* | *cm³/g* | *cm³/g* | *cm³/g* |
| 1 | 0.9324 | 0.9392 | 0.9460 | 0.9444 | 0.9518 | 0.9592 | 0.9666 |
| 1,000 | .9163 | .9176 | .9199 | .9227 | .9288 | .9349 | .9410 |
| 2,000 | .8994 | .9000 | .9005 | .9015 | .9060 | .9106 | .9152 |
| 3,000 | .8842 | .8846 | .8850 | .8856 | .8889 | .8923 | .8956 |
| 4,000 | .8711 | .8715 | .8719 | .8724 | .8755 | .8782 | .8810 |
| 5,000 | .8599 | .8602 | .8604 | .8606 | .8634 | .8661 | .8689 |
| 6,000 | .8490 | .8494 | .8498 | .8505 | .8534 | .8563 | .8592 |
| 7,000 | .8402 | .8405 | .8408 | .8413 | .8438 | .8465 | .8490 |
| 8,000 | .8320 | .8321 | .8321 | .8322 | .8345 | .8369 | .8393 |
| 9,000 | .8249 | .8252 | .8253 | .8255 | .8274 | .8297 | .8320 |
| 10,000 | .8179 | .8171 | .8172 | .8176 | .8200 | .8224 | .8246 |

TABLE 3. *Specific volumes of rubber-sulfur vulcanizate containing 28 percent of sulfur*

| Pressure | Specific volume at— | | | | | | |
|---|---|---|---|---|---|---|---|
| | 20° C | 30° C | 40° C | 50° C | 60° C | 70° C | 80° C |
| *atm* | *cm³/g* | *cm³/g* | *cm³/g* | *cm³/g* | *cm³/g* | *cm³/g* | *cm³/g* |
| 1 | 0.8730 | 0.8758 | 0.8786 | 0.8814 | 0.8840 | 0.8867 | 0.8895 |
| 1,000 | .8563 | .8588 | .8613 | .8637 | .8660 | .8683 | .8706 |
| 2,000 | .8400 | .8422 | .8444 | .8468 | .8485 | .8505 | .8525 |
| 3,000 | .8260 | .8277 | .8295 | .8310 | .8326 | .8343 | .8359 |
| 4,000 | .8130 | .8149 | .8168 | .8187 | .8205 | .8223 | .8240 |
| 5,000 | .8029 | .8045 | .8060 | .8075 | .8090 | .8105 | .8120 |
| 6,000 | .7931 | .7948 | .7964 | .7980 | .7996 | .8012 | .8027 |
| 7,000 | .7842 | .7860 | .7873 | .7886 | .7900 | .7913 | .7925 |
| 8,000 | .7761 | .7774 | .7786 | .7798 | .7810 | .7822 | .7834 |
| 9,000 | .7697 | .7710 | .7722 | .7733 | .7745 | .7757 | .7768 |
| 10,000 | .7628 | .7639 | .7650 | .7660 | .7671 | .7683 | .7694 |

## 3. Work of Compression

The work of compression defined as

$$W = \int_{P_1}^{P_2} P \left(\frac{\partial V}{\partial P}\right)_T dP$$

was calculated by graphical integration of the pressure-volume data of tables 1 to 3 by mechanical methods. The values obtained are given in tables 4 to 6. These data represent work done on the specimen by the external compressive forces. The work is observed to be only slightly affected by temperature, but strongly pressure dependent. Graphs of work as a function of pressure show the approximate linearity at high pressures noted by Bridgman [3]. It would appear from these data, however, that too much curvature still exists to permit successful use of a linear relationship for extrapolation [3]. The work of compression decreases with increasing sulfur content as expected. Such decrease is due directly to the lower compressibility of the higher sulfur content rubbers. It is to be noted that mathematical integrations of the appropriate partial derivatives of the empirical equations [1] yield results in good agreement with the data of tables 4 to 6 that were obtained graphically. Thus the empirical equations may be considered to represent both the compressibility and the temperature dependence of the compressibility fairly closly. It will also be noted in table 5 that no discontinuity in the work of compression occurs at $T_g$. This result follows directly from the previous report [2] in which no discontinuity in $(\partial V/\partial P)_T$ was observed at $T_g$.

TABLE 4. *Work of compression of rubber-sulfur vulcanizate containing 10 percent of sulfur*

| Pressure, $P$ | Work of compression between 1 atm and $P$ at— | | | | | | | |
|---|---|---|---|---|---|---|---|---|
| | 10° C | 20° C | 30° C | 40° C | 50° C | 60° C | 70° C | 80° C |
| *atm* | *j/g* | *j/g* | *j/g* | *j/g* | *j/g* | *j/g* | *j/g* | *j/g* |
| 1,000 | 1.4 | 1.4 | 1.4 | 1.4 | 1.5 | 1.5 | 1.6 | 1.6 |
| 2,000 | 4.8 | 5.0 | 5.3 | 5.4 | 5.6 | 5.7 | 5.8 | 6.2 |
| 3,000 | 9.5 | 9.7 | 10.6 | 11.0 | 11.4 | 11.8 | 12.2 | 12.7 |
| 4,000 | 14.1 | 14.7 | 15.9 | 16.6 | 17.8 | 18.2 | 18.8 | 19.7 |
| 5,000 | 19.1 | 19.9 | 21.4 | 22.6 | 23.8 | 24.5 | 25.7 | 26.9 |
| 6,000 | 24.7 | 25.6 | 27.5 | 28.6 | 30.2 | 31.3 | 32.5 | 33.9 |
| 7,000 | 30.3 | 31.6 | 33.8 | 35.2 | 36.9 | 38.0 | 39.6 | 41.2 |
| 8,000 | 36.4 | 37.8 | 40.1 | 41.6 | 43.9 | 44.8 | 47.0 | 49.0 |
| 9,000 | 42.8 | 44.7 | 47.5 | 48.9 | 51.7 | 52.9 | 55.2 | 57.7 |
| 10,000 | 50.0 | 52.0 | 55.2 | 56.6 | 59.7 | 61.0 | 63.8 | 65.5 |

TABLE 5. *Work of compression of rubber-sulfur vulcanizate containing 18 percent of sulfur*

| Pressure, $P$ | Work of compression between 1 atm and $P$ at— | | | | | | |
|---|---|---|---|---|---|---|---|
| | 20° C | 30° C | 40° C | 50° C | 60° C | 70° C | 80° C |
| *atm* | *j/g* | *j/g* | *j/g* | *j/g* | *j/g* | *j/g* | *j/g* |
| 1,000 | 1.0 | 1.0 | 1.1 | 1.3 | 1.4 | 1.4 | 1.4 |
| 2,000 | 3.4 | 3.5 | 3.6 | 4.1 | 4.1 | 4.2 | 5.8 |
| 3,000 | 7.2 | 7.3 | 7.8 | 8.0 | 7.9 | 8.0 | 10.6 |
| 4,000 | 11.8 | 11.9 | 12.1 | 12.8 | 12.6 | 12.8 | 16.5 |
| 5,000 | 17.0 | 17.4 | 17.5 | 18.2 | 17.9 | 18.1 | 22.6 |
| 6,000 | 22.9 | 23.2 | 23.3 | 23.9 | 23.9 | 23.9 | 28.6 |
| 7,000 | 28.7 | 29.1 | 29.3 | 30.0 | 30.3 | 29.9 | 35.0 |
| 8,000 | 35.1 | 35.3 | 35.5 | 36.2 | 36.9 | 36.8 | 42.2 |
| 9,000 | 41.5 | 42.1 | 42.2 | 43.0 | 44.0 | 43.8 | 49.3 |
| 10,000 | 48.2 | 49.2 | 49.4 | 50.1 | 51.6 | 51.5 | 56.7 |

TABLE 6. *Work of compression of rubber-sulfur vulcanizate containing 28 percent of sulfur*

| Pressure, $P$ | Work of compression between 1 atm and $P$ at— | | | | | | |
|---|---|---|---|---|---|---|---|
| | 20° C | 30° C | 40° C | 50° C | 60° C | 70° C | 80° C |
| *atm* | *j/g* | *j/g* | *j/g* | *j/g* | *j/g* | *j/g* | *j/g* |
| 1,000 | 0.9 | 0.9 | 1.0 | 0.9 | 1.0 | 1.0 | 1.0 |
| 2,000 | 3.3 | 3.6 | 3.6 | 3.6 | 3.7 | 3.7 | 3.8 |
| 3,000 | 7.0 | 7.3 | 7.4 | 7.5 | 7.6 | 7.8 | 7.9 |
| 4,000 | 11.5 | 11.8 | 11.8 | 12.2 | 12.3 | 12.4 | 12.3 |
| 5,000 | 16.5 | 16.8 | 16.9 | 17.3 | 17.4 | 17.4 | 17.8 |
| 6,000 | 21.9 | 22.4 | 22.6 | 22.9 | 23.3 | 23.4 | 23.5 |
| 7,000 | 27.8 | 28.2 | 28.5 | 28.9 | 29.4 | 29.4 | 29.5 |
| 8,000 | 33.7 | 34.2 | 34.5 | 35.1 | 35.6 | 35.6 | 35.9 |
| 9,000 | 39.9 | 40.6 | 40.9 | 41.6 | 42.4 | 42.4 | 42.9 |
| 10,000 | 46.4 | 47.4 | 48.0 | 48.7 | 49.7 | 49.8 | 50.3 |

## 4. Heat of Compression

The heat of compression defined as

$$Q = -T \int_{P_1}^{P_2} \left(\frac{\partial V}{\partial T}\right)_P dP$$

was calculated by graphical integration of a graph of $T(\partial V/\partial T)_P$ versus $P$ by mechanical methods.

The values so obtained are given in tables 7 to 9. These data, which are all intrinsically negative, represent the heat given off by the specimens when compressed. As noted previously, the expansivities are not known to a high accuracy and the data of tables 7 to 9 must not be interpreted too literally. In particular, the apparent excessive decrease of expansivity with increasing pressure is responsible for the low values of heat shown in table 8 at low pressures. The marked increase of heat also ob-

TABLE 7. *Heat of compression of rubber-sulfur vulcanizate containing 10 percent of sulfur*

| Pressure, $P$ | Heat of compression between 1 atm and $P$ at— | | | | | | | |
|---|---|---|---|---|---|---|---|---|
| | 10° C | 20° C | 30° C | 40° C | 50° C | 60° C | 70° C | 80° C |
| *atm* | *j/g* | *j/g* | *j/g* | *j/g* | *j/g* | *j/g* | *j/g* | *j/g* |
| 1,000 | 17.1 | 18.0 | 18.7 | 19.4 | 20.0 | 20.6 | 21.3 | 22.0 |
| 2,000 | 31.1 | 32.4 | 33.7 | 34.8 | 36.0 | 37.3 | 38.5 | 39.7 |
| 3,000 | 42.0 | 43.8 | 45.6 | 46.9 | 48.5 | 50.2 | 51.7 | 53.3 |
| 4,000 | 50.2 | 52.3 | 54.5 | 56.4 | 58.2 | 60.2 | 62.0 | 63.9 |
| 5,000 | 56.3 | 58.5 | 61.1 | 63.4 | 65.4 | 67.6 | 69.7 | 71.9 |
| 6,000 | 60.8 | 63.3 | 65.9 | 68.5 | 70.7 | 73.0 | 75.4 | 77.8 |
| 7,000 | 63.9 | 66.6 | 69.4 | 72.2 | 74.6 | 77.0 | 79.6 | 82.1 |
| 8,000 | 66.0 | 68.9 | 71.9 | 74.8 | 77.4 | 81.5 | 84.2 | 87.0 |
| 9,000 | 67.3 | 70.3 | 73.5 | 76.4 | 79.3 | 83.4 | 86.4 | 89.3 |
| 10,000 | 67.9 | 70.9 | 74.1 | 77.1 | 80.0 | 84.2 | 87.1 | 90.1 |

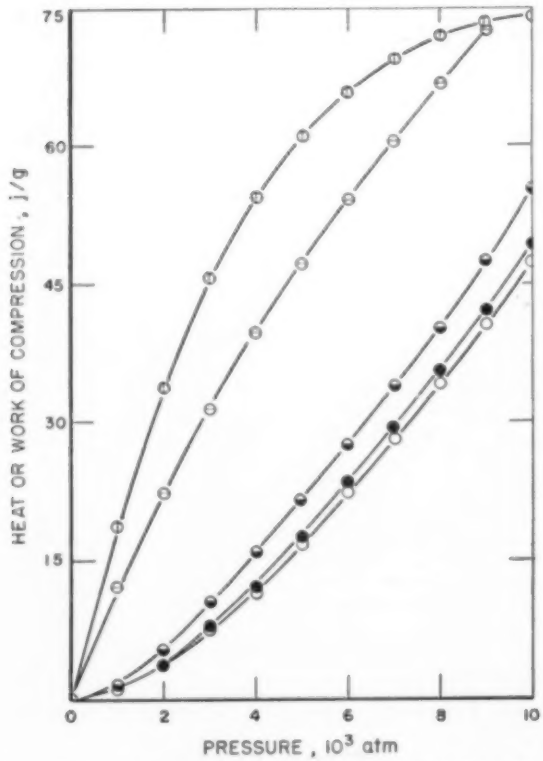


FIGURE 3. *Work and heat of compression of rubber-sulfur vulcanizates at 30° C.*

10 percent of sulfur: ⓘ, heat of compression; ◒, work of compression.
18 percent of sulfur: ●, work of compression.
28 percent of sulfur: ⊖, heat of compression; ○, work of compression.

TABLE 8. *Heat of compression of rubber-sulfur vulcanizate containing 18 percent of sulfur*

| Pressure, $P$ | Heat of compression between 1 atm and $P$ at— | | | | | | |
|---|---|---|---|---|---|---|---|
| | 20° C | 30° C | 40° C | 50° C | 60° C | 70° C | 80° C |
| *atm* | *j/g* | *j/g* | *j/g* | *j/g* | *j/g* | *j/g* | *j/g* |
| 1,000 | 7.0 | 7.1 | 7.4 | 20.8 | 21.6 | 22.2 | 22.7 |
| 2,000 | 9.8 | 10.1 | 10.6 | 36.6 | 38.0 | 39.2 | 40.2 |
| 3,000 | 11.4 | 11.8 | 12.3 | 49.2 | 51.4 | 53.2 | 54.7 |
| 4,000 | 12.5 | 13.1 | 13.6 | 59.6 | 62.4 | 64.8 | 66.9 |
| 5,000 | 13.1 | 13.8 | 14.3 | 69.0 | 72.4 | 75.3 | 78.0 |
| 6,000 | 13.6 | 14.6 | 15.0 | 77.5 | 81.4 | 85.0 | 88.2 |
| 7,000 | 14.1 | 15.1 | 15.6 | 85.8 | 90.4 | 94.4 | 97.9 |
| 8,000 | 14.6 | 15.7 | 16.2 | 93.9 | 99.0 | 103.5 | 107.3 |
| 9,000 | 15.0 | 16.2 | 16.6 | 101.4 | 107.4 | 112.3 | 116.1 |
| 10,000 | 15.4 | 16.6 | 17.0 | 109.4 | 115.8 | 121.2 | 124.9 |

TABLE 9. *Heat of compression of rubber-sulfur vulcanizate containing 28 percent of sulfur*

| Pressure, $P$ | Heat of compression between 1 atm and $P$ at— | | | | | | |
|---|---|---|---|---|---|---|---|
| | 20° C | 30° C | 40° C | 50° C | 60° C | 70° C | 80° C |
| *atm* | *j/g* | *j/g* | *j/g* | *j/g* | *j/g* | *j/g* | *j/g* |
| 1,000 | 11.6 | 12.0 | 12.5 | 13.0 | 13.4 | 13.6 | 14.0 |
| 2,000 | 21.5 | 22.3 | 23.2 | 24.0 | 24.7 | 25.3 | 26.0 |
| 3,000 | 30.2 | 31.4 | 32.5 | 33.7 | 34.7 | 35.6 | 36.6 |
| 4,000 | 38.0 | 39.6 | 41.0 | 42.5 | 43.8 | 44.9 | 46.2 |
| 5,000 | 45.3 | 47.1 | 48.9 | 50.6 | 52.1 | 53.6 | 55.1 |
| 6,000 | 52.1 | 54.2 | 56.2 | 58.1 | 59.9 | 61.6 | 63.4 |
| 7,000 | 58.5 | 60.7 | 62.9 | 65.1 | 67.1 | 69.0 | 71.1 |
| 8,000 | 64.5 | 66.9 | 69.3 | 71.6 | 73.9 | 76.0 | 78.3 |
| 9,000 | 70.2 | 72.6 | 75.2 | 77.7 | 80.2 | 82.6 | 85.1 |
| 10,000 | 75.5 | 78.1 | 80.6 | 83.3 | 86.0 | 88.7 | 91.5 |

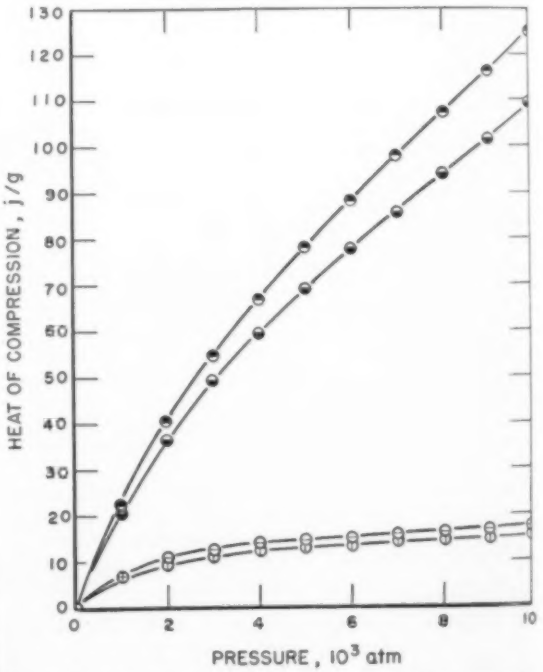


FIGURE 4. *Heat of compression of rubber-sulfur vulcanizate containing 18 percent of sulfur.*

◓, 80° C; ◒, 50° C; ⊖, 40° C; ⓘ, 20° C.

served in table 8 at temperatures above $T_g$ is real and follows necessarily from the increased expansivity above $T_g$.

Typical data for work and heat of compression are shown in figures 3 and 4.

## 5. Internal Energy Change on Compression

The internal energy change on compression is obtained by subtracting corresponding values of heat of compression from work of compression, considering both values as intrinsically positive. The results obtained are shown in tables 10 to 12. Any discrepancies noted in results obtained from subtracting data given here in tables 4 to 6 and 7 to 9 with the data of tables 10 to 12 arises from the fact that all calculations were performed initially in experimental units of $cm^3$-atm/g before converting to the units reported here. Considering first the results of tables 10 and 12, which may be considered to be essentially numerically correct for reasons discussed earlier, it is noted that on isothermal compression the internal energy initially decreases and at an elevated pressure starts to increase with increasing pressure. This behavior has been noted by Bridgman [3], who has offered the explanation that under ordinary conditions the molecular forces are predominately attractive so that on compression the heat liberated initially overcompensates the work performed on compression. At some elevated pressure, however, this process must reverse because the forces must ultimately become repulsive. Therefore, it is to be expected that at some pressure above the experimental range, the internal energy change will reverse sign and become positive. This pressure of reversal cannot be reliably estimated on the basis of these data. It is to be noted, however, that the pressure of reversal on the basis of these data increases with increasing temperature as required by Bridgman's [3] explanation and also increases with increasing hardness of rubber. The data of table 11 are more interesting. The marked change in internal energy change on passing through the thermal transition is to be noted. This change, while numerically uncertain, is of unquestionable validity since $(\partial V/\partial T)_P$ changes markedly at $T_g$, whereas $(\partial V/\partial P)_T$ does not. The low pressure at which the internal energy change reverses sign at

TABLE 10. *Change in internal energy on compression of rubber-sulfur vulcanizate containing 10 percent of sulfur*

| Pressure, $P$ | Change in internal energy between 1 atm and $P$ at— | | | | | | | |
|---|---|---|---|---|---|---|---|---|
| | 10° C | 20° C | 30° C | 40° C | 50° C | 60° C | 70° C | 80° C |
| *atm* | *j/g* | *j/g* | *j/g* | *j/g* | *j/g* | *j/g* | *j/g* | *j/g* |
| 1,000 | −15.8 | −16.6 | −17.2 | −17.9 | −18.4 | −20.2 | −19.8 | −20.4 |
| 2,000 | −26.2 | −27.4 | −28.4 | −29.3 | −30.4 | −31.6 | −32.6 | −33.4 |
| 3,000 | −32.5 | −34.0 | −34.8 | −36.0 | −37.1 | −38.4 | −39.5 | −40.6 |
| 4,000 | −36.2 | −37.6 | −38.6 | −39.8 | −40.4 | −42.0 | −43.3 | −44.2 |
| 5,000 | −37.3 | −38.7 | −39.7 | −40.8 | −41.7 | −43.1 | −44.0 | −45.0 |
| 6,000 | −36.2 | −37.7 | −38.4 | −39.8 | −40.5 | −41.6 | −42.9 | −43.9 |
| 7,000 | −33.6 | −35.2 | −35.6 | −37.0 | −37.7 | −38.9 | −40.0 | −40.9 |
| 8,000 | −29.6 | −31.1 | −31.8 | −33.1 | −33.4 | −36.7 | −37.2 | −37.9 |
| 9,000 | −24.4 | −25.6 | −26.1 | −27.6 | −27.6 | −30.6 | −31.2 | −31.5 |
| 10,000 | −17.8 | −18.9 | −19.0 | −20.5 | −20.3 | −23.2 | −23.3 | −23.6 |

TABLE 11. *Change in internal energy on compression of rubber-sulfur vulcanizate containing 18 percent of sulfur*

| Pressure, $P$ | Change in internal energy between 1 atm and $P$ at— | | | | | | |
|---|---|---|---|---|---|---|---|
| | 20° C | 30° C | 40° C | 50° C | 60° C | 70° C | 80° C |
| *atm* | *j/g* | *j/g* | *j/g* | *j/g* | *j/g* | *j/g* | *j/g* |
| 1,000 | −6.0 | −6.1 | −6.3 | −19.5 | −20.3 | −20.8 | −21.4 |
| 2,000 | −6.7 | −6.6 | −6.9 | −32.5 | −33.9 | −34.9 | −34.4 |
| 3,000 | −4.2 | −4.5 | −4.4 | −41.2 | −43.4 | −45.1 | −44.1 |
| 4,000 | −0.7 | −1.2 | −1.5 | −46.8 | −49.8 | −52.0 | −50.5 |
| 5,000 | +3.9 | +3.5 | +3.2 | −50.8 | −54.4 | −57.2 | −55.4 |
| 6,000 | +9.2 | +8.6 | +8.3 | −53.6 | −57.6 | −61.2 | −59.6 |
| 7,000 | +14.6 | +14.0 | +13.8 | −55.8 | −60.1 | −64.6 | −62.9 |
| 8,000 | +20.5 | +19.6 | +19.3 | −57.6 | −62.2 | −66.7 | −65.1 |
| 9,000 | +26.5 | +25.9 | +25.6 | −58.4 | −63.4 | −68.5 | −66.8 |
| 10,000 | +32.9 | +31.6 | +32.3 | −59.3 | −64.3 | −70.7 | −68.2 |

TABLE 12. *Change in internal energy on compression of rubber-sulfur vulcanizate containing 28 percent of sulfur*

| Pressure, $P$ | Change in internal energy between 1 atm and $P$ at— | | | | | | |
|---|---|---|---|---|---|---|---|
| | 20° C | 30° C | 40° C | 50° C | 60° C | 70° C | 80° C |
| *atm* | *j/g* | *j/g* | *j/g* | *j/g* | *j/g* | *j/g* | *j/g* |
| 1,000 | −10.6 | −11.1 | −11.6 | −12.0 | −12.4 | −12.6 | −13.0 |
| 2,000 | −18.2 | −18.7 | −19.8 | −20.5 | −21.1 | −21.5 | −22.2 |
| 3,000 | −23.1 | −24.1 | −25.1 | −26.2 | −27.0 | −27.8 | −28.7 |
| 4,000 | −26.4 | −27.7 | −29.2 | −30.4 | −31.4 | −32.5 | −33.9 |
| 5,000 | −28.9 | −30.3 | −31.9 | −33.2 | −34.7 | −36.2 | −37.3 |
| 6,000 | −30.7 | −31.6 | −33.5 | −35.2 | −36.6 | −38.2 | −39.8 |
| 7,000 | −30.7 | −32.5 | −34.4 | −36.2 | −37.7 | −39.7 | −41.5 |
| 8,000 | −30.8 | −32.6 | −34.8 | −36.6 | −38.3 | −40.5 | −42.4 |
| 9,000 | −30.3 | −32.1 | −34.2 | −36.1 | −37.8 | −40.1 | −42.2 |
| 10,000 | −29.1 | −30.6 | −32.6 | −34.6 | −36.4 | −36.8 | −41.2 |

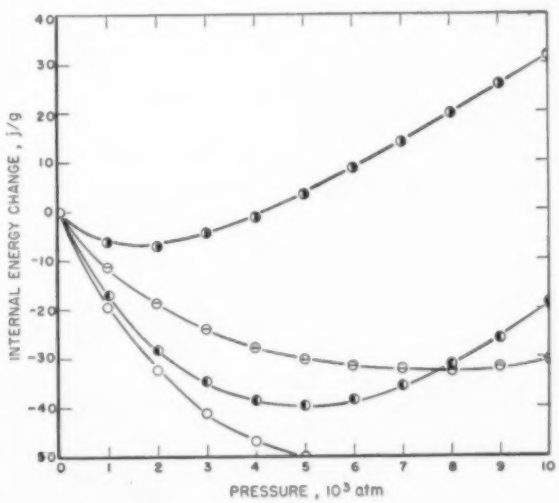


FIGURE 5. *Typical isothermal internal-energy-change behavior.*

10 percent of sulfur at 30° C, ◐.
18 percent of sulfur: ◑, 30° C; ○, 50° C.
28 percent of sulfur at 30° C, ⊖.

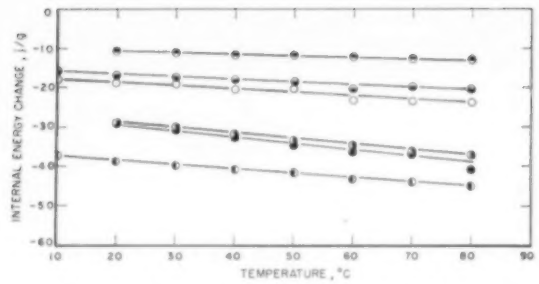


FIGURE 6. *Typical isobaric internal-energy-change behavior for low and high-sulfur contents.*

10 percent of sulfur: ◒, 1,000 atm; ◖, 5,000 atm; ○, 10,000 atm
28 percent of sulfur: ◓, 1,000 atm; ◗, 5,000 atm; ●, 10,000 atm

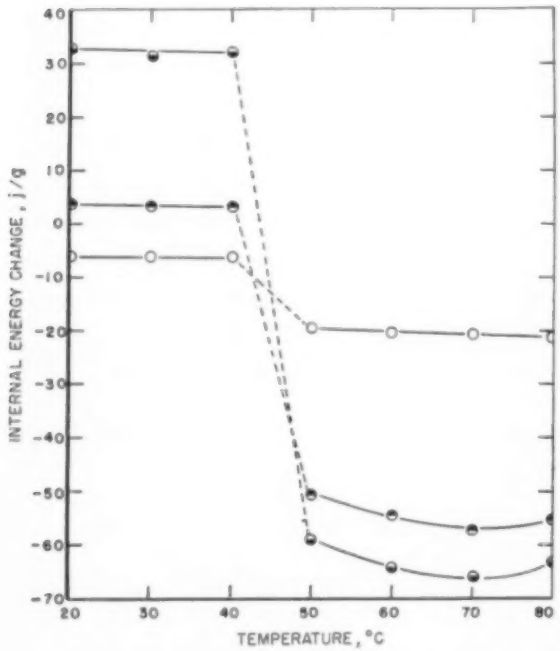


FIGURE 7. *Isobaric internal-energy-change behavior at intermediate sulfur content.*

18 percent of sulfur: ○, 1,000 atm; ◓, 5,000 atm; ◒, 10,000 atm.

the lower temperatures is highly suspect as mentioned previously as the expansivities in this region of temperature appeared to possess anomalously high pressure dependence. There is no doubt, however, that at temperatures below $T_g$ the internal energy change reverses sign at a lower pressure than at temperatures above $T_g$. This result also must arise by virtue of the change in $(\partial V/\partial T)_P$ at $T_g$.

Typical data for internal energy change are shown in figures 5, 6, and 7.

## 6. Change in Heat Capacity

The change in heat capacity with pressure may be calculated from the relationship $(\partial C_P/\partial P)_T = -T(\partial^2 V/\partial T^2)_P$. Because it was previously assumed that $(\partial V/\partial T)_P$ was constant within experimental error, such calculations have no basis in fact in these experiments. It may be concluded with assurance that any change in $C_P$ with pressure is quite small.

The difference between heat capacities at constant pressure and constant volume may be evaluated from the relationship $C_P - C_V = -T(\partial V/\partial T)_P^2/(\partial V/\partial P)_T$ which involves only first derivatives. Full data for this difference are not given here. Partial results for two rubbers of interest are given in tables 13 and 14 in terms of specific heats. In table 13, the typical behavior is observed with the difference decreasing rapidly with increasing pressure and approaching a negligible value at high pressures. Isobarically little temperature dependence is noted which follows from the fact that the expansivity was taken as independent of temperature. In table 14, similar behavior is noted above or below $T_g$ but on passing through $T_g$ isobarically a marked change in $C_P - C_V$ is noted. This result is a direct consequence of the experimental finding that no appreciable change in compressibility occurs at $T_g$ that is analogous to the change in expansivity. The change in the difference between specific heats on passing through $T_g$ amounts to approximately 0.5 j/g. It is probably fortuitous that this figure agrees closely with the change in specific heat at constant pressure for natural rubber observed by Bekkedahl [5] on passing through $T_g$.

TABLE 13. *Difference in specific heats at constant pressure and constant volume for rubber-sulfur vulcanizate containing 10 percent of sulfur*

| Pressure | $C_P - C_V$, (j/g)/deg C | | | | | | | |
|---|---|---|---|---|---|---|---|---|
| | 10° C | 20° C | 30° C | 40° C | 50° C | 60° C | 70° C | 80° C |
| *atm* | | | | | | | | |
| 1 | 0.40 | 0.40 | 0.39 | 0.38 | 0.38 | 0.37 | 0.36 | 0.36 |
| 1,000 | .32 | .31 | .31 | .30 | .30 | .30 | .30 | .30 |
| 2,000 | .22 | .22 | .22 | .22 | .22 | .22 | .22 | .22 |
| 3,000 | .22 | .22 | .21 | .21 | .21 | .21 | .20 | .20 |
| 4,000 | .15 | .14 | .14 | .13 | .13 | .13 | .13 | .12 |
| 5,000 | .09 | .09 | .08 | .08 | .08 | .08 | .08 | .08 |

TABLE 14. *Difference in specific heats at constant pressure and constant volume for rubber-sulfur vulcanizate containing 18 percent of sulfur*

| Pressure | $C_P - C_V$, (j/g)/deg C | | | | | | |
|---|---|---|---|---|---|---|---|
| | 20° C | 30° C | 40° C | 50° C | 60° C | 70° C | 80° C |
| *atm* | | | | | | | |
| 1 | 0.22 | 0.20 | 0.21 | 0.70 | 0.69 | 0.67 | 0.66 |
| 1,000 | .03 | .03 | .03 | .56 | .55 | .53 | .52 |
| 2,000 | .01 | .01 | .01 | .37 | .35 | .34 | .33 |
| 3,000 | .00 | .00 | .00 | .24 | .24 | .23 | .23 |
| 4,000 | .00 | .00 | .00 | .20 | .21 | .21 | .21 |
| 5,000 | .00 | .00 | .00 | .23 | .24 | .25 | .26 |

If it is assumed that $C_P$ is not materially changed by increasing pressure, further conclusions may be drawn as shown in the following treatment.

It can be shown that the change in the difference of specific heats probably arises from a change in $C_P$ and not $C_V$ and that $C_V$ is, therefore, very probably unchanged on passing through $T_g$. To show this, the derivative of the difference of specific heats with respect to temperature is taken and is found to be equal to

$$\frac{\Delta(C_P-C_V)}{\Delta T}=(C_P-C_V)\left[\frac{1}{T}+2\left(\frac{\partial^2 V}{\partial T^2}\right)_P\Big/\left(\frac{\partial V}{\partial T}\right)_P-\left(\frac{\partial^2 V}{\partial P\partial T}\right)_{T,P}\Big/\left(\frac{\partial V}{\partial P}\right)_T\right].$$

On considering the terms in the bracket, it can be concluded that in a small temperature interval including $T_g$, $1/T$ is negligible. It has been shown [2] that the temperature coefficient of compressibility is small compared to the compressibility, so that the third term is also negligible. It is known, however, that the temperature coefficient of expansivity is large in this temperature interval so that the ratio of $(\partial^2 V/\partial T^2)/(\partial V/\partial T)$ is of the order of $\frac{1}{2}$ or $\frac{1}{3}$ in this interval. Therefore any change of $C_P-C_V$ on passing through $T_g$ arises predominantly from a change in expansivity. Because the basic distinction between $C_P$ and $C_V$ involves this expansivity, it follows that $C_V$ is most probably unaffected by passing through $T_g$, except for the normal small variation to be expected to arise from temperature changes alone. Although the suggested constancy of $C_V$ on passing through $T_g$ must have significance as regards the processes responsible for the changes at $T_g$, no possible explanations of this behavior can be proposed at this time.

Using the data presented, it is possible to calculate $C_V$ by means of the relationship

$$C_V\equiv\left(\frac{\partial E}{\partial T}\right)_V=\left(\frac{\partial E}{\partial T}\right)_P+\left(\frac{\partial E}{\partial P}\right)_T\left(\frac{\partial P}{\partial T}\right)_V,$$

where $E$ is the internal energy. All terms on the right side of this equation are obtainable from the present data. However, attempts to verify the suggested constancy of $C_V$ in passing through $T_g$, or to calculate $C_V$ for any specimen were unsuccessful. The reasons for this failure are to be attributed to the predominant effect of the expansivity integral in determining the values of $\Delta E$, and the expansivity itself in determining the values of $(\partial P/\partial T)_V$. As pointed out previously, the expansivity is not believed to be sufficiently well determined to justify reliance on the results of such calculations.

## 7. Pressure Coefficient

The pressure coefficient $-(\partial P/\partial T)_V$ may be calculated from the ratio of expansivity to compressibility. There seems little point in reproducing these values which are generally of the order of 10 to 20 atm per deg C. It is to be noted, however, that by virtue of the change in expansivity, the pressure coefficient is discontinuous at $T_g$. Sufficient data are presented here to permit the calculation of these values if they are of interest.

## 8. Discussion

The data presented for three typical rubbers of high sulfur content are believed to be representative of the $PVT$ data obtained here. Calculations of a similar nature have not been carried out on all samples tested due to the laborious nature of the calculations and the fact that the other samples yielded quite similar experimental results. The calculations described above have been carried through with one other rubber containing 22 percent of sulfur with results similar in all important respects to those obtained on the 18-percent-sulfur vulcanizate described here. Specific qualifications concerning the numerical accuracy of the data have been emphasized, but significant behavior of the calculated quantities has been shown to be a direct consequence of the experimental observations where $T_g$ is involved or to agree otherwise with the results obtained by Bridgman [3] for solids and liquids. While the general trends of most quantities reported are believed to be of interest, it would appear that the most significant result lies in the suggestion that $C_V$ very probably does not change discontinuously at $T_g$. Inasmuch as significant differences may exist in glass-transition temperatures found by Scott [4] and in the present data, it is planned to measure the specific volume—temperature relationships of the specimens used in these studies, using dilatometers at 1 atm and modifications of the present high pressure equipment at elevated pressures. The values so obtained will be used to recalculate portions of the data presented here. Any significant differences will be reported at a future date.

## 9. References


[1] C. E. Weir, J. Research NBS **50,** 3 (1953) RP2403.
[2] C. E. Weir, J. Research NBS **50,** 6 (1953) RP2421.
[3] P. W. Bridgman, The physics of high pressure (G. Bell & Sons, Ltd, London 1949).
[4] A. H. Scott, J. Research NBS **14,** 100 (1935) RP760.
[5] N. Bekkedahl and H. Matheson, J. Research NBS **15,** 503 (1935) RP844.



Washington, March 6, 1953.

...nal of Research of the National Bureau of Standards Vol. 50, No. 6, June 1953 Research Paper 2422

# Laboratory Measurement of the Corrosion of Ferrous Metals in Soils

W. J. Schwerdtfeger

A method is described for setting up soil-corrosion cells using a soil-wetting procedure that gives reproducible results. By measuring the weight losses on cell electrodes made of steel and of cast iron after exposure to various soils for 6 months, it was possible to compare the effects of corrosion on the two materials. It was also found that the electrode weight losses correlated with the weight losses and maximum pitting on wrought ferrous specimens exposed for 10 years at the field test sites. Because the laboratory soils covered the range of corrosivity peculiar to soils, it was possible to derive empirical equations for predicting weight loss and pitting at the end of 10 years for presumably any soil. It is also shown how reasonable adjustments can be made for areas other than that of the field specimens and for exposure periods other than 10 years.

## 1. Introduction

A review of the field corrosion data obtained by the National Bureau of Standards invariably results in the conclusion that no single soil property is a good measure of its corrosivity toward iron or steel. Because the normal corrosion of iron and steel underground is an electrolytic phenomenon, several accelerated laboratory and field tests based on electrical measurements have been devised that purport to measure the corrosivity of soils. Ewing [1][1] has pointed out that the majority of such tests in effect really measures soil resistivity. Whereas measurements of soil resistivity made along a pipe line might correlate very well with the evidence of corrosion on the surface of that particular pipe, it is also true that there is no general correlation between the corrosion of ferrous metal exposed to different soils and the soil resistivity.

Denison [2, 3] described a laboratory corrosion cell in which an electromotive force was developed by differential-aeration between two steel electrodes separated by soil as the electrolyte. The maximum current measured between the electrodes over a 2-week period was used as an index of soil corrosivity. A fair correlation was obtained between laboratory and field data except for the soils of relatively high resistivity. In such soils, because of local action, the anode weight losses were more significant than the cell currents as an index of soil corrosivity.

Logan, Ewing, and Denison [4] have shown by field exposure tests that the corrosion rate of iron and steel in soils varies from an almost constant rate with time in some soils to virtual cessation within a few years in other soils. Such information is of great value to those concerned with underground construction. The time required to conduct such tests in the field, however, is long, and the required information cannot be obtained, in many cases, when it is most needed. A suitable laboratory test using the soil in question and operating over a sufficiently long period to reflect any change in the rate of corrosion of iron and steel with time is most desirable. The data from such a test should be correlated with known field-exposure data so that the results can be correctly interpreted. The extensive field exposure tests of the National Bureau of Standards provide a considerable volume of data that can be used for this purpose.

The corrosion cell used for this investigation is a modification of the cell described by Denison. It lends itself to better reproducibility than the original cell and will remain operative for a longer period of time. Although electrical measurements can be made that account for all weight loss of steel exposed to soils [5], weight loss is used as the corrosion index, because electrical measurements would have to be made frequently to account for the change in corrosion rate with time.

## 2. Experimental Methods

### 2.1. Description of the Corrosion Cell

The corrosion cell and all of its components are shown in figure 1. The cell consists essentially of a weighed iron or steel anode, A, and a weighed perforated cathode, B, made of the same material, both provided with electrical connections and separated by soil of a definite moisture content. The soil is contained in two Lucite cylinders, C. Other parts of the cell that serve to hold the soil in place and thus insure good contact with the electrodes are two stainless-steel screens, D and E, the rubber stopper, H, and the rubber band, G. The components are joined with asphalt, F, which also serves as a sealer. Aeration of the cathode is accomplished by adjusting the moisture content of the soil, and access of air to the anode is restricted by mechanically working the layer of soil in contact with it, which results in a difference of potential between the electrodes. Details concerning the preparation of the cell are given in the appendix.

### 2.2. Use of the Corrosion Cell

The behavior of the corrosion cells in reflecting the effect of time on corrosion of iron or steel is illustrated by figure 2. The cell currents were measured with a zero-resistance milliammeter without permitting the cells to be on open circuit. The currents for each soil are the average values for four cells. It will be noted from the table in the figure

[1] Figures in brackets indicate the literature references at the end of this paper.

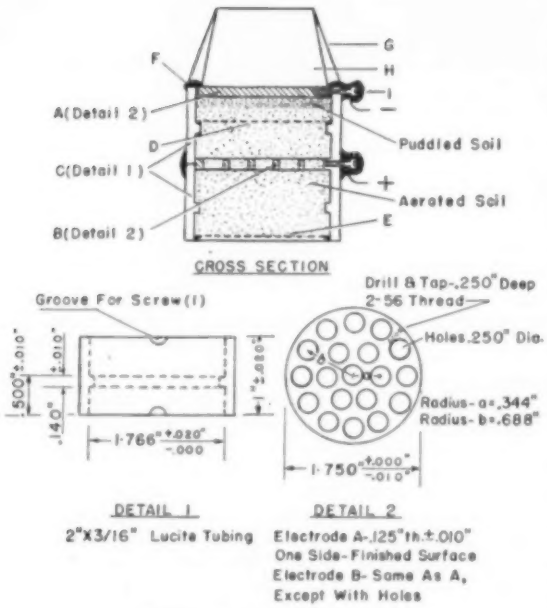


FIGURE 1. *Soil-corrosion cell.*

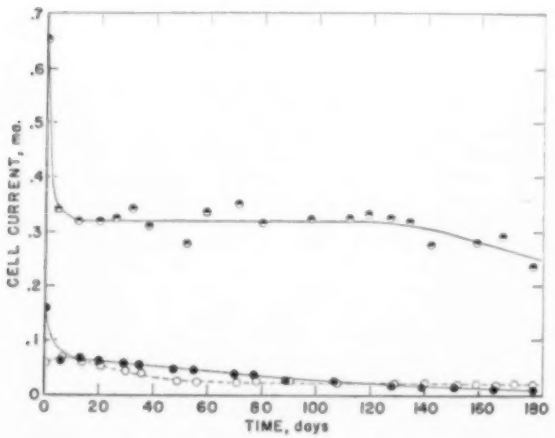


FIGURE 2. *Effect of exposure time on the corrosion of steel in soils.*

| Symbol | Soil | Resistivity | Cell current [1] | Weight loss of cell electrodes [2] | Corrosivity of soil [3] |
|---|---|---|---|---|---|
| | | *Ohm-cm* | *ma* | | |
| ◒ | 64 | 62 | 0.280 | 2.53 | Most. |
| ○ | 62 | 6922 | .030 | 1.05 | Intermediate. |
| ● | 26 | 2980 | .035 | 0.56 | Least. |

[1] Calculated from the area under a line through the points.
[2] Combined weight loss of the anode and cathode exposed for 180 days, in ounces per square foot.
[3] Order shown by the field-exposure tests.

that the electrode weight losses indicate the actual order of corrosivity of the soils, whereas the average cell currents in soils 62 and 26 are in reverse order because of the soil resistivities. However, based on field data of Denison and Romanoff [6] the curves do reflect the effect of time on the rate of corrosion of ferrous materials in the three soils. The field data reveal a fairly constant rate of corrosion of wrought materials exposed to soils 64 and 62 over a period of 14 years and a stifling effect in well-aerated soils similar to soil 26. It will be noted, figure 2, that in soil 26 the cell current gradually decreases, whereas in soils 64 and 62 after the initial decrease the currents are relatively steady.

As a result of this and other experiments, 6 months was chosen as the minimum time required for measuring soil corrosion. Although the laboratory results are based on the weight lost by the cell electrodes, the cell current serves to reveal the quality of a cell. If a diverse cell, indicated by incorrect polarity or relatively low current, exists in a particular soil group 2 weeks after assembly time, that cell should be replaced. Six months after assembly the corrosion cells are taken apart and the electrodes cleaned by methods [7] already described. The average combined loss of metal on the anodes and cathodes for the four cells is used as the corrosion index.

## 3. Comparison of the Corrosion of Steel and Cast Iron

### 3.1. Weight Loss in the Laboratory Tests

Although the laboratory corrosion test was planned primarily to show the relative effects of various soils on ferrous materials, to be shown later, the sensitivity of the test can be better evaluated if it is possible to detect differences in the corrodibility of commonly used plain ferrous materials when exposed to a given soil environment. To that end, corrosion cells were assembled with both steel and cast-iron electrodes,

TABLE 1. *Properties of the soils*

| Soil No.[a] | Soil Type | Soil Location of site | pH | Resistivity at 60 °F | Aeration [b] |
|---|---|---|---|---|---|
| | | | | *Ohm-cm* | |
| 4 | Chester loam | Jenkintown, Pa. | 5.6 | 6,670 | G |
| 5 | Dublin clay adobe | Oakland, Calif. | 7.0 | 1,346 | P |
| 8 | Fargo clay loam | Fargo, N. Dak. | 7.6 | 350 | P |
| 15 | Houston black clay | San Antonio, Tex. | 7.5 | 489 | P |
| 25 | Miami clay loam | Milwaukee, Wis. | 7.2 | 1,780 | F |
| 26 | Miami silt loam | Springfield, Ohio | 7.3 | 2,980 | G |
| 32 | Ontario loam | Rochester, N. Y. | 7.3 | 5,700 | G |
| 41 | Summit silt loam | Kansas City, Mo. | 5.5 | 1,320 | F |
| 43 | Tidal marsh | Elizabeth, N. J. | 3.1 | 60 | VP |
| 55 | Hagerstown loam | Lock Raven, Md. | 5.8 | 5,213 | G |
| 56 | Lake Charles clay | El Vista, Tex. | 7.1 | 406 | VP |
| 61 | Sharkey clay | New Orleans, La. | 5.9 | 943 | F |
| 62 | Susquehanna clay | Meridian, Miss. | 4.1 | 6,922 | F |
| 64 | Docas clay | Cholame, Calif. | 8.3 | 62 | F |
| 65 | Chino silt loam | Wilmington, Calif. | 7.2 | 148 | F |

[a] Soil number also refers to site number as specified in the NBS soil-corrosion studies.
[b] Aeration of soils: G, good; F, fair; P, poor; VP, very poor.

TABLE 2. *Comparison of the corrodibility of steel and cast iron in the laboratory*

| Soil | Loss in weight of cell electrodes in 6 months[a] | | | | | | | | | |
|---|---|---|---|---|---|---|---|---|---|---|
| | Steel[b] | | | Cast iron[c] | | | Difference between the means, $w_1-w_2$ | Standard[d] error of the difference, $\sigma_{(w_1-w_2)}$ | Value[e] of $t$ | Probability of difference due to chance |
| | Number of cells | Mean $w_1$ | Standard error, $\sigma_{w_1}$ | Number of cells | Mean $w_2$ | Standard error, $\sigma_{w_2}$ | | | | |
| | *oz/ft²* | *oz/ft²* | *oz/ft²* | *oz/ft²* | *oz/ft²* | *oz/ft²* | | | | *Percent* |
| 4 | 4 | 0.61 | 0.065 | 4 | 0.85 | 0.028 | −0.24 | 0.071 | 3.4 | <2 |
| 5 | 8 | 1.97 | .14 | 7 | 1.82 | .25 | +.15 | .29 | 0.5 | 60 |
| 8 | 4 | 0.89 | .045 | 6 | 1.46 | .13 | −.57 | .14 | 4.1 | <1 |
| 25 | 4 | .20 | .021 | 4 | 0.46 | .056 | −.26 | .060 | 4.3 | <1 |
| 26 | 4 | .56 | .049 | 4 | .65 | .037 | −.09 | .061 | 1.5 | 18 |
| 32 | 4 | .37 | .040 | 4 | .53 | .032 | −.16 | .051 | 3.1 | <2 |
| 43 | 4 | 1.36 | .18 | 4 | 3.40 | .16 | −2.04 | .24 | 8.5 | <1 |
| 56 | 4 | 2.17 | .072 | 4 | 2.33 | .11 | −0.16 | .13 | 1.2 | 30 |
| 62 | 4 | 1.05 | .098 | 4 | 1.79 | .081 | −.74 | .13 | 5.7 | <1 |
| 64 | 4 | 2.53 | .20 | 4 | 3.84 | .20 | −1.31 | .028 | 4.7 | <1 |

[a] Combined loss in weight of the anode and cathode. Area exposed, anode=2.4 in.² (15.5 cm²), cathode=3.3 in.² (21.3 cm.²)
[b] Composition of steel, in percent: 0.23 C, 0.58 Mn, 0.008 P, 0.025 S, 0.095 Si, 0.077 Cu.
[c] Composition of cast iron in percent: 3.42 C (total), 2.59 C (free), 0.83 C (combined), 1.53 Si, 0.72 P, 0.68 Mn, 0.082 S, 0.05 As.

[d] $\sigma_{(w_1-w_2)}=\sqrt{(\sigma_{w_1})^2+(\sigma_{w_2})^2}$ (See text)

[e] $t=\frac{w_1-w_2}{\sigma_{(w_1-w_2)}}$ (See text)

TABLE 3. *Comparison of steel and cast iron after 12 years of field exposure*

| Soil | Loss in weight of field specimens | | | | | | | | | |
|---|---|---|---|---|---|---|---|---|---|---|
| | Steel | | | Cast Iron | | | Difference between the means, $X_1-X_2$ | Standard error of the difference, $\sigma_{X_1-X_2}$ | Value of $t$ | Probability of difference due to chance |
| | Number of specimens | Mean $X_1$ | Standard error $\sigma_{X_1}$ | Number of specimens | Mean $X_2$ | Standard error $\sigma_{X_2}$ | | | | |
| | | *oz/ft²* | *oz/ft²* | | *oz/ft²* | *oz/ft²* | *oz/ft²* | *oz/ft²* | | *Percent* |
| 4 | 6 | 6.6 | 0.19 | 4 | 15.1 | 2.7 | −8.5 | 2.7 | 3.1 | <2 |
| 5 | 6 | 6.6 | .44 | 4 | 10.5 | 3.3 | −3.9 | 3.4 | 1.2 | 28 |
| 8 | 6 | 7.5 | .41 | 4 | 21.2 | 3.3 | −13.7 | 3.4 | 4.0 | <1 |
| 25 | 6 | 3.2 | .14 | 4 | 3.5 | .095 | −.3 | .14 | 2.1 | 5 |
| 26 | 6 | 3.6 | .14 | 4 | 4.1 | .11 | −.5 | .18 | 2.8 | <2 |
| 32 | 6 | 3.7 | .25 | 4 | 4.8 | .59 | −1.1 | .64 | 1.7 | 14 |
| 43 | 6 | 16.8 | 1.9 | 4 | 17.7 | 1.8 | −.9 | 2.6 | .3 | 70 |
| 56 * | 8 | 30.5 | 2.3 | 8 | 40.5 | 6.8 | −10.0 | 7.2 | 1.4 | 18 |
| 62 * | 8 | 6.9 | 1.0 | 8 | 5.9 | 1.1 | +1.0 | 1.5 | .6 | 55 |
| 64 * | 8 | 50.9 | 9.0 | 8 | 58.0 | 5.8 | −7.1 | 10.7 | .7 | 50 |

* Exposure 14 years.

using several soil samples collected at the test sites of the National Bureau of Standards and known to cover the range of corrosivity. The location of the test sites and some of the soil properties are given in table 1, along with other soils to be discussed later.

The results of the laboratory tests are given in table 2. In all of the soils, with the exception of soil 5, the steel electrodes were more resistant to corrosion than were the cast-iron electrodes. The significance of the difference indicated in the table is based on the standard $t$-test [8]. It will be noted that the better corrosion resistance exhibited by cast iron over steel in soil 5 may be attributed to chance.

### 3.2. Comparison of Laboratory and Field Data

A comparison of laboratory and field data pertaining to the corrosion of steel and cast iron is reasonable if the laboratory soil samples are representative of the soil in the trenches from which the field specimens were removed. The field data are shown in table 3. For all of the soils, except 56, 62, and 64, the data are based on weight losses reported by Logan [7] occurring on pipe specimens of Bessemer steel and on cast-iron pipe consisting of 2 de Lavaud specimens, 1 northern pit cast iron, and 1 southern pit cast-iron specimen. Data in table 3 pertaining to soils 56, 62, and 64, were reported by Denison and Romanoff [6].

In all soils (table 3) except soil 62, the steel specimens lost less weight than did the cast-iron specimens. The statistical significance of the difference in weight loss, as in the case of the laboratory comparison, is based on the $t$-test and, except in soils 62, 43, and 64, shows substantially the same results. For soils 43 and 62 the laboratory and field comparisons of the corrosion of steel and cast iron are inconclusive; and in the case of soil 64, the field data are so variable that any significant difference between the steel and cast iron is obscured. In soil 64, the standard errors applying to the laboratory data (table 2) are relatively small. Therefore, the laboratory results in soil 64 are to be taken as being the more significant.

The preponderance of negative values in column 8 of table 3 is not to be considered as indicating the relative behavior of the materials in soils generally.

## 4. Measurement of Soil Corrosivity

### 4.1. Correlation Between Laboratory and Field Weight Losses

In order to further evaluate the laboratory corrosion test as a measure of the relative corrosiveness of soils toward commonly used ferrous materials, the mean weight losses of steel electrodes after exposure for 6 months to the soils shown in table 1 were correlated with the average weight losses of other specimens exposed to the test sites for 10 years. The specimens at each test site totaled 8 in number and consisted of 2 of each of the following materials: Low-carbon steel, hand-puddled wrought iron, mechanically puddled wrought iron, and open-hearth iron.

In developing the laboratory test, the National Bureau of Standards was fortunate in having the cooperation of the Waterways Experiment Station, Corps of Engineers, U. S. Army. That laboratory followed the same procedure in measuring the corrosiveness of soils as described in section 2. The soil samples tested by the Waterways Experiment Station included 9 of the 10 soils studied by the National Bureau of Standards and in addition 5 soils removed from other National Bureau of Standards test sites. The 9 soils tested by both laboratories were not taken from the same samples but were removed from different parts of the trench at the 9 sites. Both laboratories used steel cell electrodes of the same chemical composition and dimensions. The composition and dimensions are given in table 2. The data obtained by both laboratories and the National Bureau of Standards field data are tabulated in table 4. Correlation between the laboratory and field weight losses is based on the text of Croxton and Cowden [8]. The coefficient of correlation between the National Bureau of Standards laboratory and field data is 0.84. The coefficient between the Waterways Experiment Station data and the National Bureau of Standards field data is 0.6, but by eliminating soil 64 the coefficient becomes 0.87.

TABLE 4. *Correlation between combined laboratory and National Bureau of Standards field data*

| Soil | Weight loss of steel electrodes after 6 months of laboratory exposure | | | Weight loss of wrought ferrous specimens after 10 years of field exposure | | Maximum pit depth on wrought ferrous specimens after 10 years of field exposure | |
|---|---|---|---|---|---|---|---|
| | National Bureau of Standards | Waterways Exp. tion | Average $w$ | Actual | Calculated $W_{10}$ | Actual | Calculated $P_{10}$ |
| | $oz/ft^2$ | $oz/ft^2$ | $oz/ft^2$ | $oz/ft^2$ | $oz/ft^2$ | *Mils* | *Mils* |
| 4 | 0.61 | 0.91 | 0.76 | 6.4 | 5.3 | 75 | 63 |
| 5 | 1.97 | 1.41 | 1.69 | 6.4 | * 13.2 | 50 | * 104 |
| 8 | .89 | | .89 | 5.5 | 6.4 | 79 | 69 |
| 15 | | 1.27 | 1.27 | 7.0 | 9.7 | 63 | 86 |
| 25 | .20 | .86 | .53 | 2.6 | 3.4 | 49 | 53 |
| 26 | .56 | .48 | .52 | 2.5 | 3.3 | 59 | 53 |
| 32 | .37 | .56 | .46 | 3.1 | 2.8 | 55 | 50 |
| 41 | | .32 | .32 | 6.1 | 1.6 | 64 | 44 |
| 43 | 1.36 | 2.18 | 1.77 | 12.6 | 13.9 | 112 | 108 |
| 55 | | .43 | .43 | 3.2 | 2.5 | 75 | 49 |
| 56 | 2.17 | 3.23 | 2.70 | 21.2 | 21.7 | 132 | 148 |
| 61 | | 1.69 | 1.69 | 7.1 | 13.2 | 72 | 104 |
| 62 | 1.05 | .91 | .98 | 6.2 | 7.2 | 78 | 73 |
| 64 | 2.53 | 1.49 | * 2.53 | 30.0 | 20.3 | 145 | 141 |
| 65 | | 1.03 | 1.03 | 11.9 | 7.6 | 100 | 75 |

* See text, section 4.

Because the soils listed in table 4 cover the range of corrosivity of soils peculiar to the United States, the data of both laboratories are used to set up the equation of best fit [9], presumably a linear relationship, between the laboratory and field weight losses, which it is again presumed will be applicable to any soil, whatever its degree of corrosivity. The standard errors associated with the weight losses were about the same for both laboratories except for the Waterways Experiment Station data pertaining to soil 64, in which the standard error was considerably larger than for all other data. As the inclusion of soil 64 adversely affected the correlation between the Waterways Experiment Station data and the field data, the Waterways Experiment Station data pertaining to this soil are omitted. Thus, by averaging the weight losses in each of 8 soils (4, 5, 25, 26, 32, 43, 56, 62, table 4) tested by the two laboratories and using the individual laboratory weight losses in the 7 other soils (8, 15, 41, 55, 61, 64, 65, table 4), the correlation between the combined laboratory weight losses and the National Bureau of Standards weight losses in the field results in a correlation coefficient of 0.83. All correlation coefficients were corrected for size of sample. Based on the correlation coefficient of 0.83, the equation relating the laboratory and field data is

$$W_{10}=8.45w-1.1, \qquad (1)$$

where $W_{10}$ is the anticipated weight loss on the commonly used ferrous specimens after 10 years of field exposure, expressed in ounces per square foot. $w$ is the mean combined weight loss in 6 months of the anode and cathode of corrosion cells, expressed in ounces per square foot. The standard error of estimate associated with this relationship is $\pm 4.1$ oz/ft$^2$.

The calculated weight losses on the National Bureau of Standards specimens based on eq (1) are tabulated in table 4, along with the actual weight losses. Relatively large discrepancies appear between the actual and calculated values in soils 5, 41, and 61. In the case of soils 41 and 61, the discrepancies might be attributed to the laboratory test. Soil 5, however, is fine in texture, very dense, and poorly aerated, and also possesses other characteristics which Denison and Ewing [10] associated with very corrosive soils. Also, a reference to some early information published by Logan, Ewing, and Yeomans [11] revealed that iron pipe removed from soil 5 was severely corroded. Probably the conditions within the trench from which the field specimens were removed were not typical of the general soil structure. Therefore, for soil 5 at least, the laboratory data are considered a better index of the potential soil corrosivity than are the field data.

### 4.2. Correlation Between Weight Loss and Maximum Penetration

The value of a laboratory corrosion test would be immeasurably increased if it could be used to predict the maximum depth of pitting under normal

field exposure. Laboratory weight losses might be interpreted in terms of pit depths if it could be shown that a correlation existed between weight loss and maximum penetration on ferrous specimens after field exposure. To test this possibility, 2 specimens of each of 4 commonly used wrought ferrous materials, previously described, exposed for 10 years at 58 National Bureau of Standards test sites were chosen. Following the statistical procedure already referred to, the average depths [2] of the deepest pits on these specimens were correlated with the average weight losses. The coefficient of correlation was calculated to be 0.79. The equation, based on this correlation, relating weight losses and pit depths for the 58 soils after 10 years of exposure is

$$P_{10}=5.2\ W_{10}+36, \tag{2}$$

where $P_{10}$ is the maximum pit depth in mils on an area of 0.4 ft,$^2$ and $W_{10}$ is the weight loss expressed in ounces per square foot. The standard error of estimate pertaining to $P_{10}$ in this equation is $\pm 18$ mils. Because of the number and variety of soils included in the derivation of eq (2), the relationship might be considered as being generally applicable to wrought ferrous materials exposed to any soil. Additional evidence of some correlation between weight loss and pitting on wrought and also cast ferrous specimens is indicated by the studies of Denison and Romanoff [6].

By combining eq (1) and (2), the maximum anticipated pit depth at 10 years is related to the laboratory weight loss for 6 months by the relation

$$P_{10}=43.9w+30, \tag{3}$$

where $P_{10}$ is expressed in mils at 10 years on an exposed area of 0.4 ft$^2$ and $w$ is as expressed for eq (1). Included in table 4 are the actual maximum pit-depths measured on the field specimens and also the calculated values based on eq (3). The lack of reasonably good agreement in soil 5 is to be expected because of the facts previously pointed out concerning this soil.

## 5. Adjustment for Time and Exposed Area

It has been shown that by means of the laboratory corrosion test a resonable estimate can be made of the weight loss and the average depth of the deepest pit that will occur on iron and steel specimens exposed in the field for 10 years. Obviously, the practical value of the test would be enhanced if it were possible to predict similar information as applied to larger exposed areas and periods of exposure other than 10 years.

Martin [12] has shown that the relation between the weight loss of iron and steel in soils and the duration of exposure may be expressed by the empirical equation

$$W=k'\ T^u$$

where $W$ is the weight loss at any time $T$, $k'$ is the weight loss on a unit area for a unit time, and $u$ is a constant peculiar to the soil.

Similarly, Logan, Ewing, and Denison [4] have shown that the average depth of the deepest pits on iron and steel may be expressed by the empirical equation

$$P=kT^nA^a,$$

where $P$ is the average depth of the deepest pits at any time $T$ on the exposed area $A$, and $k$ is the average value of the depth of the deepest pits on specimens of unit area for a unit time. The exponents $n$ and $a$ are constants, $n$ depending on the aeration and drainage of the soil, and $a$ being relatively fixed in all soils.

For a practical application of these equations to any soil, appropriate values must be selected for the exponents. Logan, Ewing, and Denison tabulated values for exponent $a$ based on exposure tests of wrought ferrous specimens in 47 soils. They concluded that the value of $a$ could not be characterized by any particular soil property. As the values reported did not vary over too wide a range, the writer believes that some average value would be appropriate for all soils. By eliminating all soils in which the associated standard errors tabulated for $a$ exceeded 20 percent, the values of $a$ for the remaining 31 soils ranged between 0.082 and 0.241, averaging 0.15, with a standard error of 0.019.

Logan, Ewing, and Dension divided the 47 soils into 4 groups based on aeration and drainage and calculated the average value of the exponent $n$ for each group. These values of $n$ and the associated standard errors are shown in table 5. Average values for $u$ and standard errors based on 14-year exposure tests of wrought ferrous materials by Denison and Romanoff [6] are included in the same table. It will be observed that the values of both $n$ and $u$ bear an inverse relation to the degree of soil aeration.

TABLE 5. *Average values of the time exponents n and u for soil groups differing in aeration*

| $n$ [a] | $\sigma_n$ | $u$ [a] | $\sigma_u$ |
|---|---|---|---|
| Group I, Good aeration | | | |
| 0.19 | 0.03 | 0.23 | 0.10 |
| Group II, Fair aeration | | | |
| 0.35 | 0.03 | 0.42 | 0.12 |
| Group III, Poor aeration | | | |
| 0.47 | 0.04 | 0.74 | 0.14 |
| Group IV, Very poor aeration | | | |
| 0.68 | 0.10 | 0.77 | 0.09 |

[a] Values for $n$ and the associated standard errors $\sigma_n$ are the mean values reported by K. H. Logan, S. P. Ewing, and I. A. Denison, Symposium on corrosion testing procedures, ASTM (Phila. Pa., 1937). Values for $u$ and the associated standard errors $\sigma_u$ are average values taken from I. A. Denison and Melvin Romanoff, J. Research NBS **44**, 47 (1950) RP2057.

[2] The average of the deepest pits on 8 specimens is also referred to as the maximum pit depth.

TABLE 6. *Time exponents n and u associated with soils of different properties*

| Soil group | I | II | III | IV |
|---|---|---|---|---|
| Values, $n$ or $u$ | 0.19 | 0.35 | 0.47 | 0.68. |
| Aeration and drainage | Good | Fair | Poor | Very poor. |
| Soil texture | Sands and sandy loams, light-textured silt loams, porous loams, clay loams. | Sandy loams, silt loams, clay loams. | Clay loams, clay | Clays and organic soils, including tidal marshes. |
| Depth of mottling in inches | None | 18 to 24 | 6 to 8 | 6 to 8. |
| Color of subsoil | Uniform | Slightly mottled—yellowish brown and yellowish gray. | Moderately mottled—gray and bluish gray. | Mottled—bluish gray. |
| Height of water table | Very low | Low | 2 to 3 ft below the surface | At the surface. |

Also, if the values for $n$ and $u$ are compared, giving consideration to the standard errors, the mean values for $n$ and $u$ overlap, except for group III. Because the values for $u$ are based on relatively few soils as compared with the values shown for $n$, the later are taken to be the more significant. For this reason, because of what has already been shown concerning the correlation between weight loss and maximum penetration, the writer believes that the values for $n$ shown in table 5 can be applied to $T$ in both the weight loss and pit-depth equations. Accordingly, this is proposed in table 6, together with the distinguishing soil properties pertaining to the four groups.

Having obtained from the laboratory test a value for the average depth of the deepest pit at 10 years, $P_{10}$ on 0.4 ft$^2$ (eq 3), the value of pitting for a time ($T$) other than 10 years and for an area ($A$) greater than 0.4 ft$^2$ is calculated from the equation

$$P = P_{10}\left(\frac{T}{10}\right)^{n}\left(\frac{A}{0.4}\right)^{0.15} \qquad (4)$$

It has been pointed out by Logan, Ewing, and Denison that the values substituted for $T$ and $A$ cannot be chosen indiscriminately. This is particularly true when substituting for $A$, because $P_{10}$ applies to 0.4 ft$^2$. A reasonable extrapolation based on soils 55 and 56 (table 4) might be considered. Assuming an area ($A$) of 20 ft$^2$ (approx. 20 ft of 3½-in. steel pipe) and an underground-exposure period ($T$) of 40 years, the maximum predicted pit depths calculated from eq (4) would be 112 mils, and 660 mils for soils 55 and 56, respectively. In these calculations, values of $n=0.19$ and $n=0.68$ were chosen for soils 55 and 56, respectively, the values being selected from table 6 on the basis of the soil properties found in table 1. Thus, in the case of soil 55 the increase in pit depth after 10 years is due chiefly to the increased area, whereas the deeper pits resulting from soil 56 are attributable mainly to the effect of time.

Weight losses at 10 years, based on the laboratory test (eq 1), can be similarly adjusted and values of weight loss ($W$) predicted for periods ($T$) other than 10 years. The weight loss becomes

$$W = W_{10}\left(\frac{T}{10}\right)^{u}, \qquad (5)$$

where $u$ is selected from table 6, based on the soil properties. The effect of area on weight loss is assumed to be linear. This equation is particularly useful in calculating the average penetration by conversion. Thus the average penetration in mils becomes

$$\overline{P} = 1.53\ W, \qquad (6)$$

where $W$ is the weight loss in ounces per square foot (eq (5)). The predicted average penetration on a steel surface exposed to soils 55 and 56 (table 4) for 40 years would be 5 mils and 81 mils, respectively. Such information is useful where loss of strength is the primary consideration.

## 6. Summary


A modification of the Denison soil-corrosion cell is described. The cells were assembled in quadruplet with both steel and cast-iron electrodes exposed to 10 soils of varying degrees of corrosivity. Because the corrosion rate of ferrous metals in soils is a function of time all measurements are based on the weight loss of the electrodes after 6 months of exposure.

In 9 of the soils, the steel electrodes lost less weight than the cast-iron electrodes. Statistically expressed, the difference in weight loss in 5 of these soils being due to chance was less than 1 percent and in 2 other soils less than 4 percent. The laboratory results compare favorably with 12-year field exposure tests.

Good correlation was also obtained between the weight losses of the corrosion cells and the weight losses occurring in the field on other wrought ferrous specimens exposed for 10 years to the same soils. Based on 10-year field exposure of wrought materials at 58 test sites throughout the United States, a fair correlation was found to exist between weight loss and maximum penetration. By making use of the latter correlation, it is shown how laboratory weight losses can be used to predict probable maximum pit depths on ferrous materials upon field exposure after 10 years.

By utilizing equations relating weight loss of ferrous field specimens to time of exposure, and the average depth of the maximum pits on the specimens to time and to exposed area, values of weight loss and pitting at the end of 10 years predicted by the laboratory test may be extrapolated to any desired area and period of exposure within reasonable limits. Suggested values of the exponents required for adjustment of the data are given.

The author gratefully acknowledges the contribution of the Waterways Experiment Station, Vicksburg, Miss., Corps of Engineers, U. S. Army. Thanks are due O. B. Ellis, Armco Steel Corp., and James T. MacKenzie, American Cast Iron Pipe Co., for furnishing the materials for the cell electrodes. The writer acknowledges the suggestions and assistance of O. N. McDorman of the National Bureau of Standards relative to the preparation of the cell and the assistance in statistical calculations by Andrew J. Griest, Jr., formerly with the National Bureau of Standards.

## 7. References

[1] Scott Ewing, Soil corrosion and pipe line protection, p. 78 (American Gas Assn., 420 Lexington Ave., New York, N. Y.).
[2] I. A. Denison, Electrolytic measurement of the corrosiveness of soils, J. Research NBS **17**, 363 (1936) RP918.
[3] I. A. Denison and R. B. Darnielle, Observation on the behavior of steel corroding under cathodic control in soils, Trans. Electrochem. Soc. **76**, 199 (1939).
[4] K. H. Logan, S. P. Ewing, and I. A. Denison, Soil corrosion testing, Symposium on corrosion testing procedures, ASTM (1937).
[5] W. J. Schwerdtfeger and O. N. McDorman, Measurement of the corrosion rate of a metal from its polarizing characteristics, J. Electrochem. Soc. **99**, 407 (1952).
[6] I. A. Denison and Melvin Romanoff, Soil-corrosion studies, 1946: Ferrous metals and alloys, J. Research NBS **44**, 47 (1950) RP2057.
[7] Kirk H. Logan, Underground corrosion, NBS Circular C450 (1945).
[8] Croxton and Cowden, Applied general statistics (Prentice-Hall, Inc., New York, N. Y., 1940).
[9] Ezekiel, Methods of correlation analysis (John Wiley & Sons, Inc., New York, N. Y., 1930; Chapman & Hall, Ltd., London, 1930).
[10] I. A. Denison and S. P. Ewing, Corrosiveness of certain Ohio soils, Soil Science **40**, 287 (1935).
[11] K. H. Logan, S. P. Ewing, and C. D. Yeomans, Soil-corrosion studies. 1. Soils, materials, and results of early observations, Tech. Pap. BS No. 368 (April 28, 1928).
[12] L. M. Martin, A preliminary study of the logarithmic relation between corrosion and time, NBS Soil Corrosion Conference 1937, unpublished.

## 8. Appendix

### 8.1. Preparation of the Corrosion Cell

The apparatus for moistening and adjusting the water content of the soil samples is shown diagramatically in figure 3. Because 4 cells are desirable for testing a soil, the apparatus provides for simultaneously moistening the soil contained in 8 Lucite cylinders. Distilled water absorbed from the water dispenser, 12, resting on the upper surface of the soil, 9, is distributed uniformly throughout the soil by a pressure difference of 30 cm of Hg. Suction is applied to 500-ml suction flasks, 3, through fritted-disk Buechner funnels, 1, (150 ml, fine) to the soil contained in the Lucite cylinders, 7. Paraffin, 8, serves to confine the suction to the soil. The battery of eight suction flasks are connected to the suction apparatus with rubber tubing and glass fittings. The vacuum in the line is controlled by valve, 5, and to each flask by valve, 4.

Details of a water dispenser, 12, are shown under detail C, figure 3. The reservoir, A, is cut from Lucite tubing of 1.75-in. OD and 0.125-in. wall thickness. The bottom edge, B, is tapered or rounded so that it will fit readily into the cylinder containing the soil. The dispenser is assembled as follows: With the reservoir placed on a flat surface in the position shown, asbestos paper, C, 0.125 in. thick cut into the form of a disk slightly larger than the inside diameter of the tubing, is pressed from the top to the bottom and sealed with molten beeswax, D. A saucer shaped stainless steel screen (16 mesh), E, held in place by friction and beeswax, serves to keep the weight of the glass beads, F, off of the asbestos. The beads (6-mm solid glass) added to within ½ in. from the top of the dispenser furnish weight to insure good contact for absorption of water by the soil. A second screen, G, identical with screen, E, is pressed over the glass beads to prevent their loss.

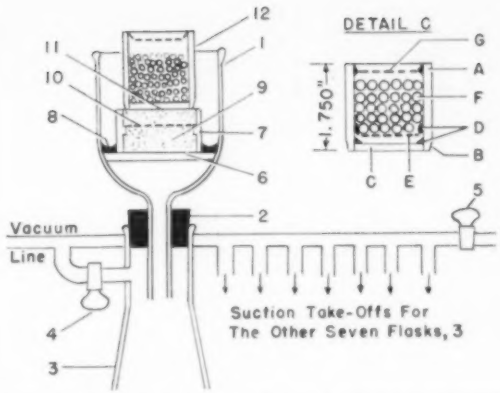


FIGURE 3. *Cross-sectional view of the soil-moistening apparatus.*

The cell electrodes (fig. 1) are prepared for the corrosion tests in the following manner: The electrodes are degreased and all burrs removed with 1G French emery cloth. After being weighed, the electrodes are fitted with 0.5 in.×2–56 steel fillister head machine screws and stranded copper wire (RC No. 18) leads, approximately 8 in. long, are soldered under the heads. The edges and unfinished surfaces of the anodes are given a heavy coat of bituminous paint. The edges and unfinished sides of the cathodes, excluding the cylindrical surface of the holes, are similarly treated. The machine screws and soldered connections are also coated to prevent corrosion and to facilitate removal of the screws at the conclusion of the test.

In setting up the corrosion cells eight Buechner funnels, 1, are fitted with rubber stoppers, 2, and positioned as shown in figure 3. Two sheets of filter paper (No. 42—5.5-cm diam), 6, are placed in each funnel to prevent direct contact between the soil and the fritted glass. The screw holes in the Lucite cylinders, 7, are filled with saturated soil and a cylinder is centered in each funnel. Paraffin is heated just to the melting point and a sufficient amount applied with a dropper to the space around each of the cylinders to adhere to both the funnel and the cylinder. Dry soil previously passed through a No. 20 standard sieve is poured into each cylinder approximately to the upper edge of the ridge and compacted by placing a cylindrically shaped brass weight 1.75 in. in diameter and 2.25 in. long on the surface of the soil. Disks of stainless-steel wire mesh, 10, are then placed on the ridges of 4 of the 8 cylinders, and the process of filling the cylinders and compacting the soil is resumed until all of the cylinders are filled. As excessive swelling usually accompanies the moistening of heavy clay soils, allowance for this may be made by filling the cylinders just short of capacity.

After the asbestos of the water dispensers is saturated with distilled water, 15 ml of water are poured into each of the reservoirs and the dispensers then positioned on the surfaces of the soil samples but separated therefrom by a sheet of filter paper, 11, cut to conform to the inside diameter of the cylinder. Vacuum equivalent to 30 cm of Hg is then applied for periods ranging from 1 to 8 hr, depending on the soil texture. Sufficient moistening of the soil is indicated by water dripping from the funnels, sweating underneath the fritted glass, or by the appearance of the soil. The valve, 4, to the particular cell is then closed and the water dispensers removed.

Usually, all sections are sufficiently wet within 20 percent of the average wetting time peculiar to the soil. If it is necessary to delay assembly of the cell, evaporation of water can be prevented by covering the soil with a pad of cheesecloth saturated with water and the funnel with an inverted crystallizing dish.

The cell components are assembled in the following manner: The adhesion between the paraffin around the Lucite cylinders and the funnels is broken with a spatula, and the four funnels containing the cylinders fitted with the screen disks D, are removed. The four funnels are inverted, and the cell sections are dropped into the palm of the hand. The four cylinders, paper-capped ends down, are placed on a flat surface, and the soil on the upper surface of the cylinders is slicked over with a spatula occasionally dipped into distilled water until all evidence of porosity has disappeared. The unpainted surfaces of four anodes (A, fig. 1) are lightly scratched with 1G French emery cloth and cleaned with distilled water. The anode is again moistened with distilled water, the screw alined with the notch in the Lucite cylinder, and with an oscillatory motion combined with some pressure, the anode is placed in good contact with the soil. Excess soil is then removed, the components wiped dry, and the junction of the anode and the cylinder sealed with molten asphalt. The paraffin seal around the Lucite is loosened with a spatula, and the cylinders are turned over so as to rest on the anodes, after which the filter paper and adhering paraffin are lifted off in preparation for the positioning of the cathodes.

The cathodes (B, fig. 1) are prepared in the manner described for the anodes and positioned over the soil in the ends of these four inverted cylinders, previously described, with the uncoated surfaces facing the anodes. The cathode perforations are then filled with dry soil. The four remaining soil cylinders are removed from the funnels and positioned over the cathodes so that the edges from which the paraffin was removed are adjacent to the cathodes. The screen disk, E, is positioned, and the components are joined with molten asphalt, as shown in figure 1. The rubber stopper, H, is then placed in position and held firmly against the anode by a No. 32 rubber band, G, wrapped once around the stopper and the cell. Each cell is placed on nonconducting supports in a 1-quart friction-top can containing about 25 ml of water to maintain a saturated atmosphere. The water level is maintained throughout the period of the test. Leads from the cell are passed through holes in the side of the can and the electrodes short-circuited by a Fahnestock clip soldered to one of the wires.

WASHINGTON, March 6, 1953.

Journal of Research of the National Bureau of Standards Vol. 50, No. 6, June 1953 Research Paper 2423

# Effect of Temperature on the Electrical Resistance and Voltage Departures (Errors) of Glass Electrodes, and Upon the Hygroscopicity of Glass

Donald Hubbard

The effect of temperature upon the electrical resistance and pH response has been studied on electrodes prepared from three types of glasses: Pyrex 7740, commercial soft-glass tubing, and Corning 015; glasses of low, intermediate, and high hygroscopicity, respectively. The results show that electrical resistance is not the determinant in most cases of voltage departure from the theoretical, and in the inherent failure of many glasses to act as satisfactory indicators of hydrogen-ion activity of aqueous solutions. For example, the electrodes prepared from Pyrex glass gave no significant pH response even when the resistance was as low as 12 megohms. The results of electrodes from glasses of intermediate hygroscopicity gave a pseudo-correspondence of pH response with resistance, whereas electrodes of Corning 015 gave voltage departures that could in no way be attributed to the electrical resistance of the electrode.

## 1. Introduction

Considerable confusion exists in the general concept as to what part the electrical resistance of a glass electrode plays in its voltage response to hydrogen-ion activity of aqueous solutions, the voltage departures (errors) that appear at high alkalinities and in the "superacid" region, and particularly in the failure of electrodes from many glasses to follow the simple dictates of the Nernst equation, $\Delta E = 0.000198T\Delta\text{pH}$. For example, the difference in performance shown between electrodes from Pyrex 7740 and a satisfactory pH-responsive glass (fig. 1) is presumed to be related somehow to a difference in resistance of the glass membranes forming the effective portion of the electrode. With the electrometer tubes available requiring grid currents of only $10^{-12}$ to $10^{-15}$ amp, a glass electrode having a resistance as great as 1,000 megohms would exhibit an IR drop (error) ranging from $10^{-3}$ to $10^{-6}$ v [1, pages 47 and 89 to 92].[1] Such errors are small, and for most practical pH measurements can be disregarded. It is obvious that glass electrodes exhibiting large voltage departures, pH errors, but having resistances less than 1,000 megohms, are failing to show full pH response not because of their high electrical resistance nor because of a lack of sensitivity of the available indicating electrometers.

The present investigation was undertaken to ascertain what individual parts the hygroscopicity (water sorption) of the glass and the electrical resistance of the glass membrane play in the over-all picture of the ability, or lack of ability, of electrodes from various glasses to act as indicators of hydrogen-ion activity of aqueous solutions over the temperature range 20° C to near the boiling point of water.

## 2. Experimental Procedures

The hygroscopicity values were obtained in the apparatus described in previous publications [2]. The experiments at elevated temperatures were carried out by immersing the humidity chamber in a thermostated water bath. Although no mechanical difficulties were encountered, this procedure for obtaining hygroscopicity was not entirely satisfactory, because of excessive condensation on the walls of the chamber at the elevated temperatures for the high humidity (approximately 98 percent) required for the experiments. However, the results appeared to be qualitatively acceptable. The hygroscopicity values reported are those obtained for 1-hour exposures.

The voltage performance of any experimental electrode was determined by the voltage change that appeared when the cell consisting of the experimental electrode and a reference electrode was transferred from a buffer solution at pH 4.1 to a buffer at pH 8.2. The reference electrode employed was either a hydrogen electrode or a glass electrode calibrated at the elevated temperatures. Thus if the experimental electrode gave full pH response, no change in voltage appeared in the two buffers at any temperatures. Typical examples of the data obtained by this procedure are illustrated in figure 1 for a commercial electrode and one prepared from Pyrex glass 7740 The above pH interval was chosen because it is a region of uniform chemical durability of the glasses studied [3]. Thus, voltage shifts are eliminated or minimized, which might be credited to a change in chemical durability [2]. The calibrated mercury-filled glass electrode [4] was preferred over the hydrogen electrode as a reference electrode because of operational simplicity and ease of temperature control by eliminating the hydrogen-gas chain. Furthermore, with both the reference and experimental electrodes filled with mercury, any small thermoelectric voltages generated at the Pt-Hg junction would be compensated by the symmetry of the system. All electromotive-force measurements were made with a Beckman pH meter, laboratory model G.

The resistance values for the experimental glass electrodes were followed at the different tempera-

[1] Figure in brackets indicate the literature references at the end of this paper.

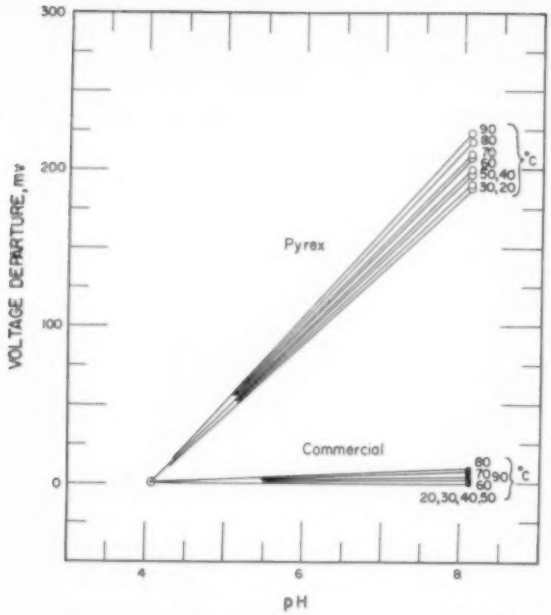


FIGURE 1. *Voltage departures at various temperatures observed over the interval* pH *4.1 to* pH *8.2 for two glass electrodes, one of which was a commercial glass-electrode and the other prepared from Pyrex glass 7740.*

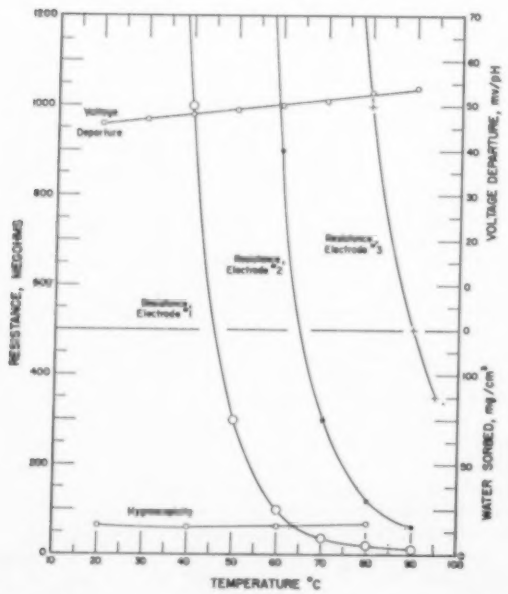


FIGURE 2. *Effect of temperature upon the resistance, hygroscopicity, and* pH *response of electrodes prepared from Pyrex glass 7740, a glass of low hygroscopicity.*

tures with an RCA Senior Voltohmyst TWV–97 A, which imposes 1.5 v across the glass membrane, while the bulb of the electrode was immersed in Britton universal buffer at pH 4.1. The electrical connections for these measurements were established by means of platinum leads, one of which was dipped into the buffer solution and the other into the mercury filling the glass electrode bulb. A number of parallel observations were made with a General Radio type 544–BS8 megohm bridge operating with 100-v drop across the terminals, to make sure that neither polarization nor the voltage generated by the battery, consisting of the two cells, glass electrode, and platinum wire, was causing spurious resistance values to be reported [5]. The higher voltage of the megohm bridge might cause polarization resistance at the glass surface or even puncture the glass membrane, whereas the low operation voltage of the Voltohmyst might be seriously affected by counter voltage generated by the battery consisting of the glass electrode and the external platinum-wire connection. Because the two instruments indicated approximately the same resistance, it seemed reasonably sure that the effects of polarization and interfering voltages were not large.

## 3. Results and Discussions

### 3.1. Electrodes Prepared from Pyrex Glass 7740; A Glass of Low Hygroscopicity

Figure 2 and table 1 show the effect of temperature upon the electrical resistance and pH response of electrodes prepared from the sample of Pyrex 7740, chemical-ware glass, and the hygroscopicity of this glass over the same temperature range. The resistance curves for these three electrodes are in accord with the long known fact that the electrical resistivity of glass decreases rapidly as the temperature is increased and follows in a general way the exponential equation

$$R = Be^{A/T},$$

where

$R$ = the resistivity,
$B$ = a constant,
$A$ = a constant involving the activation energies,
$T$ = temperature,
$\epsilon = 2.71828$, the limit of the series $(1+1/n)^n$ as $n \doteq \infty$ [6].

At times the resistance curve obtained experimentally may depart conspicuously from this shape; typical examples obtained on an electrode are illustrated by A and B in figure 3. Such S curves can be readily accounted for qualitatively by electrical surface leakage under conditions in which the resistance of the electrode bulb becomes increasingly great in comparison to the surface resistance of the glass tube. The total resistance, $R$, of the two con-

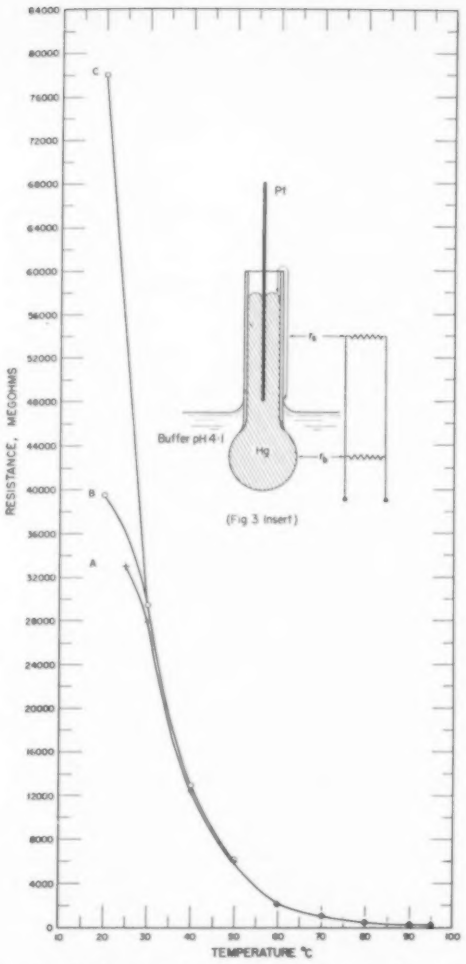


FIGURE 3. *Resistance values obtained on a single glass electrode illustrating the effect of surface conductivity upon the shape of the resistance-temperature curves.*

Curves A and B were obtained before surface treatment; C, after cleaning and drying. Insert is a schematic diagram illustrating the resistances involved. $r_s$=surface resistance, $r_b$=resistance of the glass electrode

ductors, electrode bulb and glass surface in parallel (fig. 3 insert), whose separate resistances are $r_b$ and $r_s$, is given by the relation

$$1/R=1/r_b+1/r_s, \text{ or } R=\frac{r_b r_s}{r_b-r_s}.$$

As $r_b$ becomes so very large as to approximate the resistance of an open circuit, $R$ approaches $r_s$ as a limiting value

$$1/R=1/\infty+1/r_s, \quad \text{or} \quad R=r_s.$$

These S curves are readily brought back into conformity by cleaning, drying, or treating the surface of the glass stem with appropriate water repellants, such as paraffin, organic chlorosilanes, or commercial Desicote [6].

The voltage-departure characteristics of electrode 1 as affected by temperature are also plotted in figure 2. From this curve it is evident that there was no improvement in the pH response of this Pyrex electrode, although the resistance fell to such low values as 99, 35, 19, and 12 megohms. In other words, the low resistance was not accompanied by a correspond-

TABLE 1. *Characteristic resistance, voltage departure, and hygroscopicity values observed at different temperatures for electrodes prepared from glasses of high, intermediate, and low hygroscopicity*

| No. | Temperature | Water sorbed | Voltage departure | Electrical resistance |
|---|---|---|---|---|
| | °C | mg/cm² | mv/pH | Megohms |
| **Corning 015 electrode** | | | | |
| 1 | 20 | 105 | 0 | 115 |
| | 30 | ..... | 0 | 48 |
| | 40 | 112 | 0 | 19 |
| | 50 | ..... | 0 | 9.3 |
| | 60 | 131 | 0 | 4.8 |
| | 70 | ..... | 0 | 2.5 |
| | 80 | 144 | 0 | 1.1 |
| | 90 | ..... | 0 | 0.59 |
| 2 | 20 | 105 | 5 | 495 |
| | 30 | ..... | 4 | 225 |
| | 40 | 112 | 3 | 120 |
| | 50 | ..... | 2 | 59 |
| | 60 | 131 | 1— | 33 |
| | 70 | ..... | 0 | 17 |
| | 80 | 144 | 0 | 9.3 |
| | 90 | ..... | 0 | 5.8 |
| 3 | 20 | 105 | 42 | 950 |
| | 30 | ..... | 32 | 500 |
| | 40 | 112 | 19 | 250 |
| | 50 | ..... | 12 | 110 |
| | 60 | 131 | 8— | 45 |
| | 70 | ..... | 8.5 | 21 |
| | 80 | 144 | 8.5 | 10 |
| | 90 | ..... | 9.5 | 5.2 |
| **Soft-glass electrode** | | | | |
| 1 | 20 | 26 | 0 | 8,300 |
| | 30 | ..... | 0 | 3,800 |
| | 40 | 36 | 0 | 1,800 |
| | 50 | ..... | 0 | 950 |
| | 60 | 53 | 0 | 350 |
| | 70 | ..... | 0 | 120 |
| | 80 | 87 | 0 | 41 |
| | 90 | ..... | 0 | 16 |
| 2 | 20 | 26 | ..... | ..... |
| | 30 | ..... | 52 | 31,000 |
| | 40 | 36 | 36 | 12,000 |
| | 50 | ..... | 15 | 5,300 |
| | 60 | 53 | 1 | 2,490 |
| | 70 | ..... | 0 | 1,110 |
| | 80 | 87 | 0 | 455 |
| | 90 | ..... | 0 | 207 |
| **Pyrex 7740 electrode** | | | | |
| 1 | 20 | 17 | 46 | 5,800 |
| | 30 | ..... | 47 | 2,300 |
| | 40 | 15 | 48 | 1,000 |
| | 50 | ..... | 49 | 300 |
| | 60 | 16 | 50 | 99 |
| | 70 | ..... | 51 | 35 |
| | 80 | 17.5 | 53 | 19 |
| | 90 | ..... | 54 | 12 |
| 2 | 20 | 17 | ..... | ..... |
| | 40 | 15 | ..... | ..... |
| | 60 | 16 | ..... | 900 |
| | 70 | ..... | ..... | 300 |
| | 80 | 17.5 | ..... | 120 |
| | 90 | ..... | ..... | 61 |
| 3 | 20 | 17 | ..... | ..... |
| | 40 | 15 | ..... | ..... |
| | 60 | 16 | ..... | ..... |
| | 80 | 17.5 | ..... | 1,000 |
| | 90 | ..... | ..... | 500 |
| | 95 | ..... | ..... | 350 |

ing improvement in pH response. Electrodes 2 and 3 were checked at 30° and 90° C and were also found to be unresponsive to the pH of the buffer solutions. Obviously, if electrical resistance were the major determinant in pH response of this glass, the three Pyrex electrodes would be expected to develop improved response at different temperatures in accord with their resistance curves. However, they are all useless as indicators of hydrogen-ion activity. Only upon a study of the hygroscopicity curve obtained on Pyrex glass does one get a plausible reason for the complete indifference of these electrodes to the lowered resistance at the elevated temperatures (fig. 2). The water sorbed by the glass has not changed appreciably with the increase in temperature and does not at any temperature approach a value commensurate with an effective electrode glass. [5, 7] Certainly the lowered resistance can not be attributed to water penetrating the glass. As a result, the voltage departure of the electrode in mv/pH becomes greater with increased temperature. This increased departure is largely the result of the temperature effects inherent in the derivation of the Nernst equation. Based on previous evidence, the electrodes prepared from this nonhygroscopic glass probably would have no satisfactory pH response, regardless of how thin the glass membranes were blown [5, 8, 9].

### 3.2. Electrodes Prepared from a Glass of Intermediate Hygroscopicity

Figure 4 shows the effect of temperature on the resistance and pH characteristics of two glass electrodes prepared from a commercial soft glass of intermediate hygroscopicity. The performance of these

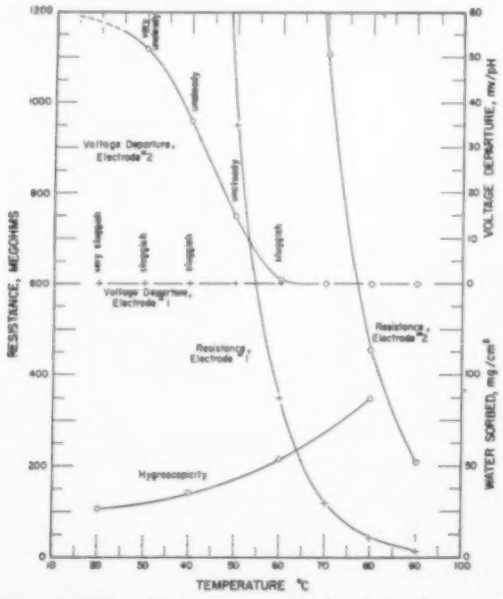


FIGURE 4. *Effect of temperature upon the electrical resistance, hygroscopicity, and* pH *response of electrodes prepared from a glass of intermediate hygroscopicity.*

electrodes more nearly follows the general conception of the part that resistance should play in determining the suitability of a glass for pH measurements. Electrode 1 at 20° C was very sluggish in drifting toward a steady voltage, whereas at 30° and 40° C the performance was still sluggish, but markedly improved. Above 50° C the resistance of the bulb fell rapidly below 1,000 megohms, and the electrode performed in an acceptable manner for high-temperature pH measurements. As the chemical durability of this glass is far superior to that of Corning 015, the life expectancy of electrodes prepared from it when used for high-temperature pH measurements would be correspondingly greater [1, 10, 11]. Electrode 2 was blown with a bulb considerably thicker than electrode 1. At 30° C the voltage departure was large and very unsteady. This electrode showed marked improvement, but was still unserviceable at 40° and 50° C. The voltage departures were small at 60° and 70° C, but the electrode performance was still sluggish. Beyond 80° C, the resistance of the bulb had fallen well below 1,000 megohms, and the over-all performance of the electrode was acceptable. As the pH response of these electrodes improved with decrease in resistance, a correlation of the pH response with the resistance values would apparently be acceptable, but not entirely adequate, as will be seen from the discussion and evaluation of the data in figure 7. However, the shape of the hygroscopicity-temperature curve is entirely different from that of Pyrex and probably is equally satisfactory in accounting for the improved performance of the glass electrode. (Compare the hygroscopicity curves in fig. 2 and 4.)

### 3.3. Electrodes from Corning 015

Figure 5 shows the electrical resistance and voltage performance of three electrodes prepared from a single sample of Corning 015 glass. Electrode 1 had low resistance values at all temperatures, ranging from 115 megohms at 20° C to 0.59 megohm at 90° C. Having been prepared from a glass of relatively high hygroscopicity and of uniform chemical durability over the pH interval chosen, this thin-walled electrode gave satisfactory performance (approximating the theoretical) over the temperature range from 20° to 90° C. Electrode 2 was blown from the same length of glass tubing as electrode 1, but with much heavier wall thickness. The resistance curve for this electrode fell below 500 megohms at 20° C and showed the usual rapid decline with increased temperature. However, this thicker electrode exhibited appreciable voltage departure at all temperatures up to 70° C, beyond which temperature it paralleled the performance of the reference electrode. Electrode 3, with a wall thickness in excess of 1 mm, still had resistance values lower than many satisfactory electrodes, but gave voltage departures over the entire temperature range from 20° to 90° C. This performance is in accord with the general knowledge that every glass has a critical thickness at which voltage departures appear [8]. Such failures of an electrode to respond to hydrogen-ion activity certainly cannot be attributed to electrical resistance

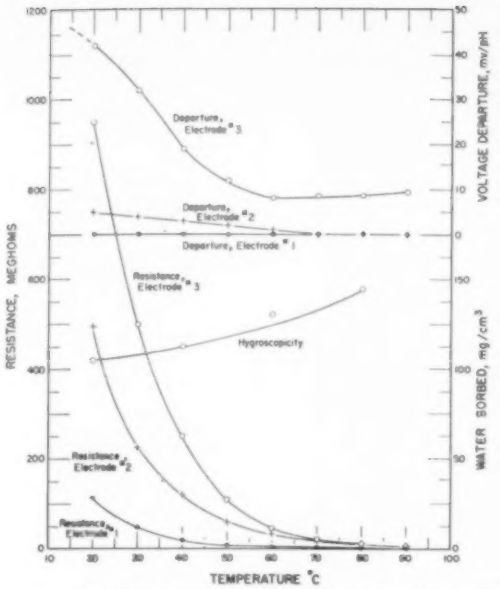


FIGURE 5. *Effect of temperature upon the electrical resistance, hygroscopicity, and* pH *response of electrodes prepared from Corning 015, a glass of high hygroscopicity.*

of the electrode, because at all temperatures the resistance is at values far below that at which the IR drop across the membrane would be as great as 1 mv. Possibly proton or $H_3O^+$ resistance due to the thickness of the membrane, lack of water penetration of the glass, or a combination of both, give a more acceptable concept. It seems probable that the glass–water–hydrogen-ion-activity equilibrium does not become established throughout the glass, even though the inherent hygroscopicity of the glass is high (fig. 5).

In order to further emphasize the lack of universal correspondence between voltage departures of glass electrodes and electrical resistance of the glass membrane, resistance values were determined for an electrode of Corning 015 over an extended pH range (conc. $H_2SO_4$ to pH 12) for temperatures from 20° to 90° C, and the results considered in relation to a conventional voltage departure curve obtained at room temperature over the same pH range (table 2, fig. 6). These results show that the voltage departures in the high alkaline and superacid ranges are not attributable to excessively high electrical resistances, nor are they associated with marked changes in electrical resistance. Their causes have been discussed elsewhere in connection with the water activity of the solutions [1], chemical durability of the glass [2], heterogeneous equilibria at the glass electrode solution interface [15], and equilibrative response to ions other than hydrogen [1, 16].

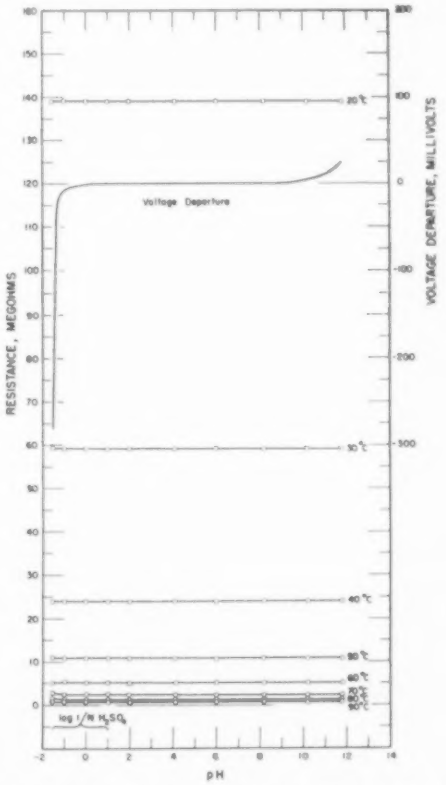


FIGURE 6. *The* pH*-resistance curves obtained on an electrode of Corning 015 over an extended* pH *range* (conc. $H_2SO_4$ *to* pH *12) for temperatures from 20° to 90° C, compared with a typical voltage departure (error) curve over the same* pH *range.*

TABLE 2. *Resistance values obtained for an electrode of Corning 015 over an extended* pH *range for temperatures from 20° to 90° C*

| Temperature | Resistance in— | | | | | | | | | |
|---|---|---|---|---|---|---|---|---|---|---|
| | $H_2SO_4$ | | | | Britton buffers at pH— | | | | | |
| | 36*N* | 10*N* | 1*N* | 0.1*N* | 2 | 4.1 | 6.0 | 8.2 | 10.2 | 11.8 |
| °*C* | *Megohms* | *Megohms* | *Megohms* | *Megohms* | *Megohms* | *Megohms* | *Megohms* | *Megohms* | *Megohms* | *Megohms* |
| 20 | 138 | 139 | 139 | 139 | 139 | 139 | 139 | 139 | 139 | 139 |
| 30 | 59.4 | 59.2 | 59 | 59 | 59.2 | 59.2 | 59.2 | 59.1 | 59.2 | 59.2 |
| 40 | 24 | 24 | 24 | 24 | 23.9 | 24 | 24 | 24 | 24 | 24 |
| 50 | 10.8 | 10.7 | 10.7 | 10.7 | 10.7 | 10.7 | 10.7 | 10.6 | 10.7 | 10.7 |
| 60 | 5 to 5.3 | 5.1 | 5 | 5 | 5 | 5 | 5 | 5 | 5 | 5 |
| 70 | 2.39 to 2.7 | 2.3 | 2.3 | 2.29 | 2.29 | 2.27 | 2.29 | 2.3 | 2.27 | 2.27 |
| 80 | 1.21 to 1.42 | 1.19 | 1.19 | 1.20 | 1.19 | 1.19 | 1.19 | 1.19 | 1.19 | 1.19 |
| 90 | .60 to .72 | .59 | .57 | .57 | .57 | .58 | .57 | .57 | .57 | .57 |

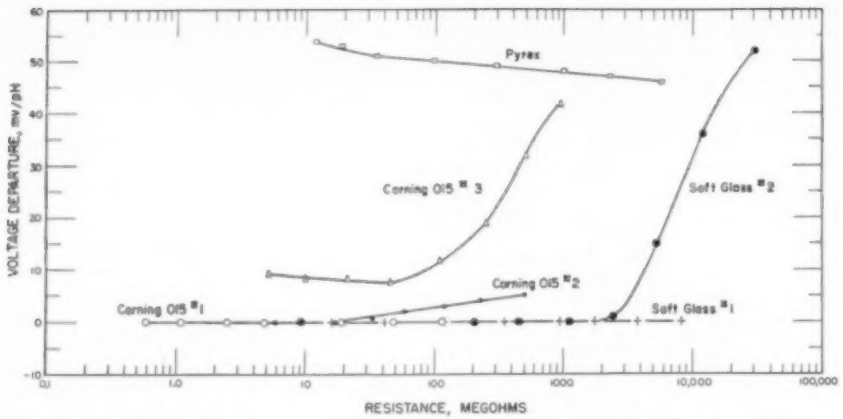


FIGURE 7. *Comparison of the voltage departure and electrical resistance values of electrodes prepared from Corning 015, a commercial soft-glass tubing, and Pyrex glass 7740.*

The resistance sequence for each of the electrodes was produced by varying the temperature.

### 3.4. Hygroscopicity versus Temperature

Although the hygroscopicity curves for the three glasses reported must be classified as being of uncertain reliability, they do warrant a brief evaluation. If adsorption were the major factor contributing to the water sorbed, the hygroscopicity curves should decrease with increased temperature [12]. As the curves for two of the glasses, figures 4 and 5, show a liberal increase with temperature, it is obvious that absorption and reaction are predominating factors.

## 4. Summary

Figure 7, in which the voltage departures (errors) are plotted as the dependent variable and resistance as the determinant, illustrates the incongruous part played by electrical resistance in the over-all picture of the pH response of glass electrodes. Not only do the pH response-resistance curves for electrodes from different glasses not coincide, but curves for electrodes from the same length of tubing (Corning 015 and soft-glass tubing) fail to exhibit similar characteristics. From the present investigation the part played by electrical resistance in determining the effectiveness of a glass for use as glass electrodes seems to be largely superficial. For example, electrodes prepared from glasses of low hygroscopicity, such as Pyrex, do not develop a staisfactory pH function even at very low resistance values. Furthermore, electrodes from glasses of high hygroscopicity and low resistance, such as Corning 015, fail to give full response to hydrogen-ion activity if the membrane thickness is excessive. From the data on the above two glasses, plus the results obtained on a glass of intermediate hygroscopicity, it appears that resistance values below 1,000 megohms are desirable, but certainly not sufficient to bring about staisfactory pH response.

Voltage departures from the theoretical pH response can appear for glass electrodes of low electrical resistance for the following reasons:

1. Low hygroscopicity of the glass from which the electrode is prepared [2, 7].
2. Membrane walls greater than a limiting thickness value, which differs for every glass [8].
3. Poor chemical durability of the glass [2]
4. High concentration of electrolytes [13, 14, 15].
5. Inhibiting films [9].

## 5. References


[1] Malcolm Dole, The glass electrode (John Wiley & Sons, Inc., New York, N. Y., 1951).

[2] Donald Hubbard, Mason H. Black, Sylvanus F. Holley, and Gerald F. Rynders, Electrode function (pH response), hygroscopicity, and chemical durability of soda-potash-silica glasses, J. Research NBS **46,** 168 (1951) RP2189.

[3] Donald Hubbard and Edgar H. Hamilton, Studies of the chemical durability of glass by an interferometer method, J. Research NBS **27,** 143 (1941) RP1409.

[4] M. R. Thompson, A metal-connected glass electrode, BS J Research **9,** 833 (1932) RP511.

[5] Richard G. Goldman and Donald Hubbard, pH response of nonhygroscopic glasses, J. Research NBS **48,** 370 (1952) RP2324.

[6] J. E. Stanworth, Physical properties of glass (Oxford University Press, Oxford, England, 1950).

[7] Donald Hubbard, Hygroscopicity and electrode function (pH response) of glasses as a measure of serviceability, J. Research NBS **36,** 511 (1946) RP1719.

[8] J. J. Diamond and Donald Hubbard, Thickness of glass electrodes, J. Research NBS **47,** 443 (1951) RP2270.

[9] Donald Hubbard and Gerald F. Rynders, Thickness of inhibiting films on glass electrode surfaces, J. Research NBS **41,** 163 (1948) RP1915.

[10] Henry H. Cary and Warren P. Baxter, U. S. Patent 2383709 (1945).

[11] George A. Perley, Composition of pH-responsive glasses, Anal. Chem. **21,** 391 (1949).

[12] Herbert Freundlich, Colloid and capillary chemistry (E. P. Dutton & Co., Inc., New York, N. Y.).

[13] D. A. MacInnes and D. Belcher, Further studies on the glass electrode, J. Am. Chem. Soc. **53,** 3315 (1931).

[14] Donald Hubbard and Gerald F. Rynders, Voltage anomalies of the glass electrode and the chemical durability of the glass, J. Research NBS **39,** 561 (1947) RP1848.

[15] Donald Hubbard and Richard G. Goldman, Heterogeneous equilibria at the glass electrode-solution interface, J. Research NBS **48,** 428 (1952) RP2333.

[16] B. Lengyel and E. Blum, The behavior of the glass electrode in connection with its chemical composition. Trans. Faraday Soc. **30,** 461 (1934).


WASHINGTON, April 9, 1953.

Journal of Research of the National Bureau of Standards Vol. 50, No. 6, June 1953 Research Paper 2424

# On the Numerical Solution of Parabolic Partial Differential Equations[1]

Gertrude Blanch

The numerical results presented here relate to a two-dimensional parabolic partial differential equation containing a nonlinear term. Denoting the independent variables by $t$ and $x$, a lattice is introduced, with intervals $k$ and $h$ in the $t$-and $x$-directions, respectively. Much attention has been devoted recently to the study of the conditions on the mesh ratio, $k/h^2$, under which an approximation by a difference equation converges to the solution of the differential equation for sufficiently small $h$. Some known results are summarized in sections 1 and 2, and three approximation formulas are given, one of order two, and two of order four. The feasibility of using approximation formulas of order higher than the differential equation is studied in later sections. The primary objective of this paper is to seek the *most economical* mesh ratio for a given approximation formula, that is, of all mesh ratios that will lead to a preassigned upper bound of error in the approximation, to choose that mesh ratio that will lead to the least amount of work. It is shown in section 3 that the largest admissible mesh ratio is not necessarily the most economical one and that a great deal depends on the form of the differential system and the boundary conditions.

In section 4 a generalization is given of the method of Hartree and Womersley (1937) for improving a solution from two difference approximations. The method is shown to be very effective for suitable boundary conditions. Five numerical examples are presented and analyzed in section 5. An appendix, with detailed derivations of the formulas used, is given for the benefit of those who may want to apply the formulas to specific studies.

## 1. Definitions; Basic formulas

Once the existence of a unique solution to a differential equation has been established, and an approximating function has been found that converges to the solution under suitable conditions, there remains the problem of providing an effective numerical treatment of the approximation. Our study concerns itself with one phase of this problem, for the case when the approximating function is expressed by a difference equation. We shall further limit the discussion to a specific type of differential equation, namely,

$$\frac{\partial u}{\partial t}=\frac{\partial^2 u}{\partial x^2}+f(x,t,u) \quad 0\le x\le x_a; \quad 0\le t\le t_N \tag{1}$$

with given initial and boundary conditions. Let us introduce a lattice covering the region, at intervals $h$ in the $x$-direction and $k$ in the $t$-direction. Let $\lambda=k/h^2$ be the *mesh ratio*. It is a trivial restriction to assume that $x_a=sh$, where $s$ is an integer.

NOTATION. For the sake of brevity, we shall write $u(x,t)=u_{m,n}$, if $(x,t)$ is a lattice point.

$$\left[\frac{\partial^p g}{\partial x^r \partial t^{p-r}}\right]_{k,n}=\frac{\partial^p g_{k,n}}{\partial x^r \partial t^{p-r}},$$

where $g$ is any function under consideration. Furthermore, following the usual convention for even central differences, we define,

$$\delta_x^{2p} u_{m,n}=\sum_{w=-p}^{w=p}(-1)^{p+w}\binom{2p}{p+w}u_{m+w,n}. \tag{2}$$

The point in the $x,t$-plane with coordinates $x=mh$, $t=nk$ will be denoted by $(m,n)$.

Let $u$ be regular at $(m,n)$. Then for $k$ sufficiently small there is a Taylor series in $t$ around $(m,n)$

$$u_{m,n+1}=u_{m,n}+\sum_{p=1}^{\infty}\frac{k^p}{p!}\frac{\partial^p u_{m,n}}{\partial t^p}. \tag{3}$$

If in (3) terms involving $p\ge 2$ are dropped, and if $\partial u/\partial t$ is replaced by the right-hand side of (1), with $\partial^2 u/\partial x^2$ approximated by central differences, we get the well-known approximation to $u$:

$$\begin{aligned} v_{m,n+1}&=v_{m,n}+\lambda\delta^2_{m,n}+kf_{m,n}\\ &=(1-2\lambda)v_{m,n}+\lambda(v_{m-1,n}+v_{m+1,n})+kf_{m,n}. \end{aligned} \tag{4}$$

Similarly, if terms through $p=2$ are retained, we obtain,

$$\begin{aligned} v_{m,n+1}&=v_{m,n}+\left[\lambda\delta^2+\left(\frac{\lambda^2}{2}-\frac{\lambda}{12}\right)\delta^4\right]v_{m,n}+k\varphi_{m,n}\\ &=\left(1-\frac{5}{2}\lambda+3\lambda^2\right)v_{m,n}+\left(\frac{4}{3}\lambda-2\lambda^2\right)(v_{m-1,n}+v_{m+1,n})\\ &\quad+\left(\frac{\lambda^2}{2}-\frac{\lambda}{12}\right)(v_{m-2,n}+v_{m+2,n})+k\varphi_{m,n}, \end{aligned} \tag{5}$$

[1] The preparation of this paper was sponsored (in part) by the Office of Naval Research, USN.

where

$$\varphi_{m,n}=kf_{m,n}+\tfrac{1}{2}k^2\left(\frac{df_{m,n}}{dt}+\frac{d^2f_{m,n}}{dx^2}\right).$$

Formulas (4) and (5) need modification at the boundary to satisfy given initial and boundary conditions to a required accuracy. This modification can, in general, be made. In the present study we shall assume that all required derivatives exist and are continuous. For parabolic equations this is not a serious restriction, for let us assume that we have generated values of $v$ for a given $t$. From (4) and (5) it is clear that these serve as boundary values in a subdomain for generating the set of values for the next $t$ in the lattice. In imposing the continuity restrictions, we therefore merely imply that regions close to the given boundary, which may have "corners" or other discontinuities, will be treated separately. This in fact must usually be done in practice, either by choosing a lattice that is much finer than that required over the major portion of the region or by special approximations that are appropriate for the particular problem. Our main concern here is with the choice of the mesh ratio, $\lambda$, for the major portion of the domain where the function is presumed to be regular. The manner in which an error (or variation) in the boundary conditions is propagated over the rest of the domain must, of course, be examined; but this problem is no different at the boundary of the given domain than at any of the subdomains (that is, at the successive values of $t$ in the lattice). This problem will not be considered here.

*Truncation terms.* Let $\sigma_{m,n}=u_{m,n}-v_{m,n}$. It can be verified that corresponding to (4),

$$\sigma_{m,n+1}=\sigma_{m,n}+\lambda\delta^2\sigma_{m,n}+k\,\frac{\partial\overline{f}_{m,n}}{\partial u}\,\sigma_{m,n}+kT_{2,m,n}, \quad (6)$$

where

$$T_{2,m,n}=h^2\left[\left(\frac{\lambda}{2}-\frac{1}{12}\right)\frac{\partial^4u_{m,n}}{\partial x^4}+\theta_1\right]+O(h^3). \quad (7a)$$

Another form for $T_{2,m,n}$ is given below:

$$T_{2,m,n}=h^2\left[\frac{\lambda}{2}\,\frac{\partial^2u_{m,n}}{\partial t^2}-\frac{1}{12}\,\frac{\partial^4u_{m,n}}{\partial x^4}\right]+O(h^3). \quad (7b)$$

Corresponding to (5),

$$\sigma_{m,n+1}\cong\sigma_{m,n}+\lambda\delta^2+\left(\frac{\lambda^2}{2}-\frac{\lambda}{12}\right)\delta^4\sigma_{m,n}+\left[k\,\frac{\partial\overline{\varphi}}{\partial u}\right]_{m,n}\sigma_{m,n}+kT_{4,m,n}, \quad (8)$$

where two expressions for $T_{4,m,n}$ are given below.

$$T_{4,m,n}=h^4\left[M(\lambda)\,\frac{\partial^6u_{m,n}}{\partial x^6}+\theta_2\right]+O(h^5), \quad (9a)$$

$$T_{4,m,n}=h^4\left[\frac{\lambda^2}{6}\,\frac{\partial^3u_{m,n}}{\partial t^3}+\left(\frac{1}{90}-\frac{\lambda}{12}\right)\frac{\partial^6u_{m,n}}{\partial x^6}\right]+O(h^5) \quad (9b)$$

where

$$M(\lambda)=\frac{\lambda^2}{6}-\frac{\lambda}{12}+\frac{1}{90}. \quad (10)$$

In the above $\theta_1$ and $\theta_2$ depend on $f$ and its derivatives; if $f=0$, then $\theta_1=\theta_2=0$. Further, $\partial\overline{f}/\partial u$ and $\partial\overline{\varphi}/\partial u$ imply evaluation of these functions at $(m,n)$ corresponding to a value of $\overline{u}$ intermediate between $u_{m,n}$ and $v_{m,n}$. Again, (6), (7), (8), and (9) need modification in the immediate vicinity of the boundary.

Definition. $T_{r,m,n}$ will be said to be of order $r$ if it contains $h^r$ as a factor, but not $h^{r+1}$.

## 2. Stability Considerations; Bounds for the Errors in the Approximations

Definition. The solution $v(x,t)$ of an approximating difference equation will be defined as *stable* if it is bounded for all finite $t$, independently of $h$.

Consider the special case when $f(x,t,u)=0$, and $u(x,0)=A(x)$ is defined and bounded for $-\infty<x<\infty$. It will be convenient to refer to the differential eq (1) under these special conditions as the *basic homogeneous* equation. Let this basic homogeneous equation be approximated by a difference equation of order $2p$, so that we can write,

$$v_{m,n+1}=\sum_{w=0}^{p}b_w\delta^{2w}v_{m,n}\equiv\sum_{w=0}^{p}a_wv_{m+w,n}, \quad (11)$$

where the coefficients $b_w$ and $a_w$ are suitable constants. It is easy to show that $\Sigma a_w=1$; in general, the coefficients $a_w$ will be functions of $\lambda$. Let $q$ be an upper bound of $|A(x)|$. If it is possible to choose $\lambda$ so that all the coefficients $a_w$ are nonnegative, we shall have, from (11),

$$|v_{m,1}|\leq\Sigma a_w|v_{m+w,0}|\leq q\Sigma a_w=q,$$

and by induction on $n$ we can establish that $|v_{m,n}|\leq q$ for all $m,n$; hence $v(x,t)$ is stable. The condition that all $a_w$ be nonnegative is therefore a sufficient, though not a necessary condition [2] for the stability of $v(x,t)$ in the case of the basic, homogeneous

[2] The above definition of stability and the observation that (11) is stable when all the coefficients $a_w$ are nonnegative were mentioned by F. John in seminar talks at the Institute for Numerical Analysis.

equation. We shall refer to the range of $\lambda$ for which the basic, homogeneous equation is stable as the "admissible" range of $\lambda$. In what follows $\lambda$ will always be chosen to lie within the admissible range; this may not guarantee that the solution $v(x,t)$ will be stable for arbitrary boundary conditions and functions $f(x,t,u)$. However, the choice of $\lambda$ within this range usually simplifies the error analysis for any set of boundary conditions, even when (1) is not homogeneous.

Turning now to the first approximation formula defined by (4), it is clear that the admissible range of $\lambda$ is $0<\lambda\leq\frac{1}{2}$. The corresponding equations for $\sigma_{m,n}$ are given in (6). Let $\tau$ be an upper bound of $|T_{2,m,n}|$ and let $\omega$ be an upper bound of $|\partial f/\partial u|$, this upper bound to be independent of $h$. If $\sigma_{m,0}=0$, eq (6) yields, for a wide range of initial and boundary conditions, $|\sigma_{m,1}|<k\tau$. Since $\lambda$ is in the admissible range, we have further

$$|\sigma_{m,n+1}|\leq|\sigma_{m,n}|(1+k\omega)|+k\tau.$$

Now $(1+k\omega)^N\leq e^{t\omega}$, where $t=Nk$; hence at time $t$,

$$|\sigma_{m,N}|\leq t\tau e^{t\omega}. \tag{12}$$

Boundary conditions may impose modification of (12). If the conditions are such that no negative power of $h$ is added as a factor to the right-hand side of the inequality (12), then it can be shown from the form of $T_{2,m,n}$ that an upper bound of $\tau$ can be found that has $h^2$ as a factor. It follows then from (12) that $v_{m,n}\to u_{m,n}$ as $h\to 0$.

Let us now consider the second approximation formula, defined by (5). The coefficients of $v_{m+w,n}|\pm w=0,1,2]$ in (5) will all be positive if $0<\lambda\leq\frac{2}{3}$. The approximation $v(x,t)$ to the basic homogeneous equation will therefore be stable for this range of $\lambda$, and by the same analysis as before, we can show that $v(x,t)$ approaches $u(x,t)$ as $h$ approaches zero, for a wide range of boundary conditions.

## 3. Criteria for the Choice of a Suitable Mesh Ratio

The error $\sigma_{m,n}$ is a function of $h,\lambda$, and of the boundary conditions associated with the differential equation. Given an upper bound of error that can be tolerated in the solution, the problem involves choosing $h$ and $\lambda$ (the latter within the admissible range) so as to meet requirements with the least amount of work. We shall assume that for a given approximation scheme, the work is proportional to the number of lattice points at which $u_{m,n}$ must be evaluated. This is not strictly true. For let us define a *profile* as a set of values of $v_{m,n}$ for a fixed $n$, and all $m\leq s$. If, for example, successive profiles are generated from preceding ones on an IBM machine such as the card programmed calculator, then merging operations may be required at the end of a profile which may consume some time. Thus a grid of 10 points in the $x$-direction and 100 points in the $t$-direction may take more time to generate than a grid of 20 points in the $x$-direction and 50 points in the $t$-direction. Nevertheless, the assumption that the work is proportional to the number of lattice points is close enough to reality to be useful. Of course, the complexity of the programming must be considered; thus an approximation formula of order four may take more machine cycles (hence more time) than one of order two. However, for the same approximation scheme, the choice of $\lambda$ does not change the amount of work radically. Let $X=sh$ be the range of $x$ and $t_1=Nk$ the range of $t$. The number of lattice points in the region is $Ns=(Xt_1/hk)=Xt_1/\lambda h^2$. As $Xt_1$ is fixed, the work required for a given approximation scheme is therefore inversely proportional to $\lambda h$.[3]

If the exact solution for $\sigma_{m,n}$ were known, it would be theoretically possible to study the magnitude of the error for various choices of $\lambda$ and $h$ corresponding to a given approximation scheme. The precise solution $\sigma_{m,n}$ is not easy to find. However, from (12), it is clear that an upper bound which can be approximated has $|T_{r,m,n}|$ as a factor. We shall, therefore, aim to choose $\lambda$ and $h$ in such a manner as to make $|T_{r,m,n}|$ small. Moreover, for both approximation formulas (4) and (5), the successive terms of $h^2T_{r,m,n}$ involve $h^{r+p}\partial^{r+p}u/\partial x^{r+p}$ and $h^{r+p}\partial^{r+p}f/\partial x^{r+p}$. We shall require that for all choices of $\lambda$, the interval $h$ be sufficiently small so as to satisfy

$$|\delta^{r+p}u|>c|\delta^{r+p+1}u|,\quad p\geq 0,\quad 0<c<1, \tag{13}$$

almost everywhere. From the known relations connecting derivatives with differences, it is clear that (13) implies that successive terms of $T_{r,m,n}$ will be numerically smaller than preceding ones. The phrase "almost everywhere" for the condition (13) needs explanation. It may happen that in a region where $\delta^{r+p}u$ changes sign, a few entries of $\delta^{r+p}u$ may be numerically smaller than corresponding entries in the higher differences. Such a case may also arise near critical points. In particular the condition (13) shall be satisfied by the initially given values and $f(x,0,u)$. In practice one often requires that $c$ be $\frac{1}{10}$ or $\frac{1}{5}$. For one powerful check on the accuracy of computed values is obtained from the pattern of successive differences of the entries. Hence, even if the criterion (13) were unnecessary from the viewpoint of estimating an upper bound of error in the solution, it would still be a desirable condition to impose, in order to insure that the computed values difference with reasonable ease. We shall further require that the term of $T_{r,m,n}$ involving the lowest power of $h$ shall approximate the magnitude of $T_{r,m,n}$ to within a factor of two. The fact that a restriction is thereby imposed on $h$ must be clearly kept in mind. In general a value of $h$ small enough to satisfy (13) will not necessarily make $|T_{r,m,n}|$ small enough to meet requirements for a given upper bound of error in

[3] It is no serious restriction to consider the range $t_1$ as an integral multiple of $h$.

the solution. In the instance when it does not, the problem posed is to choose $\lambda$ and $h$ judiciously, so as to bring the truncating error within permissible bounds with the least amount of work. But if the required accuracy is rather low, it may well happen that after $h$ is chosen small enough to satisfy (13), the error measured by $T_{r,m,n}$ may already be small enough to meet all requirements. In that case the largest $\lambda$ within the admissible range will, of course, lead to the least amount of work.

With these observations we shall now attempt to study the dependance of the truncation term on $\lambda$ and on $h$. Ideally, it would be desirable to classify differential equations into several types, according to the value of $\lambda$ which is appropriate for equations belonging to the type in question. A complete classification is difficult to set down, but an attempt in this direction is made by considering two types:

TYPE I. This type is characterized by the following conditions:

$$\frac{df}{dt}+\frac{d^2f}{dx^2}=\frac{d^4f}{dx^4}=0. \tag{14}$$

When (14) holds, it follows that

$$\frac{\partial^2 u}{\partial t^2}=\frac{\partial^4 u}{\partial x^4}, \quad \frac{\partial^3 u}{\partial t^3}=\frac{\partial^6 u}{\partial x^6}.$$

It can be shown that for systems belonging to type I, the terms of $T_{r,m,n}$, $r\leq 4$, do not involve $f(x,t,u)$ or its derivatives. The basic homogenous equation belongs to this type.

TYPE II. This type is characterized by the condition that successive derivatives of $u(x,t)$ with respect to $t$ are known to be much smaller than corresponding derivatives with respect to $x$ (usually of twice the order) with which they are associated in truncation terms such as (7b) and (9b). It is quite easy to find systems belonging to this type; the numerical illustration given in section 5 belongs to type II.

Consider differential systems of type I, and let us start with the case when formula (4) is used. The corresponding truncation term, $T_{2,m,n}$, is given by (7a). It has been observed by Milne, as well as by Thomas and others, that if $\lambda$ is chosen as $\frac{1}{6}$, then the leading term of $T_{2,m,n}$ vanishes, so that the order of $T_{2,m,n}$ becomes four. With $\lambda=\frac{1}{6}$ and $h$ small enough to satisfy the conditions for an upper bound of $|T_{2,m,n}|$—enough to meet the requirements for a given upper bound of error in the solution—a certain amount of work will be done, which we shall measure in units of $Z=1/\lambda h^3$, as it has been shown that for a rectangular lattice the work is proportional to $Z$, approximately. If another $\lambda$ and $h$ were chosen, then we shall ask whether, for the *same amount of work*, and using the same formula (4), greater accuracy can be obtained in the solution, assuming that accuracy to be measured by the magnitude of the truncation term. In other words, we shall compare various choices of $\lambda$ and $h$, for a constant $Z$. It can be readily shown that for equations belonging to type I, no other choice of $h$ and $\lambda$, keeping $Z$ constant, will be as good. In this sense it is correct to state that $\lambda=\frac{1}{6}$ is the best choice for formula (4). However, one important point has been overlooked. We have seen that $h$ is not completely free, for $h$ must be small enough to meet the minimum conditions imposed by (13). It may happen that after $h$ has been taken small enough to insure that (13) is satisfied, the conditions for an upper bound of error in the solution can be satisfied with some range of $\lambda>\frac{1}{6}$. In that case, we would certainly get a more *accurate* solution by choosing $\lambda=\frac{1}{6}$, but that would be more accuracy that required, and work could be saved by choosing a larger $\lambda$. We conclude that even for equations of type I, the choice of $\lambda=\frac{1}{6}$ will be best only if a relatively high accuracy is required in the solution. Moreover, in practice the differences of $u(x,t)$ can usually be judged only from the initially given profile, at the time when $\lambda$ and $h$ are chosen, so that a *safe* interval $h$ (rather than the maximum permissible for the given profile) is often chosen, and it may happen that the value of $h$ considered necessary may, as stated, bring the error within the tolerance limits for all choices of $\lambda$.

Still considering systems that belong to type I, let us now examine approximations of order four. The expression for the truncation term $T_{4,m,n}$ is given in (9a) and the term of order four is

$$h^4A_4(x,t,\lambda)=h^4\left(\frac{\lambda^2}{6}-\frac{\lambda}{12}+\frac{1}{90}\right)\frac{\partial^6 u_{m,n}}{\partial x^6}=h^4M(\lambda)\,\frac{\partial^6 u_{m,n}}{\partial x^6}.$$

It can be readily verified that $M(\lambda)$ is positive for all choices of $\lambda$, hence the leading term of $T_{4,m,n}$ cannot be eliminated completely, as in the case of the simpler approximation of order two. However, we may seek that value of $\lambda$ which will make the unit of work, $Z=1/\lambda h^3$, a minimum, subject to a given permissible upper bound of $|T_{4,m,n}|$. By hypothesis, $h$ is small enough so that $h^4A_4(x,t,\lambda)$ approximates the magnitude of $|T_{4,m,n}|$; hence if $C$ is the permissible tolerance of $|T_{4,m,n}|$, we wish to satisfy

$$h^4|A_4(x,t,\lambda)|=h^4M(\lambda)\left|\frac{\partial^6 u}{\partial x^6}\right|\leq C, \tag{15}$$

Since $|\partial^6 u/\partial x^6|$ is independent of the choice of parameters $h$ and $\lambda$, the inequality expressed in (15) can be satisfied by taking

$$h^4M(\lambda)=C_1; \quad C_1\leq C/\left|\frac{\partial^6 u}{\partial x^6}\right|. \tag{16}$$

Thus we seek to determine $h$ and $\lambda$, which minimize $Z$,

subject to the condition

$$h^4M(\lambda)=C_1. \tag{17}$$

From (17), $h=C_1/[M(\lambda)]^{\frac{1}{4}}$. Substituting this value of $h$ into $Z$ and differentiating the resulting expression of $Z$ with respect to $\lambda$, we obtain the following condition for a minimum of $Z$:

$$F=3\lambda M'(\lambda)-4M(\lambda)=0,$$

or

$$60\lambda^2+15\lambda-8=0. \tag{18}$$

The positive root of (18) is $\lambda_1=0.26095$ . . ., and it can be verified that $F'(\lambda_1)$ is positive, so that $Z$ is indeed a minimum for this value of $\lambda$. Since $\lambda$ lies within the admissible range, it can be used for the mesh ratio, in conjunction with a suitable value of $h$ which satisfies (18). In practice, $\lambda=0.25$ will normally be used, because an irrational value of $\lambda$ is inconvenient.

It will be instructive to examine the following schedule, which gives $M(\lambda)$, $h$, and the work unit $Z$ *for a constant value of* $h^4M(\lambda)$, and various values of $\lambda$ within the admissible range, in units of the corresponding quantities when $\lambda=\frac{1}{2}$.

| $\lambda$ | $M(\lambda)=\left(\frac{\lambda^2}{6}-\frac{\lambda}{12}+\frac{1}{90}\right)$ | $h$ | $Z=1/(\lambda h^3)$ |
|---|---|---|---|
| $\frac{1}{6}$ | 0.001851 | $1.565h_1$ | $0.782z_1$ |
| $\frac{1}{5}$ | .001111 | $1.778h_1$ | $.444z_1$ |
| $\frac{1}{4}$ | .000694 | $2.000h_1$ | $.25z_1$ |
| $\frac{3}{10}$ | .001111 | $1.778h_1$ | $.297z_1$ |
| $\frac{1}{3}$ | .001851 | $1.568h_1$ | $.391z_1$ |
| $\frac{3}{8}$ | .003299 | $1.354h_1$ | $.536z_1$ |
| $\frac{1}{2}$ | .011111 | $h_1$ | $z_1$ |
| $\frac{2}{3}$ | .029630 | $0.783h_1$ | $1.565z_1$ |

Compared with a unit of work $Z_1$ for the case $\lambda=\frac{1}{2}$, only $\frac{1}{4}Z_1$ is required when $\lambda=\frac{1}{4}$. The largest admissible value of $\lambda$ is the poorest of all, from the viewpoint of the amount of work required. Again, a word of caution is required. For the same magnitude of the error in the leading term of $T_{4,m,r}$ and different choices of $\lambda$, the above schedule shows that with $\lambda=\frac{1}{4}$, $h$ can be chosen twice as large as that required when $\lambda=\frac{1}{2}$. If $h$ is made twice as large, the eighth difference in the $x$-direction is multiplied by about $2^8$, and the differences must be reexamined to see whether this larger value of the eighth difference still satisfies the fundamental conditions imposed by (13) namely that successive differences in the $x$-direction beyond the fourth be numerically smaller than preceding ones. Moreover, it has been pointed out before that the maximum $h$ corresponding to which (13) is satisfied may already be such that $T_{4,m,n}$ is within the required tolerance for all admissible values of $\lambda$. In that case it is of course best to choose $\lambda=\frac{2}{3}$ or one close to it.

The following question arises: since the simpler approximation (4) has a truncating error of order four when $\lambda=\frac{1}{6}$, and $T_{4,m,n}$ is also of order four, is there any gain in using the approximation formula of higher order? The answer to this question is complicated by the fact that the time required to generate a profile corresponding to the higher approximation may be considerably longer than that for the simpler approximation. Much will depend not only on the computing instrument which will be used, but also on the complexity of the boundary conditions. If the IBM card programmed calculator is to be used, and the boundary conditions are not too complex, the simpler approximation (4) can perhaps be generated in only two-thirds of the time per profile, compared with the more elaborate fourth order approximation given in (5). There are, however, compensating factors which make the higher approximation worth considering. Let us assume we are dealing with a case where the "best" values of $\lambda$ are used in the approximation of order two and the one of order four. For the same $h$ used in both cases, the number of lattice points is inversely proportional to $\lambda$. Hence, we shall use only two-thirds the number of lattice points when the higher approximation is used. This would about compensate for the longer time it may take to generate each profile. There is, however, a gain in accuracy when the higher approximation is used. For the coefficient of $h^4(\partial^6u/\partial x^6)$ in (9a), corresponding to the simpler approximation, is 1/540 when $\lambda=\frac{1}{6}$. On the other hand, the coefficient of the corresponding term in the higher approximation with $\lambda=\frac{1}{4}$ is only 0.000694; or less than three-eighths that of the simpler approximation. Furthermore, in cases where the maximum permissible $h$ is such that $T_{4,m,n}$ is already within the required tolerance limit for all values of $\lambda$, we may be able to take $\lambda=\frac{2}{3}$, or close to it, when the higher approximation is used. Such a choice of $\lambda$ would cut the number of lattice points to $\frac{1}{4}$ that required for the simpler approximation, with $\lambda=\frac{1}{6}$, and that might more than compensate for the greater difficulty in generating $v(x,t)$ by the higher approximation.

Let us now consider differential systems that belong to type II. Since, by hypothesis, the derivatives in the $t$-direction are negligible compared with those in the $x$-direction, (7b) shows that the leading term in $T_{2,m,n}$ is practically independent of $\lambda$, and this term cannot be eliminated by any choice of $\lambda$. Hence, it is reasonable to take the maximum admissible $\lambda$, or one close to it. Similarly, the leading term of $T_{4,m,n}$ is complex in structure, and there is no optimum $\lambda$ that stands out as suitable for all functions falling under this type. For a given problem, it may be possible to compute estimates of the various terms that contribute to the truncation error. Or if the problem involves a family of parameters, in the boundary condition, then available results for some members of the family may lead to an optimum choice of $\lambda$ and $h$ for the remaining ones.

For equations falling under type II the higher approximation formula usually has distinct advantages over the simpler one of order two. For in this case the truncation term is necessarily of a lower order of magnitude in the higher approximation formula than in the simpler one; moreover, a larger mesh ratio, namely, $\frac{2}{3}$, can be taken. Whenever the boundary conditions are such that the coding problem is manageable, the higher approximation formula is to be recommended.

It might be well to remark that in some cases the solution may be an oscillating function of $x$ but not of $t$. Such functions may fall under type II, and a Fourier approximation may actually be better than a finite difference approximation. However, there is no reason to expect that all, or even a good portion of functions belonging to type II, can be most simply treated by Fourier approximations. A finite difference approximation such as (4) or (5) is often preferred, because of its simplicity, to other types of approximations (by Fourier series or perhaps "implicit" difference approximations). Our concern here, as stated before, is to study the dependence of the solution on the choice of $\lambda$, after either (4) or (5) has been selected as the approximation formula.

## 4. Method of Improving the Solution from Two Difference Approximations

The method to be explained below has been presented in [1] [4] by Hartree and Womersley, who ascribe the idea to L. F. Richardson [5]. In [1] the method is applied to a somewhat different type of approximation—a mixed difference—differential scheme, suitable for computation by a differential analyzer. The results will here be extended to difference approximations of any other.

Let us suppose that values of $v_{m,n}$ have been generated by an approximation formula, corresponding to a true solution $u_{m,n}$, and let us assume that it is possible to write

$$\sigma_{m,n} = u_{m,n} - v_{m,n} = h^r C_r(x, t, \lambda) + h^{r+1} C_{r+1}(x, t, \lambda) + \ldots \quad , \tag{19}$$

where the functions $C_j(x,t,\lambda)$ are independent of $h$. It can be shown that corresponding to a wide range of boundary conditions the expression for $\sigma_{m,n}$ does assume the form (19) for both approximation formulas (4) and (5).

Consider now the case when $v_{m,n}$ has been generated by the use of an interval $h_1$ in the $x$-direction and a mesh-ratio $\lambda$. Let these values of $v_{m,n}$ be designated by $v_{m,n}(h_1)$. Now let another computation be made, based on the same mesh ratio $\lambda$, but at an interval $h_2$ in $x$, where $h_2 = \rho h_1$, $0 < \rho < 1$. These values will be designated [5] by $v_{m,n}(h_2)$. It is presumed that the same approximation formula will be used in both cases. Clearly,

$$v_{m,0}(h_1) = v_{m,0}(h_2) = u_{m,0}; \quad v_{s,n}(h_1) = v_{s,n}(h_2) = u_{s,n}.$$

By hypothesis, we have from (19)

$$u_{m,n} - v_{m,n}(h_1) = h_1^r C_r + h_1^{r+1} C_{r+1} + h_1^{r+2} C_{r+2} + \ldots \quad . \tag{20}$$

Similarly, remembering that $h_2 = \rho h_1$ and that $C_j$ is independent of $h$,

$$u_{m,n} - v_{m,n}(h_2) = \rho^r h_1^r C_r + \rho^{r+1} h_1^{r+1} C_{r+1} + \rho^{r+2} h_1^{r+2} C_{r+2} + \ldots \quad . \tag{21}$$

Multiply (20) by $\rho^r$ and subtract from (21). This gives, after transposing some terms and dividing by $(1-\rho^r)$,

$$u_{m,n} = v_{m,n}(h_1,h_2) - \frac{\rho^r(1-\rho)}{1-\rho^r} h^{r+1} C_{r+1} - \rho^r \frac{(1-\rho^2)}{1-\rho^r} h^{r+2} C_{r+2} + \ldots \quad , \tag{22}$$

where

$$v_{m,n}(h_1,h_2) = \frac{v_{m,n}(h_2) - \rho^r v_{m,n}(h_1)}{1-\rho^r}. \tag{23}$$

We shall refer to the process defined in (23) as the "$\rho^r$" correction. In [1] it is recommended that $\rho$ be taken as $\frac{1}{2}$. This is a desirable choice for numerical work, since every other value in the $x$-direction at the smaller interval is available at the larger interval. Similarly, every fourth value in the $t$-direction will be available at both intervals. There are many ways of applying corrections of this type. One way, for example, is to generate four values in the $t$-direction at the finer interval, then generate the corresponding values at the larger interval; apply the $\rho^r$ correction to the last profile, and use these corrected values as initial data for generating the next profile. Such a use of the correction scheme would, of course, require interpolating for values of $v(h_1,h_2)$ for every other value of $x$, since we can correct only for those points that are available at both intervals. The coding of this method would be complicated. The simplest way of using the correction scheme is to actually make two completely separate computations for all required values of $n$, and then to apply the correction process only to those functional values that are required. Often the last profile generated is of most interest, and in that case it may be enough to correct the values on the last computed profile only.

The process furnishes a powerful check on the convergence rate of the approximations, and since the work done at the larger interval is one-eighth that done at the smaller interval if $\rho = \frac{1}{2}$, the added labor is not too costly, when the two computations are carried separately. Moreover, the coding is the same

[4] Figures in brackets indicate the literature references at the end of this paper.

[5] In the subsequent discussions we shall write $v(h_2)$, or $v(h_1,h_2)$ to indicate $v_{m,n}(h_2)$ or $v_{m,n}(h_1,h_2)$, when no ambiguity is likely to arise.

for both approximation schemes. For the special case when $r=2$, (22) and (23) reduce to

$$u_{m,n}=v_{m,n}(h_1,h_2)-\frac{\rho^2h^4C_3}{1+\rho}-\rho^2h^4C_4+\cdots, \quad (24)$$

where

$$v_{m,n}(h_1,h_2)=\frac{v_{m,n}(h_2)-\rho^2v_{m,n}(h_1)}{1-\rho^2}. \quad (25)$$

The "$\rho^r$" correction has been applied in the numerical examples given in section 5 with highly satisfactory results. In [1] Hartree and Womersley give *sufficient* conditions on the nature of the boundary for the method to be valid; the method can probably be used over a wider class of functions than those specified in [1].

If $h_1$ is sufficiently small, $v(h_1,h_2)$ will always be an improvement over $u(h_2)$, since the truncation term is of lower order of magnitude in $v(h_1,h_2)$. The question arises: how small must $h$ be to insure that $v(h_1,h_2)$ shall be an improvement over $u(h_2)$? Let the truncation term, $T_{r,m,n}$, now be identified by $T_{r,m,n}(h)$, when associated with an interval $h$ in the $x$ directions, and let

$$\sigma(h_1,h_2)=u-v(h_1,h_2); \quad \sigma(h)=u=v(h);$$

$$T_{r,m,n}(h_1,h_2)=\frac{T_{r,m,n}(h_2)-\rho^rT_{r,m,n}(h_1)}{1-\rho^r}. \quad (26)$$

It is more difficult to get a good estimate of $\sigma$ than of $T_{r,m,n}$. Just as in section 3, we shall, therefore, inquire under what conditions the inequality

$$|T_{r,m,n}(h_1,h_2)|<|T_{r,m,n}(h_2)| \quad (27)$$

will be satisfied. A numerically smaller truncation term will usually be associated with a smaller total error. For the approximation formulas considered here the truncation term is of the form

$$T_{r,m,n}(h_2)=\sum_{p=r}^{\infty}\rho^ph^pg_p(x,t,u).$$

Moreover, the condition following eq (13) guarantees that

$$T_{r,m,n}(h_2)\cong\rho^rh^rg_r(x,t,u). \quad (28)$$

But no similar statement was made about $T_{r,m,n}(h_1)$. Now from

$$T_{r,m,n}(h_1,h_2)=\frac{-\sum_{p=1}^{\infty}\rho^r(1-\rho^p)h^{r+p}g_{r+p}(x,t,u)}{(1-\rho^r)}.$$

If we can satisfy

$$|hg_{r+p}(x,t,u)|\leq|\rho^cg_{r+p-1}(x,t,u)|, \quad (29)$$

where

$$\rho^c=1-\rho^r, \quad (30)$$

then from (27) and (30) it can be shown by summing the absolute values of the terms of $T_{r,m,n}(h_1,h_2)$ that (27) is satisfied. When $\rho=\frac{1}{2}$ and $r=2$, the condition (29) implies that $\rho^c=\frac{3}{4}$. If $\rho=\frac{1}{2}$ and $r=4$, then $\rho^c=\frac{15}{16}$, or what is equivalent, successive terms of $T_{r,m,n}$ at the larger interval are required to be just smaller numerically than preceding terms. Under such conditions $v(h_1,h_2)$ will always be an improvement over $u(h_2)$.

In the foregoing, it has been assumed that $v_{m,n}$ can be computed exactly by the prescribed formula, and that all initial and boundary conditions are exact. This can seldom be realized in practice, and there will be rounding errors committed at every step of the computation, due to carrying a fixed number of decimals or significant figures in the computations. The cumulative effect of such errors can perhaps be studied statistically, or upper bounds for errors of this type [2] can be found. In the numerical examples given in section 5, the cumulative round-off error was very small, after 100 steps in $t$.

## 5. Numerical Examples

The problem selected for analysis was the following one:

$$\frac{\partial u}{\partial t}=\frac{\partial^2u}{\partial x^2}+f(x,u). \quad (31)$$

$$\text{At } t=0, \quad u=(10x^2+x^3+0.64)^{1/2}=A(x);$$

$$\text{at } x=1, \quad u=(11.64+t)^{1/2}=B(t).$$

$$\left[\frac{\partial u}{\partial x}\right]_{x=0}=0; \quad f(x,u)=\frac{-(3x+9.5)}{u}+\frac{(10x+1.5x^2)^2}{u^3}.$$

This particular form was chosen because it represents a case in which derivatives with respect to $t$ are much smaller numerically than corresponding derivatives with respect to $x$, with which they are associated in truncation terms such as those of (7b). The differential system belongs to type II of section 3. It is known that the exact solution to the problem is

$$u=(10x^2+x^3+0.64+t)^{1/2}.$$

The choice of a nonlinear form of the differential equation was deliberate. It was made in order to study the cumulative error in cases where a considerable number of operations, that involve the approximate values of $u$, have to be performed at each step.

The following five sets of solutions were generated:

EXAMPLE 1.

Formula:

$$v_{m,n+1}=v_{m,n}+\lambda\delta^2 v_{m,n}+kf_{m,n};\quad v_{m,o}=A(x);$$

$$v_{s,n}=B(t);\quad sh=1.$$

$$v_{-1,n}=v_{1,n}+\frac{h^3}{3}\left[\frac{\partial f}{\partial x}\right]_{x=0}=v_{1,n}-\frac{h^3}{v_{0,n}}.$$

Parameters: $h=0.05=h_2$; $k=0.00125$; $\lambda=\frac{1}{2}$.
Range of $t$: $0\leq t\leq 0.125$.
Number of lattice points: $20\times 100=2{,}000$.
Initial values and the computed values of $v_{s,n}$ for the last profile are given in table 1.

TABLE 1. *Solution of the difference equation*

$$v_{m,n+1}=v_{m,n}+\lambda\delta^2 v_{m,n}+kf(x,u);\quad v_{-1,n}=v_{1,n}-\frac{h^3}{v_{0,n}}$$

$$At\ t=0,\quad v(x,0)=(10x^2+x^3+0.64)^{\frac{1}{2}};\quad At\ x=1,\quad v(1,t)=(11.64+t)^{\frac{1}{2}}$$

$$f(x,v)=\frac{-(3x+9.5)}{v}+\frac{(10x+1.5x^2)^2}{v^3};\quad \lambda=\tfrac{1}{2},\quad h_2=0.05;\quad k=.00125$$

$$u=\sqrt{10x^2+x^3+t+0.64}$$

| $x$ | $v(x,0)$ | At $t=0.125$ | | |
|---|---|---|---|---|
| | | $v(x,t)$ | $u(x,t)$ | $u(x,t)-v(x,t)$ |
| 0.00 | 0.8000000 | 0.8720400 | 0.8746427 | +.0026027 |
| .05 | .8155520 | .8864322 | .8888897 | +.0024575 |
| .10 | .8608136 | .9285124 | .9305912 | +.0020788 |
| .15 | .9318664 | .9950813 | .9966819 | +.0016006 |
| .20 | 1.0237187 | 1.0819105 | 1.0830512 | +.0011407 |
| .25 | 1.1316470 | 1.1848335 | 1.1855905 | +.0007570 |
| .30 | 1.2517987 | 1.3003062 | 1.3007690 | +.0004628 |
| .35 | 1.3812585 | 1.4255420 | 1.4257892 | +.0002472 |
| .40 | 1.5178933 | 1.5584295 | 1.5585249 | +.0000954 |
| .45 | 1.6601581 | 1.6973964 | 1.6973876 | −.0000088 |
| .50 | 1.8069311 | 1.8412718 | 1.8411952 | −.0000766 |
| .55 | 1.9573898 | 1.9891819 | 1.9890638 | −.0001181 |
| .60 | 2.1109240 | 2.1404665 | 2.1403270 | −.0001395 |
| .65 | 2.2670741 | 2.2946235 | 2.2944770 | −.0001465 |
| .70 | 2.4254896 | 2.4512642 | 2.4511221 | −.0001421 |
| .75 | 2.5858993 | 2.6100866 | 2.6099568 | −.0001298 |
| .80 | 2.7480902 | 2.7708507 | 2.7707399 | −.0001108 |
| .85 | 2.9118937 | 2.9333664 | 2.9332788 | −.0000876 |
| .90 | 3.0771740 | 3.0974789 | 3.0974182 | −.0000607 |
| .95 | 3.2438210 | 3.2630627 | 3.2630315 | −.0000312 |
| 1.00 | 3.4117444 | 3.4300145 | 3.4300145 | 0 |

EXAMPLE 2.
Formula: The same as in example 1.
Parameters: $h=0.1=h_1$; $k=0.005$; $\lambda=\frac{1}{2}$.
Range of $t$: The same as in example 1.
Number of lattice points: $10\times 25=250$.
Initial values and the computed values of $v_{m,n}$ for the last profile are given in table 2.

TABLE 2. *Solution of the difference equation described in table 1 and values of* $v(h_1,h_2)$

Parameters: $h_1=0.1$; $k=0.005$, $\lambda=\frac{1}{2}$.

$v(x,t,h_1,h_2)\equiv v(h_1,h_2)=[v(h_2)-\rho^2 v(h_1)]/(1-\rho^2)$; $\rho=\frac{1}{2}$.

$v(h_2)$ given in table 1.

| $x$ | $v(x,0)$ | At $t=0.125$ | | | | |
|---|---|---|---|---|---|---|
| | | $v(x,t)$ | $u(x,t)$ | $u(x,t)-v(x,t)$ | $v(h_1,v_2)$ | $u(x,t)-v(h_1,h_2)$ |
| 0.0 | 0.8000000 | 0.8638878 | 0.8746427 | +.0107549 | 0.8747574 | −.0001147 |
| .1 | .8608136 | .9221349 | .9305912 | +.0084563 | .9306382 | −.0000470 |
| .2 | 1.0237187 | 1.0784844 | 1.0830512 | +.0045668 | 1.0830525 | −.0000013 |
| .3 | 1.2517987 | 1.2989434 | 1.3007690 | +.0018256 | 1.3007605 | +.0000085 |
| .4 | 1.5178933 | 1.5581507 | 1.5585249 | +.0003742 | 1.5585224 | +.0000025 |
| .5 | 1.8069311 | 1.8415191 | 1.8411952 | −.0003239 | 1.8411893 | +.0000059 |
| .6 | 2.1109240 | 2.1408939 | 2.1403270 | −.0005669 | 2.1403240 | +.0000030 |
| .7 | 2.4254896 | 2.4517066 | 2.4511221 | −.0005845 | 2.4511167 | +.0000054 |
| .8 | 2.7480902 | 2.7711921 | 2.7707399 | −.0004522 | 2.7701369 | +.0000030 |
| .9 | 3.0771740 | 3.0976676 | 3.0974182 | −.0002494 | 3.0974160 | +.0000022 |
| 1.0 | 3.4117444 | 3.4300145 | 3.4300145 | 0 | | 0 |

EXAMPLE 3.

Formula: The same as in example 1.

Parameters: $h=1/14$; $k=1/1176$; $\lambda=\frac{1}{6}$.

Range of $t$: The same as in example 1.

Number of lattice points: $14\times147=2058$.

Initial values and the computed values of $v_{m,n}$ for the last profile are given in table 3.

The formula for examples 1 to 3 comes from (4).

TABLE 3. *Solution of the difference equation described in table 1*

Parameters: $h=1/14$, $k=1/1176$; $\lambda=1/6$, $x=mh$.

| $m$ | $v(x,0)$ | At $t=0.125$ | | |
|---|---|---|---|---|
| | | $v(x,t)$ | $u(x,t)$ | $u(x,t)-v(x,t)$ |
| 0 | 0.8000000 | 0.8692554 | 0.8746428 | +.0053874 |
| 1 | .8314955 | .8987549 | .9035402 | +.0047853 |
| 2 | .9203245 | .9824630 | .9858991 | +.0034361 |
| 3 | 1.0531018 | 1.1087660 | 1.1108660 | +.0021000 |
| 4 | 1.2164087 | 1.2656385 | 1.2667479 | +.0011094 |
| 5 | 1.4003800 | 1.4438567 | 1.4443213 | +.0004646 |
| 6 | 1.5985781 | 1.6371338 | 1.6372086 | +.0000748 |
| 7 | 1.8069311 | 1.8413398 | 1.8411953 | −.0001445 |
| 8 | 2.0228433 | 2.0537601 | 2.0535080 | −.0002521 |
| 9 | 2.2446210 | 2.2725815 | 2.2722948 | −.0002867 |
| 10 | 2.4711277 | 2.4965649 | 2.4962917 | −.0002732 |
| 11 | 2.7015788 | 2.7248430 | 2.7246151 | −.0002279 |
| 12 | 2.9354176 | 2.9567941 | 2.9566326 | −.0001615 |
| 13 | 3.1722397 | 3.1919624 | 3.1918811 | −.0000813 |
| 14 | 3.4117444 | 3.4300145 | 3.4300145 | 0 |

EXAMPLE 4.

Formula:

$$v_{m,n+1} = v_{m,n} + \lambda\,(\delta^2 - \tfrac{1}{12}\,\delta^4)\,v_{m,n} + k f_{m,n} \qquad (32)$$

$$v_{-m,n} = v_{m,n} + \frac{m^3h^3}{3}\left[\frac{\partial f}{\partial x}\right]_{x=0} = v_{m,n} - \frac{m^3h^3}{v_{0,n}}, \quad m = 1, 2.$$

It will be convenient to rewrite (32) in the following form:

$$v_{m,n+1} = \sum_{q=-2}^{q=2} a_q v_{m+q,n} + k f_{m,n}, \qquad (33)$$

where

$$a_{-2} = a_2 = -\tfrac{1}{12}\lambda; \quad a_{-1} = a_1 = \tfrac{4}{3}\lambda; \quad a_0 = 1 - 2.5\,\lambda.$$

Parameters: $h = 0.0625$; $k = 0.0014$; $\lambda = 0.3584$.
Range of $t$: $0 \le t \le 0.1288$.
Number of lattice points: $16 \times 92 = 1472$.

Formula (32) is a modification of (5). It is obtained by dropping the terms of (3) involving $p \ge 2$. However, the second derivative with respect to $x$ is approximated by differences, including the fourth order. The resulting formula is almost as accurate as (5) for this problem, since derivatives with respect to $t$ are very small numerically. In view of the fact that (5) was modified, it is necessary to examine (33) to determine the admissible range of $\lambda$. It is clear from (33) that all the coefficients $a_q$ cannot be made positive by any choice of $\lambda$; hence the stability criteria given earlier do not apply. However, it has been shown in [2] that if there exists a positive number $M$, independent of $x$ and $t$, such that the coefficients $a_q$ of (33) satisfy

$$\left|\sum_{p=-2}^{p=2} a_q \exp(iqy)\right| \le \exp(-My^2), \quad \text{for } |y| \le \pi, \qquad (34)$$

then the basic homogeneous differential equation,[5] is stable. From that result we may then deduce the stability of (32) or (33).

[5] In [2] the theorem applies to a more general case. Similar results relating to stability are given in [4].

TABLE 4. *Solution of the difference equation*

$$v_{m,n+1} = v_{m,n} + \left(\lambda\delta^2 - \frac{\lambda\delta^4}{12}\right) v_{m,n} + k f_{m,n}$$

$$v_{-m,n} = v_{m,n} + \frac{m^3h^3}{3}\left[\frac{\partial f}{\partial x}\right]_{x=0} = v_{m,n} - \frac{m^3h^3}{v_{0,n}}$$

$v_{m,0} = u_{m,0}$; $v_{s,n} = u_{s,n}$; $\delta^4 v_{s-1,n} = \delta^4 v_{s-2,n}$; $ah = 1$

$f(x,v)$ defined in table 1.

Parameters: $h = 0.0625$; $k = 0.0014$; $\lambda = 0.3584$.

| $x$ | $v(x,0)$ | At $t = 0.1288$ | | |
|---|---|---|---|---|
| | | $v(x,t)$ | $u(x,t)$ | $u(x,t) - v(x,t)$ |
| 0.0000 | 0.8000000 | 0.8767367 | 0.8768124 | +.0000757 |
| .0625 | .8242006 | .8988926 | .8989475 | +.0000545 |
| .1250 | .8934221 | .9627974 | .9628100 | +.0000125 |
| .1875 | .9990767 | 1.0615954 | 1.0615804 | −.0000150 |
| .2500 | 1.1316470 | 1.1872134 | 1.1871920 | −.0000214 |
| .3125 | 1.2833862 | 1.3326403 | 1.3326211 | −.0000192 |
| .3750 | 1.4487872 | 1.4925905 | 1.4925762 | −.0000143 |
| .4375 | 1.6241314 | 1.6633207 | 1.6633105 | −.0000102 |
| .5000 | 1.8069311 | 1.8422337 | 1.8422269 | −.0000068 |
| .5625 | 1.9955052 | 2.0275254 | 2.0275206 | −.0000048 |
| .6250 | 2.1886961 | 2.2179277 | 2.2179247 | −.0000030 |
| .6875 | 2.3856893 | 2.4125343 | 2.4125324 | −.0000019 |
| .7500 | 2.5858993 | 2.6106854 | 2.6106848 | −.0000006 |
| .8125 | 2.7888957 | 2.8118924 | 2.8118925 | +.0000001 |
| .8750 | 2.9943567 | 3.0157864 | 3.0157871 | +.0000007 |
| .9375 | 3.2020364 | 3.2220847 | 3.2220858 | +.0000011 |
| 1.0000 | 3.4117444 | 3.4305684 | 3.4305684 | 0 |

EXAMPLE 5.

Formula: The same as in example 4.
Parameters: $h_1=0.125$; $k=0.0056$; $\lambda=0.3584$.
Range of $t$: The same as in example 4. Results are given in table 5.

TABLE 5. *Solution of the difference equation described in table 4*

Parameters: $h_1=0.125$; $k=0.0056$; $h=0.3584$

$v(x,t,h_1,h_2)=v(h_1,h_2)=[v(h_2)-\rho^4(v(h_1))]/[1-\rho^4]$; $\rho=\frac{1}{2}$

$v(h_2)$ given in table 4.

| $x$ | $v(x,0)$ | At $t=0.1288$ | | | | |
|---|---|---|---|---|---|---|
| | | $v(x,t)$ | $u(x,t)$ | $u(x,t)-v(x,t)$ | $v(h_1,h_2)$ | $u(x,t)-v(h_1,h_2)$ |
| 0 | 0. 8000000 | 0. 8753628 | 0. 8768124 | +. 0014496 | 0. 8768282 | −. 0000158 |
| 0. 125 | . 8934221 | . 9623470 | . 9628099 | +. 0004629 | . 9628274 | −. 0000175 |
| . 250 | 1. 1316470 | 1. 1872934 | 1. 1871920 | −. 0001014 | 1. 1872081 | −. 0000161 |
| . 375 | 1. 4487872 | 1. 4926595 | 1. 4925762 | −. 0000833 | 1. 4925859 | −. 0000097 |
| . 500 | 1. 8069311 | 1. 8422296 | 1. 8422269 | −. 0000027 | 1. 8422340 | −. 0000071 |
| . 625 | 2. 1886961 | 2. 2178929 | 2. 2179247 | +. 0000318 | 2. 2179300 | −. 0000053 |
| . 750 | 2. 5858993 | 2. 6106245 | 2. 6106847 | +. 0000602 | 2. 6106895 | −. 0000048 |
| . 875 | 2. 9943567 | 3. 0157128 | 3. 0157869 | +. 0000741 | 3. 0157913 | −. 0000044 |
| 1. 000 | 3. 4117444 | 3. 4305684 | 3. 4305684 | 0 | | 0 |

In all the above examples, $v_{m,n}$, $u_{m,n}$, and $u_{m,n}-v_{m,n}$ were generated. Fourth differences were generated in all the examples, even where the computing formula did not call for them. These fourth differences were jotted down by the operator of the card programmed IBM calculator, and any lack of continuity in the differences was a warning that the machine was not functioning properly. The operations were carried out with a board wired to perform eight-place multiplication. The calculations were carried to the fullest possible accuracy, that is, to seven decimals in $v_{m,n}$ and to eight decimals in some of the subsidiary computations for $(v_{m,n+1}-v_{m,n})$. This accuracy is far in excess of the truncation error, for small values of $x$.

A "$\rho^2$" correction was applied to the values of the last available profile, as explained in section 4, based on the entries in examples 1 and 2. The results are given in example 2. Similarly, a $\rho^4$ correction was applied to the last profile in examples 4 and 5; the results are given in example 5.

## 5.1. Observations

### (a) The $\rho^r$ Correction Process

It is to be noted that in spite of the fact that in the last profile $v_{0,n}$ differs from the true values by 0.0026 in example 1 and by more than 0.01 in example 2, the values of $v(h_1,h_2)$ resulting from the $\rho^2$ correction are correct to within 0.00011 or better. It can be verified from the tabulated entries that

$$[u-v(h_1)]/[u-v(h_2)]\simeq h_1^2/h_2^2.$$

It follows that to gain an accuracy comparable to that of $v(h_1,h_2)$ without the "$\rho^2$" correction, an interval of $h=0.01$ would be needed, and hence the amount of work would be 125 times that used in example 1.

The improvement due to the "$\rho^4$" correction in examples 4 and 5 is not quite so striking. However, even here there is considerable improvement for small values of $x$, and it must be remembered that the formula used does include an $h^2$ term in the truncation error, which is not eliminated by the $\rho^4$ correction, although the error from this term is somewhat lessened. However, for $x$ larger than $\frac{1}{2}$, $v(h_2)$ in example 4 is closer to the true value than $v(h_1,h_2)$. An explanation for this may come from the following considerations: Assume

$$u-v(h_2)=\sum_{p=0}^{\infty}\rho^{p+2}h^{p+2}C_{p+2}. \tag{35}$$

then it follows that

$$u-v(h_1,h_2)=\frac{\rho^2h^2C_2}{1+\rho^2}+\frac{\rho^3(1-\rho)}{1+\rho^4}h^3C_3 - \frac{\rho^4(1-\rho)}{1-\rho^4}h^5C_5-\ldots. \tag{36}$$

It is to be noticed that the terms involving $h^2$ and $h^3$ are numerically smaller in (36) than in (35). However, the term involving $h^5$ is somewhat larger, if $\rho=\frac{1}{2}$, and all subsequent terms will be larger. In fact, it can be readily verified that if a "$\rho^r$" correction is applied, then compared with a term involving $\rho^{p+r}h^{p+r}C_{p+r}$ in (35), there is the corresponding term $[-\rho^r(1-\rho^p)/(1-\rho^r)h^{p+r}C_{p+r}$ in $[u-v(h_1,h_2)]$, which is, of course, numerically larger; but usually the leading term after the elimination is smaller than the term eliminated, namely, $h^r\rho^rC_r$. The "$\rho^4$" approximation, as applied in examples 4 and 5, is rather unusual in that a very small term of order two is left. If all the terms of (35) are small numerically, it may happen that the combination of the leading terms in $|u-v(h_1,h_2)|$ may be somewhat larger than in $|u-v(h_2)|$. In such cases, however, the difference between $v(h_1,h_2)$ and $v(h_2)$ will itself be small; hence, although it may not be known which is the better answer, it is to be expected that the order of magnitude of the error in $v(h_1,h_2)$ is not greater than $|v(h_2)-v(h_1,h_2)|$.

(b) The Rounding Error

The last place of $u(x,t)$ is not guaranteed, hence we can judge the rounding error only to the extent that the sixth decimal place is affected. It is to be noticed that in example 4, which seems to be the most accurate, the difference $u_{m,n}-v_{m,n}$ is systematic as far as sign is concerned. This is evidence of the fact that no large rounding-off error accumulated, after 100 steps in $t$, even though a nonlinear differential equation was used, and a considerable number of arithmetic operations were performed at each step.

(c) The Effect of Varying $\lambda$

Let us compare the error pattern in example 1, where $\lambda=\frac{1}{4}$, with that of example 3, where $\lambda=\frac{1}{6}$. In spite of the fact that somewhat more work was performed in generating values in example 3, the results are not as good—although the error in both examples is in the same decimal place; but the error in example 3 is about twice as large. This, in fact, is precisely what was to be expected. For as observed in section 3, in cases coming under type II, where derivatives with respect to $t$ are relatively small, the error is not appreciably affected by $\lambda$; hence, it is almost proportional to $h^2$. The ratio of the two values of $h^2$ is $(20/14)^2\cong 2.04$. The numerical illustration verifies the observation that $\lambda=\frac{1}{6}$ is *not* necessarily the best mesh ratio for the formula given in (4). The boundary conditions and the form of $f(x,t,u)$ determine the type that the differential system belongs to, and it is only after the problem is studied from this viewpoint that a suitable choice of $\lambda$ can be made.

In connection with example 3 corresponding to $\lambda=\frac{1}{6}$, it was not desirable to generate values at double the interval in the $x$-direction, for purposes of applying a "$\rho^{2r}$" correction. For if the formula given in (4) were used to compute $v_{-1,1}$, we would get a *negative* value of $(v_{0,1}-v_{0,0})$. Even if the true answer were not known, a knowledge of the more accurate values of $v_{m,n}$ from the smaller value of $h$ would warn us that a negative value of $(v_{0,1}-v_{0,0})$ is incorrect. It will be instructive to write down the differences of $v_{m,0}$ (the known initial profile) at double the interval used in example 3, and to use a value $v_{-1,0}$ computed from formula (4). The values of $v_{m,0}$ and some of the differences are given below:

$h=\frac{1}{3}$; $t=0$.

| $m$ | $v_{m,0}$ | $\delta^2v$ | $\delta^3v$ | $\delta^4v$ | $\delta^5v$ |
|---|---|---|---|---|---|
| −1 | 0. 9166802 | | | | |
| | | . 2370047 | | | |
| 0 | . 8000000 | | −. 0612450 | | |
| | | . 1757597 | −. 0896745 | −. 0284295 | |
| 1 | . 9203245 | | | | +. 0741146 |
| | | . 0860852 | −. 0439894 | +. 0456851 | |
| 2 | 1. 2164087 | | | | −. 0197723 |
| | | . 0420958 | −. 0180766 | +. 0259128 | |
| 3 | 1. 5985781 | | | | |
| | | . 0240192 | | | |
| 4 | 2. 0228433 | | | | |
| | | | | | |
| 5 | 2. 4711277 | | | | |

The fourth differences are not numerically smaller than the third differences, and the first entry in the fifth-difference column is very much larger numerically than the second one in the same column. Such a pattern is a warning that the interval is too large.

(d) The Effect of Using a Higher-Order Approximation Formula

Let us compare the results in examples 1 and 4. The coding for example 4 is somewhat more complicated than that for example 1, but since only 1,472 lattice points were used in example 4 compared with 2,000 in example 1, the over-all amount of work is about the same in both cases. The result after 100 steps shows that the higher approximation formula gives very much better results. To secure a maximum error of 0.00008 in $v_{m,n}$ with the approximation used in example 1, it would have been necessary to use an interval $h$ of about 0.009; hence 170 times the amount of work would have been necessary. However, if the $\rho^2$ correction were applied, the comparative results would not be quite so unfavorable to the simpler approximation. Assuming that a $\rho^2$ correc-

tion were applied to two computations by the simpler approximation, and a $\rho^4$ correction to results of the modified fourth-order approximation, the latter would still give significantly better results—one additional decimal place, in fact. To secure comparable accuracy by the simpler approximation, it would be necessary to multiply the amount of work by the factor[7] 10. The conclusion is inescapable that the higher approximation is worth while, in cases where the boundary conditions do not introduce singularities in the higher derivatives, and when the coding problem is manageable.

---

The author acknowledges gratefully the many constructive suggestions which were given by Dr. Fritz John during the progress of the study.

## 6. References

[1] D. R. Hartree and J. R. Womersley, A method for the numerical or mechanical solution of certain types of partial differential equations, Proc. Roy. Soc., London [A] **161,** 353 to 366 (1937).

[2] Fritz John, On integration of parabolic equations by difference methods, Communications on Pure and Applied Math. **5,** 155–211 (1952).

[3] L. M. Milne-Thomson, The calculus of finite differences (Macmillan Co., London, 1933).

[4] George O'Brien, Morton A. Hyman and Sidney Kaplan, A study of the numerical solution of partial differential equation, J. Math. Phys. **29,** No. 4, 223 to 251 (Jan. 1951).

[5] L. F. Richardson and J. Arthur Gaunt, The deferred approach to the limit. Part I: Single lattices, Richardson. Part II: Interpenetrating lattices, Gaunt, Phil. Trans. Roy. Soc., London [A] **226,** 299 to 361 (July 1927).

## 7. Appendix

DEFINITION. We define $z\ (m,M;n,N)$ to be a region in the $x,t$-plane, which contains the region

$$(m-M)h \le x \le (m+M)h; \quad nk \le t \le (n+N)k.$$

### 7.1. Expressions for Derivatives[8] in Terms of Differences

$$\frac{\partial^2 u}{\partial x^2} = \frac{1}{h^2}\left[\left(\delta^2 - \frac{1}{12}\delta^4 + \frac{1}{90}\delta^6\right)u_{m,n}\right] - \frac{h^6}{560}\frac{\partial^8 u_{x_1,nk}}{\partial x^8}, \tag{37}$$

$$\frac{\partial^4 u_{m,n}}{\partial x^4} = \frac{1}{h^4}\left[\left(\delta^4 - \frac{1}{6}\delta^6\right)u_{m,n}\right] + h^4\left[\frac{7}{240}\frac{\partial^8 u_{x_2,n}}{\partial x^8} - \frac{h^2}{4200}\frac{\partial^{10} u_{x_2,n}}{\partial x^{10}}\right], \tag{38}$$

$$\frac{\partial^6 u_{m,n}}{\partial x^6} = \frac{1}{h^6}\delta^6 u_{m,n} - h^2\left[\frac{1}{4}\frac{\partial^8 u_{x_1,n}}{\partial x^8} - \frac{7h^2}{720}\frac{\partial^{10} u_{x_2,n}}{\partial x^{10}} + \frac{h^4 \partial^{12} u_{x_3,n}}{18480\,\partial x^{12}}\right], \tag{39}$$

where the points $(x_j,nk)$ are in $Z(m,3;n,0)$, $j=1,2,\ldots,6$.

[7] This is on the assumption that after the $\rho^2$ correction, the leading term of $\sigma_{m,n}$ has the factor $h^2$. Since the work is inversely proportional to $h^2$ for the same $\lambda$, improving the entries by a factor of $M$ means doing $M$ times the amount of work.

[8] See chapter VII, reference [3].

If $h$ is sufficiently small, successive terms of (37), (38), and (39) are of a lower order of magnitude than preceding ones, and if terms involving $h$ in the numerator are dropped, then the truncation error is of the order of magnitude of the first term neglected.

### 7.2. Relations Between Derivatives in the $t$- and $x$-Directions

By differentiating (1) we can establish:

$$\frac{\partial^2 u}{\partial t^2} = \frac{\partial^2}{\partial x^2}\left(\frac{\partial u}{\partial t}\right) + \frac{df}{dt} = \frac{\partial^4 u}{\partial x^4} + \frac{d^2 f}{dx^2} + \frac{df}{dt}. \tag{40}$$

$$\frac{\partial^2 u}{\partial x \partial t} = \frac{\partial^3 u}{\partial x^3} + \frac{df}{dx} \tag{41}$$

$$\frac{\partial^3 u}{\partial x \partial t^2} = \frac{\partial^5 u}{\partial x^5} + P_{31}; \quad P_{31} = \frac{d^3 f}{dx^3} + \frac{d^2 f}{dx dt}. \tag{42}$$

$$\frac{\partial^3 u}{\partial t^3} = \frac{\partial^6 u}{\partial x^6} + P_{32}; \quad P_{32} = \frac{d^4 f}{dx^4} + \frac{d^3 f}{dt^2} + \frac{d^3 f}{dt dx^2}. \tag{43}$$

In the above, $P_{31}$ and $P_{32}$ are functions of $x$ and $t$. Where not otherwise specified, they will be understood to correspond to $x=mh$, $t=nk$. If $f(x,t,u)$ involves $u$, the derivatives of $f$ may involve various derivatives of $u$ with respect to $x$. It will be convenient in this section to change the notation introduced previously, and to define $f_x=\partial f/\partial x$, with $t,u$ held fixed; $f_t=\partial f/\partial t$, with $x,u$ held fixed; $f_u=\partial f/\partial u$, with $x,t$ held fixed with similar definitions for $f_{x,t}, f_{x,u}$, etc. These derivatives will usually be required at $x=0$ and $t=nk$; hence evaluation of the derivatives at $(0,nk)$ will be implied unless otherwise specified, or readily understood from the context of the analysis.

### 7.3. The Boundary Conditions at x=0 for the Examples in Section 5

Since $u_{-m,0}$ has not been defined by the differential system, the expression (47) must be modified when $m=0$, or what is equivalent to it, $u_{-1,n}$ must be defined. Similarly $u_{-1,n}$ and $u_{-2,n}$ must be defined for (5) and (32). Consider the condition $(\partial u_{0,n}/\partial x)=0$. It implies

$$\frac{\partial^p u_{0,n}}{\partial t^{p-1}\partial x} = 0, \quad p \ge 2. \tag{44}$$

Now from (41) and (44)

$$0 = \frac{\partial^2 u_{0,n}}{\partial t \partial x} = \frac{\partial^3 u_{0,n}}{\partial x^3} + f_x.$$

Hence

$$\frac{\partial^3 u_{0,n}}{\partial x^3} = -f_x. \tag{45}$$

Similarly, from (6.23) and (6.30)

$$0 = \frac{\partial^3 u_{0,n}}{\partial t^2 \partial x} = \frac{\partial^5 u_{0,n}}{\partial x^5} + P_{31},$$

where

$$P_{3,1} = \left[\frac{d^3 f}{dx^3} + \frac{d^2 f}{dx dt}\right]_{0,t}.$$

If $f$ involves $u$, $P_{31}$ will involve $\partial^2 u/\partial x^2$. An explicit expression for $P_{31}$ in terms of partial derivatives will therefore be useful. It is given below.

$$P_{31} = f_{xxx} + 4f_{x,u}\frac{\partial^2 u}{\partial x^2} + f\cdot f_{x,u} - f_x \cdot f_u + f_{x,t}$$
$$= 4f_{x,u}\frac{\partial^2 u_{0,n}}{\partial x^2} + G_n = -\frac{\partial^5 u_{0,n}}{\partial x^5}, \tag{46}$$

where

$$G_n = f_{xxx} + f \cdot f_{x,u} - f_x \cdot f_u + f_{x,t}. \tag{47}$$

Using (45) the Maclaurin series around $(0, nk)$ yields

$$u_{m,n} = u_{0,n} + \frac{m^2h^2}{2}\frac{\partial^2 u_{0,n}}{\partial x^2} - \frac{m^3h^3}{6} f_x + \sum_{p=4}^{\infty} \frac{m^p h^p}{p!} \frac{\partial^p u_{0,n}}{\partial x^p}. \tag{48}$$

If we set $m = 1, 2$ and use (46), we can obtain $\partial^{2p} u_{0,n}/\partial x^{2p}$ to an accuracy comparable to approximations used over the rest of the region. The same results are obtained if we use (48), to solve for $u_{-1,n}$ and $u_{-2,n}$ (if the latter is needed). This artificial extension of the region to negative values of $m$ is convenient for numerical treatment, and is justifiable wherever (48) exists and the required derivatives are bounded. Thus we can write

$$u_{-m,n} = u_{m,n} + \frac{m^3h^3}{3} f_x - \frac{m^5h^5}{60}\frac{\partial^5 u_{0,n}}{\partial x^5} - \cdots. \tag{49}$$

If $h$ is sufficiently small, and terms involving powers of $h^{3+p}, p \geq 0$ are neglected in (49), the truncation error for $u_{-m,n}$ is of order $h^5$. Thus $T_{2,0,n}$, defined in (7a), has a term in $h^3$.

The third term on the right-hand side of (49) was also dropped in example 4, since its magnitude would have affected only the fifth decimal place at any point. This term could have been obtained, if desired, by using (46) and (37), and then setting $m = 1$ and $m = 2$ in (49), to obtain three linear equations for the unknowns $u_{-1}, u_{-2}$, and $h^3\partial^3 u/\partial x^3$.

## 7.4. The Boundary Condition at the Terminal Points $(x_a, t)$

The difference equation defined in (4) needs no special treatment for the boundary conditions at $x_a$, where $a = sm$, since $(s-1, n)$ is the last lattice point at which $v_{m,n}$ is generated, and $\delta^2 v_{s-1,n}$ is fully defined. However, when the fourth order approximation is used, as in (5), an expression is required for $v_{s+1,n}$, or for $\delta^2 u_{s,n}$. Since $u(x_a, t) = B(t)$ and all its derivatives in the $t$-direction are assumed to be known, the differential eq (1) can be used to obtain the second partial derivative in the $x$-direction, in terms of $\partial u/\partial t$ and $f(x,u)$. The relations between derivatives and differences can then be used to obtain $\delta^2 u_{s,n}$. In examples 4 and 5, the fourth difference in the $x$-direction was essentially zero at $x_a$; hence the last fourth difference was replaced by $\delta^4 u_{s-1,n}$.

Los Angeles, California, September 18, 1951.

Journal of Research of the National Bureau of Standards Vol. 50, No. 6, June 1953 Research Paper 2425

# Thermal Properties of Some Butadiene-Styrene Copolymers[1]

George T. Furukawa, Robert E. McCoskey, and Gerard J. King

The thermal properties of 41° and 122° F butadiene-styrene copolymers containing 8.58 percent of bound-styrene were investigated by means of an adiabatic calorimeter from 16° to 330° K. The 41° F copolymer was found to crystallize in the temperature range from 210° to 285° K. The 122° F copolymer did not exhibit any crystallization. The glass-transformation temperatures of the 41° and 122° F copolymers were 200° and 193° K, respectively. The effects of heat treatment upon the heat capacity and the glass-transformation temperature have been studied. The results of the heat-capacity measurements were used to compute heat capacity, enthalpy, and entropy from 0° to 330° K at 5-deg intervals.

## 1. Introduction

The literature is copious with studies involving the physical and chemical properties of various rubber polymers prepared from different recipes. These investigations have principally in mind the correlation of the observed properties with the structure of the polymers—the structure or the composition being determined by chemical methods, derived judiciously from the units that compose the polymers, or deduced from the various observed properties themselves. The situation is complicated by many variables in the recipes, such as polymerization temperature, percentage conversion, catalyst, modifier, and others, both controllable and noncontrollable, which affect the internal structure of the final product. For example, in the polymerization of dienes many of the above factors influence the degree of 1-4, 1-2, *cis*, or *trans* addition as well as cross-linking. Furthermore, in many instances the noncontrolled variables outweigh the controlled variables in determining the physical property.

Some of the physical properties of rubber polymers have been known to be dependent to a certain extent upon their previous thermal and mechanical history. For example, in the heat-capacity measurements with Hycar O. R.–15 [1][2] and GR–S [2], the direction of the temperature drift in the temperature range of glass transformation is shown to depend upon the rate at which the polymers were cooled prior to the measurements. The temperature drift observed can be explained in terms of the long relaxation times encountered for certain degrees of freedom in the polymeric substance to reach equilibrium. At the lower temperatures a given degree of freedom can be essentially frozen-in, and at the higher temperatures the attainment of equilibrium for that degree of freedom can be very rapid. The temperature drift is observed in the intermediate temperature range when the relaxation time for the degree of freedom is of the same order of magnitude as the time for the heat-capacity measurements. In the temperature range of glass transformation the relaxation time for certain degrees of freedom in polymers comes within this magnitude. Similarly, as is pointed out later, the crystallization and melting processes in polymers have a relaxation time within this range. Thus, when the polymer is cooled rapidly through the glass-transformation interval (or through the crystallization interval) a certain portion of the polymer molecules fails to undergo transition from the higher- to the lower-energy states. During the heat-capacity experiments and when heating to temperatures near the glass-transformation interval, the frozen-in degrees of freedom become gradually excited and transitions occur within the polymer in the direction of equilibrium. In this case, the polymer molecules transform into the lower-energy states with the consequent liberation of energy and upward temperature drift. On the other hand, when the polymer is cooled slowly through the glass-transformation interval, more polymer molecules have a chance to transform into the lower-energy states. Upon heating to the glass-transformation range, the polymer molecules transform into the higher-energy states accompanied by an absorption of energy and a downward temperature drift.

The glass transformation, which is associated with many polymers, supercooled liquids, and other noncrystalline solids, arises from the freezing-in or the increasing length of relaxation time for certain degrees of freedom and is characterized in calorimetry by a steep decrease in the heat capacity with decrease in temperature. The thermal coefficient of expansion decreases rapidly in a similar manner, and there are many other physical properties that are affected similarly within the same temperature range. The glass transformation is not as sharp as first-order transitions, but is spread over a 5- to 10-deg interval. As the relaxation time for equilibrium in this temperature range is of the same order of magnitude as the experimental measurements, the heat-capacity values obtained are dependent upon the rate of cooling through this interval as well as the time awaited for temperature measurements. Consequently, the heat-capacity values are somewhat scattered.

Natural rubber and other natural and synthetic

[1] This paper is based on the work sponsored by the Reconstruction Finance Corp., Synthetic Rubber Division.
[2] Figures in brackets indicate the literature references at the end of this paper.

polymers are known to crystallize over a wide range of temperature. There is only a short-range order within any crystalline polymeric substance and along a single polymer molecule both crystalline and amorphous structures exist simultaneously. Recent X-ray studies [3] have shown that the crystallinity in natural rubber increased with storage, and that even after 30 years of storage the crystallization process had not reached the state of equilibrium. The crystallization and melting processes of polymers are observed as temperature drifts in calorimetry. The lower temperature limit of this crystallization range is set by the lack of thermal motion to attain crystal configuration; and beyond the upper limit, the thermal motion is sufficient to make the time spent in a crystalline state short and the polymer is amorphous. Thus, the degree of crystallinity of the polymer at temperatures below the crystallization range, is determined to a certain extent by the rate of cooling through this range.

This report deals with the heat-capacity investigation of two butadiene-styrene copolymers containing 8.58 percent of bound-styrene and prepared at 41° F (5° C) and 122° F (50° C). These two materials were investigated to determine the effect of the polymerization temperature upon their relative crystallizability, glass-transformation temperature, and heat capacity. The effects of heat treatment upon the heat capacity and the glass-transformation temperature have been studied, and the results of the measurements were used to compute heat capacity, enthalpy, and entropy of the polymers at 5-deg intervals from 0° to 330° K.

The calorimetric method, as applied in this investigation, is sensitive to changes in the polymer in which thermal energy as little as 0.03 abs j $min^{-1}$ is evolved or absorbed. This method was used to detect temperatures at which thermal effects occurred and at which transitions took place. The temperature range of crystallization in the 41° F copolymer and the glass-transformation temperature of both copolymers were determined.

## 2. Apparatus and Method

The details of the calorimetric apparatus and method used in this investigation can be found in the previous reports dealing with 1,3-butadiene [4] and diphenyl ether [5]. A small quantity of helium gas, sealed in with each polymer sample, supplemented the vanes in enhancing the attainment of thermal equilibrium. The temperature measurements were based on the platinum resistance thermometer calibrated at this Bureau in accordance with the 1948 International Temperature Scale [6] and between 10° and 90° K on a provisional scale [7], consisting of a set of platinum resistance thermometers calibrated against a helium gas thermometer. The temperatures expressed in degrees Kelvin were obtained by adding 273.16° to the observed temperatures in degrees Celsius.

In order to study in what way the heat treatment affects the heat-capacity results, two series of experiments were carried out in the temperature range from 80° to 280° K. In one series, the polymer was shock-cooled by immersing the calorimeter in liquid nitrogen with helium gas in the space surrounding the sample container. By means of this procedure, the sample was cooled from room temperature to about 90° K in 30 min and to about 80° K in an additional 30 min. In the second series of measurements, the polymer was cooled slowly by maintaining a high vacuum around the sample container. The cooling process was prolonged by successively using dry ice and then liquid nitrogen. In several cases the 41° F polymer was left between 200° and 230° K for a number of days to increase the crystallinity by allowing a longer time for crystallization. After cooling the polymer to the desired temperature, the heat-capacity measurements were made at progressively higher temperatures, the final temperature of the first measurement being the initial temperature of the second measurement, and so forth up the temperature scale. As heat-capacity measurements with simpler substances [5, 8] show that normal temperature equilibrium was established in 6 to 7 min after the heating period, any persistent temperature drift after the eighth minute was considered to arise from the thermal effects in the polymeric material.

The net heat capacity, or the heat capacity of the polymer, was obtained by subtracting the heat capacity of the empty container from the gross heat capacity. At the lower temperatures at which the slope of the heat-capacity curve changes rapidly, the temperature increase per heating period was made as low as 2 to 3 deg to make insignificant the curvature correction to the experimental heat capacity. As the curvature does not change rapidly at the higher temperatures, larger temperature intervals of 7 to 9 deg were used. The heat capacities tabulated at 5-deg intervals in tables 4 and 7 were obtained by graphical smoothing of the net heat capacities. The heat capacities in the transition regions were obtained by methods later described.

## 3. Samples

The two 90/10 butadiene-styrene copolymers investigated were obtained from different sources. The history of the rubber polymer, designated X–454 and obtained through the Copolymer Corp., Baton Rouge, La., is not completely known. This copolymer was emulsion polymerized at 41° F (5° C) with the initial butadiene-styrene charge ratio at 90/10; the emulsifier was Dresinate 731 and the modifier was probably Sulfole B–8. The reaction was "short-stopped" at about 55-percent conversion, using ditertiary butylhydroquinone. No further information is known about this copolymer. The GL–658 copolymer prepared at 122° F (50° C) was obtained through the University of Akron-Government Laboratories [9], and the details concerning this material are found in the reference given. The copolymer was emulsion polymerized with the same initial butadiene-styrene charge ratio as the 41° F copoly-

ner, using, however, as emulsifier soap flakes (SF), and as modifying agent normal-dodecyl mercaptan (DDM). The polymerization reaction was activated by potassium persulfate and "short-stopped" at about 72-percent conversion by means of hydroquinone.

The polymers were purified by M. Tryon of the Rubber Section of the National Bureau of Standards, and the purification procedure was as follows. The material was first dissolved in benzene and centrifuged to eliminate solid particles. This solution was added dropwise into well-stirred methyl alcohol to coagulate the polymer. The coagulated polymer was then redissolved in benzene. The solution and subsequent precipitation processes were carried out three times. This procedure eliminated fatty acids and their salts, stabilizer (phenylbetanaphthylamine), and some low-molecular-weight polymers. After dissolving the polymer for the fourth time, about 0.1 percent of phenylbetanaphthylamine was added to the benzene solution as a stabilizer. Subsequently, the benzene was removed by pumping on the frozen polymer solution held at the dry-ice temperature, leaving the stabilizer behind with the polymer. This process yielded a spongy mass, which was pressed into ¼-inch sheets. The polymer samples were received from the Rubber Section in this form, and they were cut to size to fit between the vanes of the sample container. The samples were pumped at high vacuum for 3 days at 25° C and 1 day at 50° C to eliminate volatile impurities such as moisture, air, and benzene. Following this, the container was sealed with a small quantity of helium gas. The mass of the X–454 copolymer investigated was 41.336 g, and that of the GL–658 was 40.349 g.

A portion of the purified polymers was analyzed for composition. The results are given in table 1.[4] The styrene contents given in the table were computed from the carbon-hydrogen ratios corrected for the mercaptan content. The phenylbetanaphthylamine was added after the analysis.

TABLE 1. *Composition of the copolymers*

| | Percentage by weight | |
|---|---|---|
| | X–454 | GL–658 |
| Carbon | 88.869 | 88.907 |
| Hydrogen | 10.872 | 10.8982 |
| Sulfur | .056 | .136 |
| Oxygen | .235 | .16 |
| Ash | .18 | .104 |
| Styrene | 8.58 | 8.58 |
| Phenylbetanaphthylamine | .1 | .1 |

## 4. Results

### 4.1. X–454, 41° F Copolymer

The experimental details regarding heat treatments, temperature range of the measurements, and temperature drifts with the X–454 copolymer are summarized in table 2. The observed heat-capacity values are given in table 3 and plotted in figure 1. The heat-capacity measurements in runs 1, 2, and 3 were made after shock-cooling the polymer from room temperature to that of liquid nitrogen. In these experiments the upward temperature drifts, observed in the range of temperature from about 170° to 280° K, are attributed to slow changes in the polymer to lower states of energy. In run 2 the upward temperature drift at 220° K was a much as 0.09 deg per min 40 min after the end of the heating period. As shown in figure 1, the heat-capacity results in run 2 (indicated by filled-in circles) rise steeply over the temperature interval from about 195° to 205° K. Then, there follows a sudden drop and again a rise in the heat capacity. The heat-capacity rise in the interval 195° to 205° K is attributed to glass transformation. The glass-transformation temperature is taken to be 200° K. The sudden decrease that follows is caused by the crystallization of the polymer, for apparent heat capacity falls off with crystallization. The rise following this is from the melting of the polymer crystallites. The results (fig. 1) of all heat-capacity measurements are relatively high in the temperature interval 230° to 280° K, and during the heat-capacity measurements upward temperature drifts were observed in this range. It is believed that irreversible melting took place in the vicinity of the heater (central well) because during the heating process the temperature is invariably higher near the heater. For this reason the heating rate, or the power, somewhat affects the heat capacity. During the equilibrating period some of the melted crystallites recrystallize, and also new crystallites form with the increased thermal energy now available for orientation. The apparent high heat capacity is indicative of a relatively larger amount of melting in the particular heating interval in comparison to crystallization. Thus the amount of the polymer melted is greater than the amount crystallized in the temperature range 230° to 280° K,

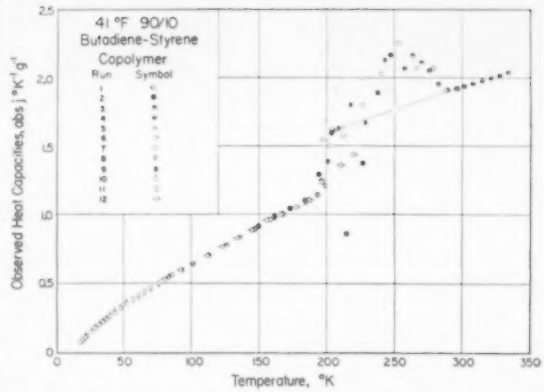


FIGURE 1. *Observed heat capacities of the X–454, 41° F butadiene (90)—styrene (10) copolymer.*

The broken line was obtained by extrapolating the heat capacities in the amorphous range.

[4] The analyses were made by R. A. Paulson and M. Tryon of the Bureau.

TABLE 2. *Heat treatments and observations with the 41° F butadiene (90)-styrene (10) copolymer X-454*

(Temperatures are in ° K)

| Run | Treatment of sample | Temperature range of measurements | Drift observation |
|---|---|---|---|
| 1 | Cooled rapidly from room temperature to 77°. | 77° to 171° | Upward drift at 171°. |
| 2 | Cooled rapidly from room temperature to 78° and heated to 143°. | 143° to 251° | Upward drift from 178° to 251°. |
| 3 | Cooled rapidly from room temperature to 251°. | 251° to 298° | Upward drift from 251° to 278°. |
| 4 | Left at room temperature overnight. | 298° to 337° | No drift. |
| 5 | Cooled slowly from room temperature to 200° and left between 200° and 230° for 3 days and cooled to 78°. | 78° to 151° | Downward drift from 131° to 151°. |
| 6 | Allowed to remain around 150° overnight and heated to 153°. | 153° to 223° | Downward drift from 153° to 172°; upward from 191° to 223°. |
| 7 | Cooled to 193° overnight with dry ice. | 193° to 300° | Downward drift from 193° to 199°; upward from 204° to 273°. |
| 8 | Cooled slowly to 200°, allowed to remain between 200° and 230° for 1 week, and cooled rapidly to 171°. | 171° to 200° | Upward drift from 188° to 200°. |
| 9 | Allowed to remain at dry ice temperature overnight. | 196° to 295°; 251° to 295° was one heat. | Downward drift at 211°; upward drift from 222° to 251°. |
| 10 | Allowed to remain at dry ice temperature for 1 week and cooled to liquid $H_2$ temperature. | 20° to 53° | No drift. |
| 11 | Continuation of run 10. | 16° to 22° and 51° to 78°. | Do. |
| 12 | Cooled slowly to 200° and allowed to remain between 200° and 230° for 3 weeks. | 194° to 213° | Upward drift from 206° to 213°. |

TABLE 3. *Observed heat capacities of 41° F butadiene (90)-styrene (10) copolymer X–454*

| Run | T | C | Run | T | C | Run | T | C |
|---|---|---|---|---|---|---|---|---|
| | °K | *abs j* °K⁻¹g⁻¹ | | °K | *abs j* °K⁻¹g⁻¹ | | °K | *abs j* °K⁻¹g⁻¹ |
| 1 | 79.91 | 0.5362 | 5 | 82.57 | 0.5491 | 10 | 21.73 | 0.1223 |
| | 85.21 | .5671 | | 91.92 | .6006 | | 25.49 | .1560 |
| | 91.68 | .6016 | | 100.51 | .6458 | | 28.43 | .1813 |
| | 100.76 | .6497 | | 112.50 | .7101 | | 31.13 | .2046 |
| | 111.49 | .7089 | | 125.78 | .7831 | | 33.71 | .2261 |
| | 122.30 | .7704 | | 136.32 | .8408 | | 36.39 | .2477 |
| | 133.59 | .8330 | | 146.32 | .8955 | | 39.17 | .2695 |
| | 144.23 | .8923 | | 157.49 | .9561 | | 42.77 | .2967 |
| | 155.00 | .9622 | | 166.89 | 1.006 | | 47.03 | .3280 |
| | 165.97 | 1.005 | | 176.80 | 1.057 | | 51.04 | .3592 |
| 2 | 148.86 | 0.9183 | 6 | 186.36 | 1.108 | 11 | 17.34 | .0847 |
| | 160.87 | .9850 | | 195.47 | 1.248 | | 19.01 | .0989 |
| | 172.34 | 1.047 | | 203.63 | 1.608 | | 21.04 | .1163 |
| | 183.34 | 1.106 | | 211.22 | 1.580 | | 56.25 | .3910 |
| | 193.65 | 1.294 | | 219.02 | 1.442 | | 60.28 | .4160 |
| | 202.91 | 1.597 | | 195.70 | 1.240 | | 64.73 | .4462 |
| | 213.69 | 0.8616 | | 201.31 | 1.507 | | 69.47 | .4721 |
| | 226.10 | 1.376 | | 211.48 | 1.630 | | 75.10 | .5036 |
| | 237.00 | 1.894 | | 226.02 | 1.802 | 12 | 197.23 | 1.548 |
| | 246.42 | 2.171 | 7 | 239.49 | 2.033 | | 203.43 | 1.622 |
| 3 | 256.69 | 2.068 | | 252.05 | 2.257 | | 209.81 | 1.367 |
| | 262.95 | 2.167 | | 265.46 | 2.077 | | | |
| | 269.15 | 2.114 | | 277.61 | 2.072 | | | |
| | 275.44 | 2.058 | | 287.55 | 1.912 | | | |
| | 281.87 | 1.957 | | 296.43 | 1.926 | | | |
| | 288.45 | 1.911 | 8 | 183.68 | 1.090 | | | |
| | 295.05 | 1.923 | | 192.47 | 1.143 | | | |
| | 301.05 | 1.940 | | 198.19 | 1.212 | | | |
| 4 | 307.56 | 1.961 | 9 | 200.27 | 1.389 | | | |
| | 314.28 | 1.982 | | 207.66 | 1.630 | | | |
| | 320.94 | 2.001 | | 216.57 | 1.803 | | | |
| | 327.28 | 2.020 | | 227.60 | 1.672 | | | |
| | 333.58 | 2.041 | | 242.04 | 2.133 | | | |

although the observed upward temperature drifts indicate crystallization to be taking place. On the other hand, in run 2, as pointed out earlier, the low heat capacity just above the glass-transformation temperature arises from a large amount of crystallization. As temperatures used in heat-capacity calculations were determined during temperature drifts, the heat-capacity values are different from the values that would be obtained if thermal equilibrium had been reached. The temperature equilibrium, however, was awaited sufficiently long so that the general nature of each heat-capacity value is preserved.

The heat-capacity curve (fig. 1) is smooth in the range of temperature in which run 4 was made. The polymer is considered to be completely amorphous above 285° K.

The remainder of the experiments were made after cooling the polymer slowly to obtain a well-crystallized and annealed sample. The results of the measurements in runs 5, 6, and 7, which were made on successive days, showed that, in general, after annealing the polymer, the heat-capacity values between 210° and 285° K became higher (see tables 2, and 3, and fig. 1). This indicates that the amount of crystallization that took place during these heat-capacity measurements was lower than in the measurements when the polymer was shock-cooled. In these experiments, the downward temperature drifts below 200° K are considered to arise from the slow transition of the polymer molecules from lower- to higher-energy states, these states being associated in some way with glass transformation. The downward temperature drifts above this temperature are attributed to slow melting of the crystallites. As relatively low heat-capacity results were obtained in the temperature interval 200° to 230° K, the polymer was held within this temperature interval for 1 week to increase the degree of crystallinity. Runs 8 and 9, carried out on successive days, are experiments with the material so treated. The heat-capacity results in these measurements were not as low as found in runs 2 and 6; however, a relatively low value was obtained at 227.60° K. The experiments in run 12 were made to determine whether a longer conditioning period would eliminate completely the low heat-capacity values. In spite of the 3-weeks' conditioning, the experiments of run 12 yielded low values. In this run, the polymer was probably not as well crystallized as expected. The interpretation of the observed results with this polymer is made difficult by the closeness of the crystallization to the glass-transformation temperature. In the crystallization interval, probably the melting and crystallization processes occur simultaneously. The direction of the temperature drift is an indication of the predominating process at the time of the measurement. Also, the direction of the drift is dependent, as in the glass-transformation temperature range, upon the previous heat treatment, the rate at which the new condition was reached from the former, and the time lapse between the attainment of the new condition and the experimental observation.

The annealing process, which increased the crystallinity in the polymer, yielded lower heat-capacity values in the temperature range below 200° K. The difference between the results of the shock-cooled and annealed polymer is about 1 percent at 185° K and about 0.5 percent at 80° K. The heat-capacity values given in table 4 were calculated from the results of the annealed polymer. The values at 15° K and below were obtained by extrapolation, using the Debye function,

$$C = 0.2489 D\left(\frac{90.54}{T}\right),$$

which was fitted to experimental values between 17° and 25° K. The heat-capacity values in the range 190° to 295° K were estimated from a heat-capacity–temperature curve, in which the values in the crystallization range were taken along the broken curve (hypothetical heat-capacity curve for amorphous copolymer), as shown in figure 1. The estimated values are given in table 4. The broken curve was obtained by linear extrapolation of the experimental values in the temperature range 290° to 330° K. Above the glass-transformation temperature, the heat-capacity curves for Hycar 0.R.–15 [1] and GR–S [2] were found to be closely linear. The results with the GL–658 copolymer, which was found to give no crystallization, are also closely linear between 250° and 330° K; extrapolation below 250° to the glass-transformation temperature, however, would result in a deviation of 4 percent at 200° K.

TABLE 4. *Heat capacity, enthalpy, and entropy of 41° F butadiene (90)-styrene (10) copolymer X–454*

| $T$ | $C$ | $(H_T-H_0)$ | $(S_T-S_0)$ | $T$ | $C$ | $(H_T-H_0)$ | $(S_T-S_0)$ |
|---|---|---|---|---|---|---|---|
| °K | abs j°K$^{-1}$ | abs j g$^{-1}$ | abs j°K$^{-1}$ | °K | abs j°K$^{-1}$ | abs j g$^{-1}$ | abs j°K$^{-1}$ |
| 0 | 0 | 0 | 0 | 175 | 1.048 | 96.36 | 1.048 |
| 5 | 0.0033 | 0.0041 | 0.0011 | 180 | 1.074 | 101.7 | 1.078 |
| 10 | .0248 | .0641 | .0086 | 185 | 1.101 | 107.1 | 1.107 |
| 15 | .0653 | .2855 | .0280 | 190 | 1.130 | 112.7 | 1.137 |
| 20 | .1074 | .7164 | .0505 | 195 | 1.18 | ..... | ..... |
| 25 | .1519 | 1.364 | .0793 | 200 | 1.56 | ..... | ..... |
| 30 | .1949 | 2.232 | .1108 | 205 | 1.61 | ..... | ..... |
| 35 | .2365 | 3.311 | .1440 | 210 | 1.63 | ..... | ..... |
| 40 | .2758 | 4.593 | .1781 | 215 | 1.65 | ..... | ..... |
| 45 | .3133 | 6.066 | .2128 | 220 | 1.67 | ..... | ..... |
| 50 | .3508 | 7.727 | .2478 | 225 | 1.68 | ..... | ..... |
| 55 | .3840 | 9.565 | .2828 | 230 | 1.70 | ..... | ..... |
| 60 | .4143 | 11.56 | .3175 | 235 | 1.72 | ..... | ..... |
| 65 | .4448 | 13.71 | .3519 | 240 | 1.74 | ..... | ..... |
| 70 | .4750 | 16.01 | .3859 | 245 | 1.75 | ..... | ..... |
| 75 | .5050 | 18.46 | .4197 | 250 | 1.77 | ..... | ..... |
| 80 | .5345 | 21.06 | .4533 | 255 | 1.79 | ..... | ..... |
| 85 | .5639 | 23.80 | .4866 | 260 | 1.80 | ..... | ..... |
| 90 | .5906 | 26.69 | .5196 | 265 | 1.82 | ..... | ..... |
| 95 | .6168 | 29.71 | .5522 | 270 | 1.84 | ..... | ..... |
| 100 | .6432 | 32.86 | .5845 | 275 | 1.85 | ..... | ..... |
| 105 | .6698 | 36.14 | .6165 | 280 | 1.87 | ..... | ..... |
| 110 | .6963 | 39.56 | .6483 | 285 | 1.89 | ..... | ..... |
| 115 | .7234 | 43.11 | .6798 | 290 | 1.90 | ..... | ..... |
| 120 | .7510 | 46.79 | .7112 | 295 | 1.923 | 309.1 | 1.947 |
| 125 | .7786 | 50.62 | .7424 | 298.16 | 1.931 | 315.2 | 1.968 |
| 130 | .8063 | 54.58 | .7735 | 300 | 1.937 | 318.8 | 1.979 |
| 135 | .8337 | 58.68 | .8045 | 305 | 1.952 | 328.5 | 2.012 |
| 140 | .8610 | 62.92 | .8353 | 310 | 1.968 | 338.3 | 2.044 |
| 145 | .8883 | 67.29 | .8660 | 315 | 1.983 | 348.2 | 2.075 |
| 150 | .9156 | 71.80 | .8965 | 320 | 1.997 | 358.1 | 2.106 |
| 155 | .9428 | 76.45 | .9270 | 325 | 2.012 | 368.2 | 2.138 |
| 160 | .9696 | 81.23 | .9574 | 330 | 2.028 | 378.3 | 2.168 |
| 165 | .9958 | 86.14 | .9876 | | | | |
| 170 | 1.022 | 91.18 | 1.018 | | | | |

The enthalpy values given in table 4, except in the range 190° to 295° K, were obtained by evaluating the expression

$$H_T - H_0 = \int_0^T C\,dT. \qquad (1)$$

$H_0$ is the enthalpy at absolute zero of temperature. The enthalpy change over the temperature interval 190° to 295° K was computed from the experimental heat-capacities obtained in run 7 by summing the product of individual net heat capacities and the corresponding temperature rise. At other temperatures, except below 15° K, the expression in eq (1) was evaluated by numerical integration, using four-point Lagrangian integration coefficients [11]. Below 15° K, the enthalpy was evaluated by using the Debye function given above.

As previously stated, in the crystallization interval the hypothetical amorphous copolymer would probably follow the broken heat-capacity curve. By integrating along this curve (see fig. 1 and table 4) the change in enthalpy of the "amorphous" copolymer between 190° and 295° K was found to be about 180 abs j g$^{-1}$. Comparing this value with the 196.46 and 198.97 abs j g$^{-1}$ obtained in runs 7 and 9, respectively, for the same temperature interval, the heat of fusion per gram would be about 16 to 19 abs j. The range of these values is close to 16.71 abs j g$^{-1}$ obtained by Bekkedahl and Matheson [10] with natural rubber. As shown by the difference in the values obtained in runs 7 and 9, these values are dependent upon the heat treatment. As the copolymer was annealed for a longer period prior to run 9 than run 7, the larger value in run 9 seems consistent.

Entropy values given in table 4 were obtained in a similar manner as were enthalpies by evaluating the thermodynamic expression:

$$S_T - S_0 = \int_0^T \frac{C\,dT}{T}. \qquad (2)$$

$S_0$ is the entropy at absolute zero of temperature. Between 190° and 295° K, the entropy change was computed using the experimental data obtained in run 7 by summing the individual $C\Delta T/T$ values. $C$ is the net heat capacity, and $\Delta T$ and $T$ are the corresponding temperature increase and midtemperature, respectively.

The enthalpy and entropy values given in table 4 were evaluated from the results of the experiments with the annealed polymer. No attempt was made to make a similar table of the results of shock-cooled experiments.

### 4.2. GL–658, 122° F Copolymer

The heat treatments and the subsequent heat-capacity experiments with the GL–658 copolymer were carried out in a similar manner as with the X–454 copolymer. The details regarding the heat treatments, temperature range of the measurements, and the drift observations with this copolymer are

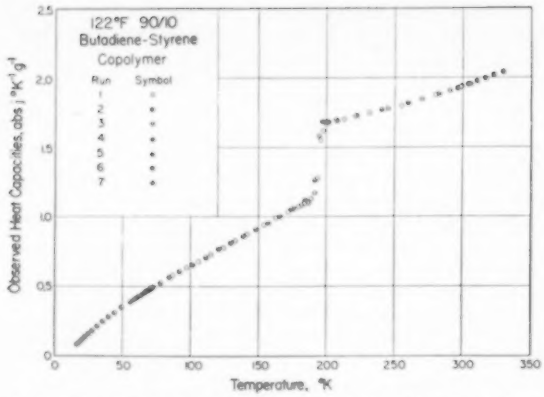


FIGURE 2. *Observed heat capacities of the GL-658, 122° F butadiene (90)-styrene (10) copolymer.*

summarized in table 5. The observed heat-capacity values are given in table 6 and plotted in figure 2. The experiments in runs 1 and 3 were made after rapidly cooling the copolymer. In these measurements upward temperature drifts were observed in the temperature range from about 167° to 195° K and no drift above 195° K. The results of runs 1, 2, and 3 show that the glass transformation occurs at about 190° to 195° K and that crystallization does not occur in this copolymer. The heat-capacity results (run 4), obtained after cooling the copolymer slowly, showed downward temperature drifts from 189° to 195° K and no drift above 195° K. The downward drift in temperature is considered to arise from slow changes in the polymer to higher states of energy. In these experiments the heat-capacity curve at the glass-transformation interval rises a few degrees sooner than the curve obtained when the copolymer was rapidly cooled. The glass-transformation temperature is taken to be 193° K, the temperature at the midpoint of the upward sweep in the curve. Between 90° and 165° K, the heats capacity results seem essentially the same, regardless of the heat treatment. The maximum spread in the over-all heat-capacity results is ±0.2 percent at the higher temperatures (above 195° K). From 165° K to the glass-transformation temperature the results show greater scattering, as much as 1 percent. The heat-capacity values show no clear correlation with heat treatment because of the obscuring effect the temperature drifts have on the heat capacity. At 177° K the temperature was drifting upward after 30 min. Thus, no further attempt was made in other experiments to reach thermal equilibrium. The temperature measurements were started at times (about 6 to 7 min after the end of heating) usually required for thermal equilibrium with simpler materials [5,8]. Experience with the X–454 copolymer and the other polymers, recently investigated at the Bureau, shows that the waiting period for thermal equilibrium can be extremely long. The heat-capacity results (runs 5, 6, and 7) below 90° K do not show any unusual effects.

TABLE 5. *Heat treatment and observations with the 122° F butadiene (90)-styrene (10) copolymer GL–658*

(Temperatures are in °K)

| Run | Treatment of sample | Temperature range of measurements | Drift observations |
|---|---|---|---|
| 1 | Cooled rapidly from room temperature to 77°. | 81° to 307° | Upward drift from 167° to 195°. No drift above 195°. |
| 2 | Left at room temperature for 2 days. | 295° to 333° | No drift. |
| 3 | Cooled rapidly from room temperature to 172°. | 172° to 311° | Upward drift from 172° to 193°. No drift above 193°. |
| 4 | Cooled slowly from room temperature over 5 days to 85°. | 87° to 294 | Downward drift from 189° to 195°. No drift above 195°. |
| 5 | Cooled from room temperature to 80° and then to 16°. | 16° to 91° | No drift. |
| 6 | Cooled from room temperature to 80° and then to 54°. | 67° to 71° | Do. |
| 7 | Cooled from room temperature to 80° and then to 55°. | 55° to 72° | Do. |

TABLE 6. *Observed heat capacities of 122° F butadiene (90)-styrene (10) copolymer GL–658*

| Run | T | C | Run | T | C | Run | T | C |
|---|---|---|---|---|---|---|---|---|
| | °K | abs j °K⁻¹g⁻¹ | | °K | abs j °K⁻¹g⁻¹ | | °K | abs j °K⁻¹g⁻¹ |
| 1 | 86.90 | 0.5793 | 3 | 175.28 | 1.059 | 5 | 16.69 | 0.0868 |
| | 96.68 | .6308 | | 181.40 | 1.083 | | 17.82 | .0965 |
| | 105.71 | .6788 | | 186.27 | 1.110 | | 19.22 | .1078 |
| | 114.79 | .7277 | | 191.03 | 1.173 | | 20.93 | .1226 |
| | 123.99 | .7781 | | 195.36 | 1.553 | | 22.94 | .1409 |
| | 132.71 | .8263 | | 199.13 | 1.676 | | 25.34 | .1624 |
| | 141.69 | .8761 | | 206.60 | 1.695 | | 28.03 | .1862 |
| | 153.76 | .9435 | | 221.43 | 1.727 | | 31.59 | .2174 |
| | 162.53 | .9902 | | 244.92 | 1.782 | | 35.63 | .2498 |
| | 171.75 | 1.036 | | 269.60 | 1.849 | | 39.88 | .2825 |
| | 179.07 | 1.073 | | 290.23 | 1.910 | | 44.39 | .3162 |
| | 183.82 | 1.098 | | 305.57 | 1.960 | | 49.14 | .3521 |
| | 188.62 | 1.133 | 4 | 91.95 | .6058 | | 71.55 | .4894 |
| | 193.21 | 1.280 | | 101.52 | .6563 | | 77.90 | .5272 |
| | 197.23 | 1.624 | | 111.01 | .7086 | | 84.43 | .5662 |
| | 201.22 | 1.684 | | 120.53 | .7615 | | 91.43 | .6053 |
| | 212.75 | 1.708 | | 129.53 | .8103 | | 66.94 | .4641 |
| | 231.34 | 1.749 | | 138.65 | .8590 | 6 | 69.25 | .4770 |
| | 254.96 | 1.809 | | 147.93 | .9077 | | 71.48 | .4897 |
| | 279.74 | 1.879 | | 156.84 | .9551 | | 55.87 | .3936 |
| | 298.54 | 1.937 | | 165.44 | 1.002 | | 58.40 | .4101 |
| | 306.22 | 1.928 | | 174.52 | 1.055 | | 60.81 | .4256 |
| | 298.89 | 1.938 | | 184.02 | 1.125 | 7 | 63.11 | .4402 |
| 2 | 303.65 | 1.954 | | 191.21 | 1.267 | | 65.84 | .4566 |
| | 310.12 | 1.975 | | 194.24 | 1.587 | | 68.97 | .4745 |
| | 316.53 | 1.997 | | 196.67 | 1.689 | | 71.95 | .4915 |
| | 322.98 | 2.024 | | 200.40 | 1.685 | | | |
| | 329.44 | 2.041 | | 207.78 | 1.699 | | | |
| | | | | 222.48 | 1.730 | | | |
| | | | | 240.52 | 1.772 | | | |
| | | | | 259.88 | 1.822 | | | |
| | | | | 282.16 | 1.887 | | | |

The results of the heat-capacity measurements were used to obtain heat-capacity values at 5-deg intervals from 0° to 330° K (table 7). The values at 15° K and below were obtained by extrapolation, using the Debye function

$$C = 0.2633\, D\left(\frac{88.7}{T}\right),$$

which was fitted to the experimental results obtained in the temperature range 17° to 25° K.

The effect of cooling rate upon the change in enthalpy between 175° and 210° K was computed from the heat-capacity data. The experiments (runs 1

TABLE 7. *Heat capacity, enthalpy, and entropy of 122° F butadiene (90)-styrene (10) copolymer G–L658*

| $T$ | $C$ | $(H_T-H_0)$ | $(S_T-S_0)$ | $T$ | $C$ | $(H_T-H_0)$ | $(S_T-S_0)$ |
|---|---|---|---|---|---|---|---|
| °K | abs j °K$^{-1}$ | abs j g$^{-1}$ | abs j °K$^{-1}$ | °K | abs j °K$^{-1}$ | abs j g$^{-1}$ | abs j °K$^{-1}$ |
| 0 | 0 | 0 | 0 | 175 | 1.055 | 97.37 | 1.067 |
| 5 | 0.0037 | 0.0046 | 0.0012 | 180 | 1.08 | ..... | ..... |
| 10 | .0278 | .0719 | .0096 | 185 | 1.11 | ..... | ..... |
| 15 | .0729 | .3174 | .0289 | 190 | 1.17 | ..... | ..... |
| 20 | .1146 | .7859 | .0557 | 195 | 1.57 | ..... | ..... |
| 25 | .1595 | 1.470 | .0860 | 200 | 1.66 | ..... | ..... |
| 30 | .2037 | 2.379 | .1191 | 205 | 1.69 | ..... | ..... |
| 35 | .2449 | 3.502 | .1536 | 210 | 1.702 | 145.5 | 1.315 |
| 40 | .2834 | 4.823 | .1888 | 215 | 1.713 | 154.0 | 1.356 |
| 45 | .3208 | 6.334 | .2244 | 220 | 1.724 | 162.6 | 1.395 |
| 50 | .3568 | 8.034 | .2602 | 225 | 1.735 | 171.3 | 1.434 |
| 55 | .3879 | 9.902 | .2958 | 230 | 1.747 | 180.0 | 1.472 |
| 60 | .4204 | 11.92 | .3309 | 235 | 1.758 | 188.7 | 1.510 |
| 65 | .4518 | 14.10 | .3658 | 240 | 1.770 | 197.6 | 1.547 |
| 70 | .4811 | 16.44 | .4004 | 245 | 1.783 | 206.4 | 1.584 |
| 75 | .5100 | 18.91 | .4345 | 250 | 1.796 | 215.4 | 1.620 |
| 80 | .5402 | 21.54 | .4684 | 255 | 1.809 | 224.4 | 1.655 |
| 85 | .5694 | 24.31 | .5020 | 260 | 1.822 | 233.5 | 1.691 |
| 90 | .5957 | 27.23 | .5353 | 265 | 1.836 | 242.6 | 1.726 |
| 95 | .6219 | 30.27 | .5682 | 270 | 1.850 | 251.8 | 1.760 |
| 100 | .6484 | 33.45 | .6008 | 275 | 1.864 | 261.1 | 1.794 |
| 105 | .6752 | 36.76 | .6331 | 280 | 1.879 | 270.5 | 1.828 |
| 110 | .7022 | 40.20 | .6651 | 285 | 1.894 | 279.9 | 1.861 |
| 115 | .7298 | 43.78 | .6970 | 290 | 1.910 | 289.4 | 1.894 |
| 120 | .7574 | 47.50 | .7286 | 295 | 1.925 | 299.0 | 1.927 |
| 125 | .7849 | 51.35 | .7601 | 298.16 | 1.936 | 305.1 | 1.948 |
| 130 | .8122 | 55.35 | .7914 | 300 | 1.942 | 308.7 | 1.960 |
| 135 | .8394 | 59.47 | .8226 | 305 | 1.958 | 318.4 | 1.992 |
| 140 | .8665 | 63.74 | .8536 | 310 | 1.975 | 328.2 | 2.024 |
| 145 | .8935 | 68.14 | .8844 | 315 | 1.992 | 338.2 | 2.055 |
| 150 | .9205 | 72.67 | .9152 | 320 | 2.009 | 348.2 | 2.087 |
| 155 | .9474 | 77.34 | .9458 | 325 | 2.026 | 358.2 | 2.118 |
| 160 | .9743 | 82.15 | .9763 | 330 | 2.043 | 368.4 | 2.149 |
| 165 | 1.001 | 87.09 | 1.007 | | | | |
| 170 | 1.028 | 92.16 | 1.037 | | | | |

and 3) made with the material cooled rapidly yielded 47.61 and 47.75 abs j $g^{-1}$, respectively, giving an average of 47.68 abs j $g^{-1}$. The result with the polymer slowly cooled (run 4) was 48.98 abs j $g^{-1}$. These results show that when the polymer is slowly cooled, the enthalpy change, between the temperature limits given, is greater by about 1.30 abs j $g^{-1}$.

The enthalpy values (table 7) at 5-deg intervals from 0° to 330° K were obtained in a similar manner as for the X–454 copolymer by evaluating eq 1. For the temperature interval 175° to 210° K, the average enthalpy change for the three experiments (1, 3, and 4) was used in constructing the table. No attempt was made to evaluate the enthalpies at other temperatures within this interval.

The entropy values were evaluated in a similar manner as were those of X–454 copolymer. These are given in table 7. The entropy change over the temperature interval 175° to 210° K used in the computations is the average of the three experiments previously mentioned.

### 4.3. Reliability of Results

The reliability of the heat-capacity measurements with the copolymers is difficult to evaluate because of the nonreproducibility of the physical state. Campbell and Allen [12] have shown in photomicrographs similarity in spherulite formation when the polymer was not raised too far above its melting temperature and recrystallized. The scattering in the heat-capacity results of X–454 copolymer does not seem to support this, however. The heat-capacity measurements with more normal materials [5, 8] in a similar calorimeter yielded results considered to have an error of 0.2 percent.[4] The results with the X-454 copolymer show the heat capacities of the two series of experiments to differ as much as 1.2 percent just below the glass-transformation temperature. Within the same series of experiments, in which the material has been treated very similarly, the results are within 0.2 percent, except near the transformation temperature. The results above the crystallization temperature (that is, above 285° K) in the amorphous region are believed to have the error of 0.2 percent. Below the glass-transformation temperature to 50° K the error of the results in the same series of experiments is considered to be 0.3 percent. Below 50° K, the error increases to several percent at 17° K.

The results with the GL–658 copolymer show as much as 1-percent scattering in the temperature range 165° K to the glass-transformation temperature. Between 90° and 165° K the results are essentially the same within ±0.2 percent, regardless of the heat treatment. Above the glass-transformation temperature at which the heat-capacity results lie on a smooth curve, the results are considered to have an error of 0.2 percent. Between 50° and 165° K, the error is believed to be 0.3 percent, and between 165° K and the glass-transformation temperature, to be 0.5 to 1 percent. Below 50° K the error increases to several percent similar to the X–454 copolymer.

Except for the transition intervals, the tabulated (tables 4 and 7) enthalpy and entropy for the two copolymers were obtained, as previously shown, from the smoothed heat capacities. These thermal quantities are dependent upon the accuracy of the heat capacity from which they were evaluated. Considering the various sources of inaccuracy, the error in the tabulated values of these quantities is believed to be 0.5 percent.

## 5. Discussion

The results of these experiments show that the increase in the polymerization temperature from 41° to 122° F eliminated crystallization effects in the 90/10 butadiene-styrene copolymer. This behavior, in which the crystallizability of polymers is increased with decreasing polymerization temperatures, has been observed by other investigators. Beu, et al. [13] and Beu [14], using an X-ray method, found such a behavior in the crystallinity of stretched polybutadienes and butadiene-styrene copolymers prepared at temperatures from −20° to +55° C. Lucas, et al. [15], using a dilatometer method, studied relative crystallizability and molecular regularity in polybutadienes, polychloroprenes, and butadiene-styrene copolymers prepared at temperatures ranging from −33° to +50° C, and found a similar behavior in the crystallizability of these polymers. More recently, Campbell and Allen [12] used a polarizing microscope

[4] For these experiments a true probable error cannot be computed statistically. The values given are estimates reached by examining contributions to the inaccuracy from all known sources. The authors estimate that there is an equal chance that the error is no larger than that indicated.



256401—53——5

to show greater crystallizability in polybutadienes prepared at lower temperatures. They found 41° F 90/10 butadiene-styrene copolymer to show a small crystallinity.

Bekkedahl and Matheson [10] measured the heat capacity of natural rubber and reported a fairly sharp melting point, giving the melting temperature as 284° K. Wood and Bekkedahl [16] found the crystallization temperature of unvulcanized natural rubber to extend from 220° to 290° K. Their measurements also show the melting temperature to depend upon the crystallization temperature. The results of the measurements with the X–454 copolymer reported herein show the crystallization temperature to extend from 210° to 285° K, with no indication of any sharp melting temperature. There is, however, at about 250° K a maximum (fig. 1) in the heat capacity. In recent unpublished heat-capacity investigations at the Bureau with 41° and 122° F polybutadienes, the crystallization temperature ranges were found to be from 200° to 295° K and 200° to 270° K, respectively.

In the heat-capacity experiments by Bekkedahl and Matheson [10] the glass-transformation temperature was reported to be 199° K. Thermal expansion measurements, in which the coefficient of thermal expansion rises steeply with temperature at the glass-transformation temperature in a similar manner as the heat-capacity curve, show glass transformation in natural rubber to occur at 200° K [17]. Ferry and Parks [18] investigated the heat capacity and thermal expansion of polyisobutylene and found the glass-transformation temperature in both measurements to be 197° K. As pointed out by Kauzmann [19], this indicates a close alliance of motions in polymers involving energy and volume. Also, glass transformation as observed in heat-capacity and thermal-expansion measurements is closely associated with the brittle-point temperature, below which rubber polymers lose rubber-like elasticity. Similarly, dielectric-relaxation time [19] is shown to increase steeply as temperature is lowered through the glass-transformation temperature. There are many suggestions [20, 21, 22] as to how molecular structure in the polymer affects the glass-transformation temperature. The size of the side groups, symmetry of the polymeric units, degree of cross-linking, and ease of rotation about the carbon-carbon bonds as might be influenced by the intramolecular structure and neighboring molecules are some of the factors that seem to affect the glass-transformation temperature. The transformation temperature in styrene-divinyl benzene copolymers [21] has been shown to increase when the number of monomer units between cross-links becomes less than 300. The crystallization process would be expected to have a similar effect [21], if the degree of crystallization is such that the number of monomer units between crystallites becomes smaller than the above figure. The heat-capacity measurements [10] with natural rubber show that this transformation temperature is higher when the material is crystallized, although attention has not been called previously to this fact. The results with the X–454 copolymer show a similar rise in the transformation temperature when the sample was annealed. As previously pointed out, the results are, however, dependent somewhat upon the time allowed before temperature measurement. On the other hand, the experiments with the 122° F copolymer, which does not crystallize, seem to show that the steep increase in the heat-capacity curve occurs a few degrees lower in the slowly cooled experiments. In comparing the glass-transformation temperatures, the experimental results with the two

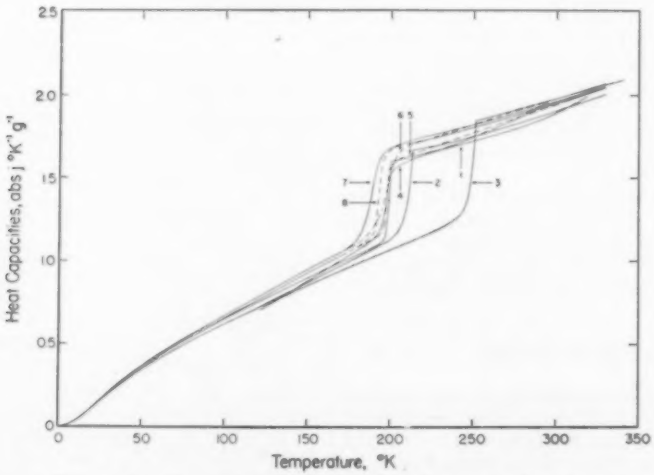


FIGURE 3. *Comparison of the heat-capacity curves of various polymers.*

1, Natural rubber [10]; 2, GR–S [2]; 3, Hycar O. R.–15 [1]; 4, polyisobutylene [19]; 5, 41° F 90/10 butadiene-styrene copolymer; 6, 41° F polybutadiene; 7, 122° F polybutadiene, and 8, 122° F 90/10 butadiene-styrene copolymer.

copolymers indicate that the change in the polymerization temperature from 122° F (50° C) to 41° F (5° C) raised the transformation temperature from 193° to 200° K. This behavior is similar to that found with the recently investigated 122° and 41° F polybutadienes, in which the glass-transformation temperatures obtained are 187° and 195° K, respectively. These results seem accordant on the basis that a higher polymerization temperature yields a polymer of lower regularity [12, 13, 14, 15] and a more open intermolecular structure to permit greater ease in the rotation of the polymer segments [21]. As previously mentioned, crystallization increases the glass-transformation temperature, and the lowering of the polymerization temperature increases the crystallizability. These effects are all consistent with the experimental results.

Tuckett [22] and Überreiter [23] have shown that in styrene-butadiene copolymers the styrene hinders free rotation, and that the increase in the bound-styrene content raises the glass-transformation temperature. The glass-transformation temperature 195° and 187° K for the 41° and 122° F polybutadienes, 200° and 193° K for the 41° and 122° F butadiene-styrene (8.58 percent) copolymers reported here, and 237° K very recently obtained at the Bureau for the 122° F butadiene-styrene (42.98 percent) copolymer are in conformity with the results of the above investigators.

The heat-capacity curves for polyisobutylene [18], natural rubber [10], Hycar O. R.–15 [1], GR–S [2], 41° and 122° F polybutadienes, and 41° and 122° F 90/10 butadiene-styrene copolymers are compared in figure 3. It is interesting to note that the heat capacities per unit mass for these polymers lie within a narrow band. The heat capacities of the two copolymers reported merge into a single curve below the glass-transformation temperature; percentage wise, however, the curves are not quite the same as shown by tables 4 and 7. The experimental values above the transformation temperature for the two copolymers differ by about 0.1 percent at 295° K, increasing to about 0.7 percent at 330° K. The two polybutadienes, previously mentioned, show similar behavior. The glass-transformation temperatures of the various polymers are compared in the figure, showing Hycar 0. R.–15 [1] to have the highest transformation temperature.

The authors are grateful to W. Bruenner and M. L. Reilly for assisting with some of the experimental work and calculations, to M. Tryon for purifying the polymer samples, and to R. A. Paulson for the chemical analysis of the polymers.

## 6. References

[1] N. Bekkedahl and R. B. Scott, J. Research NBS **29,** 87 (1942) RP 1487.
[2] R. D. Rands, Jr., W. J. Ferguson, and J. L. Prather, J. Research NBS **33,** 63 (1944) RP1595.
[3] J. M. Goppel and J. J. Arlman, Appl. Sci. Research, **A1,** 462 (1949).
[4] R. B. Scott, C. H. Meyers, R. D. Rands, Jr., F. G. Brickwedde, and N. Bekkedahl, J. Research NBS **35,** 39 (1945) RP1661.
[5] G. T. Furukawa, D. C. Ginnings, R. E. McCoskey, and R. A. Nelson, J. Research NBS **46,** 195 (1951) RP2191.
[6] H. F. Stimson, J. Research NBS **42,** 209 (1949) RP1962.
[7] H. J. Hoge and F. G. Brickwedde, J. Research NBS **22,** 351 (1939), RP1188.
[8] G. T. Furukawa, R. E. McCoskey, and G. J. King, J. Research NBS **47,** 256 (1951) RP2251.
[9] R. W. Laundrie, Butadiene-styrene copolymers for refractive index studies, University of Akron-Government Laboratories, AU–725, Project P 100.74 August 12, 1949.
[10] N. Bekkedahl and H. Matheson, J. Research NBS **15,** 503 (1935) RP844.
[11] Tables of Lagrangian Interpolation coefficients (Columbia University Press, New York, N. Y., 1944).
[12] H. N. Campbell and M. D. Allen, Ind. Eng. Chem. **43,** 413 (1951).
[13] K. E. Beu, W. B. Reynolds, C. F. Fryling, and H. L. McMurry, J. Polymer Sci. **3,** 465 (1948).
[14] K. E. Beu, J. Polymer Sci. **3,** 801 (1948).
[15] V. E. Lucas, P. H. Johnson, L. B. Wakefield, B. L. Johnson, Ind. Eng. Chem **41,** 1629 (1949).
[16] L. A. Wood and N. Bekkedahl, J. Research NBS **36,** 489 (1946). RP1718.
[17] N. Bekkedahl, J. Research NBS **13,** 411 (1934) RP717.
[18] J. D. Ferry and G. S. Parks, J. Chem. Phys. **4,** 70 (1936).
[19] W. Kauzmann, Chem. Rev. **43,** 219 (1948).
[20] K. Überreiter, Kolloid-Z. **102,** 272 (1943).
[21] H. Mark and G. S. Whitby, Scientific progress in the field of rubber and synthetic elastomers (Interscience Publishers, Inc., New York, N. Y., 1946).
[22] R. F. Tuckett, Trans. Faraday Soc. **38,** 310 (1942).
[23] K. Überreiter, Z. angew. Chem. **53,** 247 (1940).

WASHINGTON, June 9, 1952.

EAST ENGIN LIBRARY
TA 1 .458

# INDEX TO VOLUME 50


## A

Page

Acrylate, styrene, and isoprene polymers, pyrolysis of, RP2405 ..... 165
Altimeter, nonquantized frequency-modulated, RP2413 ..... 215
Angle blocks, assembled polygon for calibration of, RP2387 ..... 45
Angular standard, solid, RP2387 ..... 45
Angular velocity measurements, RP2390 ..... 69
Atomic hydrogen, sixth series in spectrum of, RP2380 ..... 1

## B

*Ball, A. F., D. C. Ginnings, D. T. Vier,* Calorimetric determination of the half-life of polonium, RP2392 ..... 75
Beryllium, intersystem transition in first spectrum of, RP2399 ..... 131
*Black, M. H., J. M. Florence, F. W. Glaze,* Transmission of near-infrared energy by some two- and three-component glasses, RP2408 ..... 187
*Blanch, G.,* On the numerical solution of parabolic partial differential equations, RP2424 ..... 343
*Bozman, W. F., C. H. Corliss, W. F. Meggers, R. E. Trees,* An intersystem transition in the first spectrum of beryllium, RP2399 ..... 131
*Bradt, P., V. H. Dibeler, F. L. Mohler,* A new technique for the mass spectrometric study of the pyrolysis products of polystyrene, RP2410 ..... 201
*Brownell, R. M. F. H. Forziati, C. M. Hunt,* Surface areas of cottons and modified cottons before and after swelling as determined by nitrogen sorption, RP2401 ..... 139
Butadiene-styrene copolymers, thermal properties, RP2425 ..... 357
*Buzzard, R. W.,* Beryllium-uranium system, RP2389 ..... 63
—, *R. B. Liss, D. P. Fickle,* Titanium-uranium system in the region 0 to 30 atomic percent of titanium, RP2412 ..... 209

## C

*Cacheris, J. C., H. P. Kalmus, H. A. Dropkin,* Nonquantized frequency-modulated altimeter, RP2413 ..... 215
Calculus of variations, RP2418 ..... 277
Calorimeter, use in measuring heats of radioactivity, RP2392 ..... 75
Chemical durability of silicates, enamels, and metals, RP2394 ..... 87
*Chung, K. L.,* Contributions to the theory of Markov chains, RP2411 ..... 203
Cobalt-60, standardization of, RP2409 ..... 197
Compression of natural rubber-sulfur vulcanizates, temperature dependence of, RP2403 ..... 153
Cooperative phenomena, tabulation of an integral arising in the theory of, RP2406 ..... 177
Copolymers, butadiene-styrene, thermal properties, RP2425 ..... 357
Copper-reducing value of dextran, RP2393 ..... 81
*Corliss, C. H., W. R. Bozman, W. F. Meggers, R. E. Trees,* An intersystem transition in the first spectrum of beryllium, RP2399 ..... 131
Corrosion of ferrous metals in soils, RP2422 ..... 329
*Corruccini, R. J., H. Shenker,* Modified 1913 reference tables for iron-constantan thermocouples, RP2415 ..... 229
Cotton, determination of surface areas, RP2401 ..... 139

## D

Damping of elastically supported element in a vacuum tube, RP2391 ..... 71
*Davis, R., K. S. Gibson, G. W. Haupt,* Spectral energy distribution of the International Commission on Illumination light sources, A, B, and C., RP2384 ..... 31
Daylight spectral energy distribution, CIE, RP2384 ..... 31
*de Bruijn, N. G., P. Erdős,* On a recursion formula and on some Tauberian theorems, RP2404 ..... 161
Dextran, molecular weight, RP2393 ..... 81
*Dibeler, V. H., P. Bradt, F. L. Mohler,* A new technique for the mass spectrometric study of the pyrolysis products of polystyrene, RP2410 ..... 201
Dielectric loss calculations from dielectric dispersion for polar polymers, RP2382 ..... 19
Differential equations, parabolic partial, numerical solution, RP2424 ..... 343
*Dropkin, H. A., H. P. Kalmus, J. C. Cacheris,* Nonquantized frequency-modulated altimeter, RP2413 ..... 215
*Dryden, M. R., H. S. Isbell, C. F. Snyder, N. B. Holt,* Determination of molecular weights of dextrans by means of alkaline copper reagents, RP2393 ..... 81

## E

*Ehrlich, P.,* A simple calculation of dielectric loss from dielectric dispersion for polar polymers, RP2382 ..... 19
Elastomer latices, synthetic, electron microscopy of, RP2419 ..... 299
Electrical resistance and voltage departures of glass electrodes, effect of temperature on, RP2423 ..... 337
Electrodes, glass, effect of temperature on electrical resistance and voltage departures of, RP2423 ..... 337
Enamels, vitreous, chemical durability, RP2394 ..... 87
*Engel, O. G.,* Epitaxial deposits of metals evaporated on salt substrates, RP2416 ..... 249
Epitaxial deposits of metals evaporated on salt substrates, RP2416 ..... 249
Equation for atmospheric refractive index at radio frequencies, constants in, RP2385 ..... 39
*Erdős, P., N. G. de Bruijn,* On a recursion formula and on some Tauberian theorems, RP2404 ..... 161
Ethanes, spectra of, RP2414 ..... 223
Expansion, thermal, of invar surveying tapes, RP2407 ..... 179

## F

*Fickle, D. P., R. W. Buzzard, R. B. Liss,* Titanium-uranium system in the region 0 to 30 atomic percent of titanium, RP2412 ..... 209
*Florence, J. M., F. W. Glaze, M. H. Black,* Transmission of near-infrared energy by some two- and three-component glasses, RP2408 ..... 187
Fluoroethanes, spectra of, RP2414 ..... 223
*Forziati, F. H., R. M. Brownell, C. M. Hunt,* Surface areas of cottons and modified cottons before and after swelling as determined by nitrogen sorption, RP2401 ..... 139
Frequency-modulated, nonquantized altimeter, RP2413 ..... 215
*Frush, H. L., H. S., Isbell,* Synthesis of lactose-1-C$^{14}$ and lactobionic-1-C$^{14}$ delta lactone from 3-β-D-galactopyranosyl-α-D-arbinose, RP2400 ..... 133
*Furukawa, G. T., R. F. McCoskey, G. J. King,* Thermal properties of some butadiene-styrene copolymers, RP2425 ..... 357

## G

Galactopranosyl-arabinose, preparation, RP2400 ..... 133
Gentiobiose, copper-reducing value, RP2393 ..... 81
*Gibson, K. S., R. Davis, G. W. Haupt,* Spectral energy distribution of the International Commission on Illumination light sources, A, B, and C., RP2384 ..... 31
*Ginnings, D. C., A. F. Ball, D. T. Vier,* Calorimetric determination of the half-life of polonium, RP2392 ..... 75
Glass electrodes, effect of temperature on electrical resistance and voltage departures of, RP2423 ..... 337
Glass transformation in polymers, RP2425 ..... 337
Glasses, three component, transmittance of near-infrared energy, RP2408 ..... 187
*Glaze, F. W., J. M. Florence, M. H. Black,* Transmission of near-infrared energy by some two- and three-component glasses, RP2408 ..... 187

## H

*Hakkarinen, W., P. D. Lowell, D. L. Randall,* National Bureau of Standards mobile low-level sounding system, RP2381 ..... 7
Half-life of polonium, calorimetric determination, RP2392 ..... 75
*Hammersley, J. M.,* Tables of complete elliptic integrals, RP2386 ..... 43
*Haupt, G. W., R. Davis, K. S. Gibson,* Spectral energy distribution of the International Commission on Illumination light sources, A, B, and C., RP2384 ..... 31
*Haven, C. E., A. G. Strang,* Assembled polygon for the calibration of angle blocks, RP2387 ..... 45
Heat of radioactivity of polonium, RP2392 ..... 75
*Hidnert, P., R. K. Kirby,* A new method for determining linear thermal expansion of invar geodetic surveying tapes, RP2407 ..... 179
*Hobbs, E. V., S. Levy, W. D. Kroll, L. Mordfin,* Damping of elastically supported element in a vacuum tube, RP2391 ..... 71
*Holt, N. B., H. S. Isbell, C. F. Snyder, M. R. Dryden,* Determination of molecular weights of dextrans by means of alkaline copper reagents, RP2393 ..... 81
*Hubbard, D.,* Effect of temperature on the electrical resistance and voltage departures (errors) of glass electrodes, and upon the hydroscopicity of glass, RP2423 ..... 337
—, *R. G. Pike,* An interferometer procedure applied to the study of the chemical durability of silicates, enamels, and metals, RP2394 ..... 87
*Humphreys, C. J.,* The sixth series in the spectrum of atomic hydrogen, RP2380 ..... 1
*Hunt, C. M., F. H. Forziati, R. M. Brownell,* Surface areas of cottons and modified cottons before and after swelling as determined by nitrogen sorption, RP2401 ..... 139
Hydrogen, atomic, sixth series in spectrum of, RP2380 ..... 1
Hydrogen-ion response and electrical resistance of glass electrodes, effect of temperature on, RP2423 ..... 337
Hydronamic effects of gales on Lake Erie, RP2396 ..... 99
Hygroscopicity of glass, effect of temperature on, RP2423 ..... 337

## I

Infrared energy, transmittance by some three-component glasses, RP2408 ..... 187
Infrared spectra of fluoroethanes, RP2414 ..... 223
Integrals, tables of complete elliptic, RP2386 ..... 43
Interferometer procedure for determining chemical durability of silicates, enamels, and metals, RP2394 ..... 87
International Commission on Illumination light sources, spectral energy distribution, RP2384 ..... 31
Intersystem transition in the first spectrum of beryllium, RP2399 ..... 131
Invar surveying tapes, thermal expansion, RP2407 ..... 179
Iodine-131, standardization of, RP2409 ..... 197
Iron-constantan thermocouples, reference tables, RP2415 ..... 229
*Isbell, H. S., H. L. Frush,* Synthesis of lactose-1-C$^{14}$ and lactobionic-1-C$^{14}$ delta lactone from 3-β-D-galactopyranosyl-α-D-arabinose, RP2400 ..... 133
—, *C. F. Snyder, N. B. Holt, M. R. Dryden,* Determination of molecular weights of dextrans by means of alkaline copper reagents, RP2393 ..... 81
Isomaltose, copper-reducing value, RP2393 ..... 81
Isoprene, styrene, and acrylate polymers, pyrolysis of, RP2405 ..... 165

## K

*Kalmus, H. P., J. C. Cacheris, H. A. Dropkin,* Nonquantized frequency-modulated altimeter, RP2413 ..... 215
*Keulegan, G. H.,* Hydrodynamic effects of gales on Lake Erie, RP2396 ..... 99
*King, G. J., G. T. Furukawa, R. F. McCoskey,* Thermal properties of some butadiene-styrene copolymers, RP2425 ..... 357
*Kirby, R. K., P. Hidnert,* A new method for determining linear thermal expansion of invar geodetic surveying tapes, RP2407 ..... 179
*Kroll, W. D., S. Levy, F. V. Hobbs, L. Mordfin,* Damping of elastically supported element in a vacuum tube, RP2391 ..... 71

## L

Lactobionic acid-1-C$^{14}$, preparation and crystallization of lactone, RP2400 ..... 133
Lactose-1-C$^{14}$, method for preparation, RP2400 ..... 133
Lake Erie wind tides, RP2396 ..... 99
*Levy, S., E. V. Hobbs, W. D. Kroll, L. Mordfin,* Damping of elastically supported element in a vacuum tube, RP2391 ..... 71

Light sources, CIE, spectral energy distribution, RP2384 ..... 31
*Liss, R. B., R. W. Buzzard, D. P. Fickle*, Titanium-uranium system in the region 0 to 30 atomic percent of titanium, RP2412 ..... 209
*Lowell, P. D., W. Hakkarinen, D. L. Randall*, National Bureau of Standards mobile low-level sounding system, RP2381 ..... 7
*Luxenberg, H.*, Torsion of anisotropic elastic cylinders by forces applied on the lateral surface, RP2417 ..... 263

M

*Madorsky, S. L., S. Straus*, Pyrolysis of styrene, acrylate, and isoprene polymers in a vacuum, RP2405 ..... 165
*Mandel, J., R. R. Stromberg, M. Swerdlow*, Electron microscopy of synthetic elastomer lattices, RP2419 ..... 299
*Mann, W. B., H. H. Seliger*, Refinements in radioactive standardization by $4\pi$ beta counting, RP2409 ..... 197
Markov chains, contributions to theory of, RP2411 ..... 203
Mass spectrometric study of pyrolysis products of polystyrene, RP2410 ..... 201
Mathematical tables, complete elliptic integrals, RP2386 ..... 43
Mathematical tables, Struve function, RP2383 ..... 21
*McCoskey, R. E., G. T. Furukawa, G. J. King*, Thermal properties of some butadiene-styrene copolymers, RP2425 ..... 357
*Meggers, W. F., W. R. Bozman, C. H. Corliss, R. E. Trees*, An intersystem transition in the first spectrum of beryllium, RP2399 ..... 131
Metal, sheet, determination of shear stress-strain relation:
RP2397 ..... 111
RP2398 ..... 125
Metals chemical durability, RP2394 ..... 87
Metals, evaporated on salt substrates, epitaxial deposits of, RP2416 ..... 249
Metals, ferrous, corrosion in soils, RP2422 ..... 329
Meteorological sounding system, NBS low-level, RP2381 ..... 7
Microscopy, electron, of synthetic elastometer lattices, RP2419 ..... 299
*Miller, J. A., W. Ramberg*, Stress-strain relation in shear from twisting test of annulus, RP2398 ..... 125
—, —, Twisted square plate method and other methods for determining the shear stress-strain relation of flat sheet, RP2397 ..... 111
*Mohler, F. L., P. Bradt, V. H. Dibeler*, A new technique for the mass spectrometric study of the pyrolysis products of polystyrene, RP2410 ..... 201
Moisture and temperature distributions, low-level sounding system for, RP2381 ..... 7
Molecular weight of dextran, determination by means of alkaline copper reagents, RP2393 ..... 81
*Mordfin, L., S. Levy, E. V. Hobbs, W. D. Kroll*, Damping of elastically supported element in a vacuum tube, RP2391 ..... 71

N

National Bureau of Standards mobile low-level sounding system, RP2381 ..... 7
Nitrogen sorption determination of surface areas of cotton, RP2401 ..... 139
Numerical solution of parabolic partial differential equations, RP2424 ..... 343

P

Parabolic partial differential equations, numerical solution, RP2424 ..... 343
Particle size, determination of synthetic elastomer lattices, RP2419 ..... 299
Phosphorus-32, standardization of, RP2409 ..... 197
*Pike, R. G., D. Hubbard*, An interferometer procedure applied to the study of the chemical durability of silicates, enamels, and metals, RP2394 ..... 87
*Plyler, E. K., D. Simpson*, Infrared spectra of pentachlorofluorethane, 1,2-dichlorotetrafluorethane, and 1-bromo-2-fluorethane, RP2414 ..... 223
Polonium, half-life, calorimetric determination, RP2392 ..... 75
Polygon, assembled, for calibration of angle blocks, RP2387 ..... 45
Polymers, polar, dielectric loss calculation from dielectric dispersion, RP2382 ..... 19
Polymers, styrene, acrylate, and isoprene, pyrolysis of, RP2405 ..... 175
Polystyrene, mass spectrometric study of pyrolysis products of, RP2410 ..... 201
Polytetrafluoroethylene transitions and phases of, RP2395 ..... 95
Pressure-volume-temperature relationships of natural rubber-sulfur vulcanizates, RP2403 ..... 153
Pyrolysis of styrene, acrelate, and isoprene polymers in a vacuum, RP2405 ..... 165
Pyrolysis products of polystyrene, mass spectrometric study, RP2410 ..... 201

R

Radio frequencies, atmospheric refractive index at, constants in equation for, RP2385 ..... 39
Radio-wave propagation measurements, low-level sounding system for determination of moisture and temperature distributions for use in, RP2381 ..... 7
Radioactive standardization by $4\pi$ beta counting, RP2409 ..... 197
Radioactivity of polonium, calorimetric determination, RP2392 ..... 75
*Ramberg, W., J. A. Miller*, Stress-strain relation in shear from twisting test of annulus, RP2398 ..... 125
—, —, Twisted square plate method and other methods for determining the shear stress-strain relation of flat sheet, RP2397 ..... 111
*Randall, D. L., P. D. Lowell, W. Hakkarinen*, National Bureau of Standards mobile low-level sounding system, RP2381 ..... 7
Recursion formula, RP2404 ..... 161
Reference tables for iron-constantan thermocouples, RP2415 ..... 229
Refractive index, atmospheric, at radio frequencies, constants in equation for, RP2385 ..... 39
Resistors, multimegohm, measurement, RP2402 ..... 147
Rubber-sulfur system at high pressures, thermodynamics of, RP2421 ..... 321
Rubber-sulfur vulcanizates, temperature dependence of compression of, RP2403 ..... 153
Rubbers, second-order transitions of at high pressures, RP2420 ..... 311

S

Salt substrates, epitaxial deposits of metals evaporated on, RP2416 ..... 249
Scaler circuit, use of in measuring frequency, RP2390 ..... 69
*Schwerdtfeger, W. J.*, Laboratory measurement of the corrosion of ferrous metals in soils, RP2422 ..... 329
*Scott, A. H.*, Measurement of multimegohm resistors, RP2402 ..... 147
Second order transitions of rubbers at high pressures, RP2420 ..... 311
*Seliger, H. H., W. B. Mann*, Refinements in radioactive standardization by $4\pi$ beta counting, RP2409 ..... 197
Shear flow, turbulent, spectrum of energy in, RP2388 ..... 51
Shear stress-strain relation of sheet metal, determination of:
RP2397 ..... 111
RP2398 ..... 125
*Shenker, H., R. J. Corruccini*, Modified 1913 reference tables for iron-constantan thermocouples, RP2415 ..... 229
Silicates, chemical durability, RP2394 ..... 87
*Simpson, D., E. K. Plyler*, Infrared spectra of pentachlorofluorethane, 1,2-dichlorotetrafluoroethane, and 1-bromo-2-fluoroethane, RP2414 ..... 223
*Smith, E. K., Jr., S. Weintraub*, The constants in the equation for atmospheric refractive index at radio frequencies, RP2385 ..... 39
*Snyder, C. F., H. S. Isbell, N. B. Holt, M. R. Dryden* Determination of molecular weights of dextrans by means of alkaline copper reagents, RP2393 ..... 81
Sodium lactobionate-1-C$^{14}$, preparation RP2400 ..... 133
Soils, corrosion of ferrous metals in, RP2422 ..... 329
Sounding system, NBS low-level meteorological, RP2381 ..... 7
Spectra of substituted ethanes, RP2414 ..... 223
Spectral energy distribution of CIE light sources, RP2384 ..... 31
Spectrum of atomic hydrogen, sixth series in, RP2380 ..... 1
Spectrum of beryllium, first, intersystem transition in, RP2399 ..... 131
Spectrum of energy in turbulent shear flow, RP2388 ..... 51
*Stein, M. L.*, On methods for obtaining solutions of fixed end-point problems in the calculus of variations, RP2418 ..... 277
*Strang, A. G., C. E. Hazen*, Assembled polygon for the calibration of angle blocks, RP2387 ..... 45
*Straus, S., S. L. Madorsky*, Pyrolysis of styrene, acrylate, and isoprene polymers in a vacuum, RP2405 ..... 165
Stress-strain relation in shear, twisted square plate method, RP2397 ..... 111
Stress-strain relation in shear from twisting test of annulus, RP2398 ..... 125
Stresses in beam of elliptic cross section, RP2417 ..... 263
Stroboscopic light source, RP2390 ..... 69
*Stromberg, R. R., M. Swerdlow, J. Mandel*, Electron microscopy of synthetic elastomer latices, RP2419 ..... 299
Struve function of order three-halves, RP2383 ..... 21
Styrene, acrylate, and isoprene polymers, pyrolysis of, RP2405 ..... 165
Styrene-butadiene copolymers, thermal properties, RP2425 ..... 357
Sugars, carbon-14 labeled, preparation, RP2400 ..... 133
*Sulzer, P. G., M. Wales, L. C. Williams*, Pulsed light system for multiple-cell ultracentrifuge rotor, RP2390 ..... 69
Surface areas of cottons, determination, RP2401 ..... 139
Surveyor's tapes, thermal expansion, RP2407 ..... 179
Swelling, effect on surface areas of cotton, RP2401 ..... 139
*Swerdlow, M., R. R. Stromberg, J. Mandel*, Electron microscopy of synthetic elastomer latices, RP2419 ..... 299

T

Tables, reference, for iron-constantan thermocouples, RP2415 ..... 229
Tapes, surveying, thermal expansion, RP2407 ..... 179
Tauberian theorems, RP2404 ..... 161
*Tchen, C. M.*, On the spectrum of energy in turbulent shear flow, RP2388 ..... 51
Temperature and moisture distributions, low-level sounding system for, RP2381 ..... 7
Temperature dependence of compression of natural rubber-sulfur vulcanizates of high sulfur content, RP2403 ..... 153
Temperature, effect on electrical resistance and voltage departures of glass electrodes, RP2423 ..... 337
Theory of cooperative phenomena, tabulation of an integral arising in, RP2406 ..... 177
Theory of Markov chains, contributions to, RP2411 ..... 203
Thermal expansion of invar surveying tapes, RP2407 ..... 179
Thermal properties of some butadiene-styrene copolymers, RP2425 ..... 357
Thermocouples, iron-constantan, reference tables, RP2415 ..... 229
Thermodynamics of the rubber-sulfur system at high pressures, RP2421 ..... 321
*Tikson, M.*, Tabulation of an integral arising in the theory of cooperative phenomena, RP2406 ..... 177
Titanium-uranium system in the region 0 to 30 percent of titanium, RP2412 ..... 209
Torsion of anisotropic elastic cylinders by forces applied on the lateral surface, RP2417 ..... 263
Transition, intersystem, in first spectrum of beryllium, RP2399 ..... 131
Transitions and phases of polytetrafluoroethylene, RP2395 ..... 95
Transitions, second-order, of rubber at high pressures, RP2420 ..... 311
Transmittance of near-infrared energy by some three-component glasses, RP2408 ..... 187
*Trees, R. E., W. F. Bozman, C. H. Corliss, W. F. Meggers*, An intersystem transition in the first spectrum of beryllium, RP2399 ..... 131
Twisted square-plate method and other methods for determining shear stress-strain relation of flat sheet, RP2397 ..... 111

U

Uranium-beryllium system, RP2389 ..... 63
Uranium-titanium system in the region of 0 to 30 percent of titanium, RP2412 ..... 209

V

Vacuum tube, damping of elastically supported element in, RP2391 ..... 71
*Vier, D. T., D. C. Ginnings, A. F. Ball*, Calorimetric determination of the half-life of polonium, RP2392 ..... 75
Vulcanizates of high sulfur content, temperature dependence of compression of, RP2403 ..... 153

W

*Wales, M., P. G. Sulzer, L. C. Williams*, Pulsed light system for multiple-cell ultracentrifuge rotor, RP2390 ..... 69
*Weintraub, S., E. K. Smith, Jr.*, The constants in the equation for atmospherical refractive index at radio frequencies, RP2385 ..... 39
*Weir, C. E.*, Second-order transitions of rubbers at high pressures, RP2420 ..... 311
—, Temperature dependence of compression of natural rubber-sulfur vulcanizates of high sulfur content, RP2403 ..... 153
—, Thermodynamics of the rubber-sulfur system at high pressures, RP2421 ..... 321
—, Transitions and phases of polytetrafluoroethylene (Teflon), RP2395 ..... 95
*Williams, L. C., M. Wales, P. G. Sulzer*, Pulsed light system for multiple-cell ultracentrifuge rotor, RP2390 ..... 69
Wind forces on bodies of water, RP2396 ..... 99
Wind tides of Lake Erie, RP2390 ..... 99

East Engineering

# Journal of Research

of the

National Bureau of Standards

JUNE 1953

VOLUME 50 NUMBER 6

U. S. DEPARTMENT OF COMMERCE
Sinclair Weeks, Secretary
NATIONAL BUREAU OF STANDARDS
A. V. Astin, Director

JUNE • 1953
VOLUME • 50
NUMBER • 6

# JOURNAL OF RESEARCH

of the

## NATIONAL BUREAU OF STANDARDS

### PERIODICALS OF THE NATIONAL BUREAU OF STANDARDS

The National Bureau of Standards is engaged in fundamental and applied research in physics, chemistry, mathematics, and engineering. Projects are conducted in fifteen fields: electricity, optics and metrology, heat and power, atomic and radiation physics, chemistry, mechanics, organic and fibrous materials, metallurgy, mineral products, building technology, applied mathematics, electronics, ordnance development, radio propagation, and missile development. The Bureau has custody of the national standards of measurement and conducts research leading to the improvement of scientific and engineering standards and of techniques and methods of measurement. Testing methods and instruments are developed; physical constants and properties of materials are determined; and technical processes are investigated.

### JOURNAL OF RESEARCH

Internationally known as a leading scientific periodical, the Journal presents research papers by authorities in the specialized fields of physics, mathematics, chemistry, and engineering. Complete details of the work are presented, including laboratory data, experimental procedures, and theoretical and mathematical analyses. Annual subscription: domestic, $5.50; foreign, $6.75.

### TECHNICAL NEWS BULLETIN

Summaries of current research at the National Bureau of Standards are published each month in the Technical News Bulletin. The articles are brief, with emphasis on the results of research, chosen on the basis of their scientific or technologic importance. Lists of all Bureau publications during the preceding month are given, including Research Papers, Handbooks, Applied Mathematics Series, Building Materials and Structures Reports, and Circulars. Each issue contains 12 or more two-column pages; illustrated. Annual subscription: domestic, $1.00; foreign, $1.35.

### BASIC RADIO PROPAGATION PREDICTIONS

The Predictions provide the information necessary for calculating the best frequencies for communication between any two points in the world at any time during the given month. The data are important to all users of long-range radio communications and navigation, including broadcasting, airline, steamship, and wireless services, as well as to investigators of radio propagation and ionosphere. Each issue, covering a period of one month, is released three months in advance and contains 16 large pages, including pertinent charts, drawings, and tables. Annual subscription: domestic, $1.00; foreign, $1.25.

---

Order all publications from the Superintendent of Documents
U. S. Government Printing Office, Washington 25, D. C.

The printing of this publication has been approved by the Director of the Bureau of the Budget, May 12, 1953.

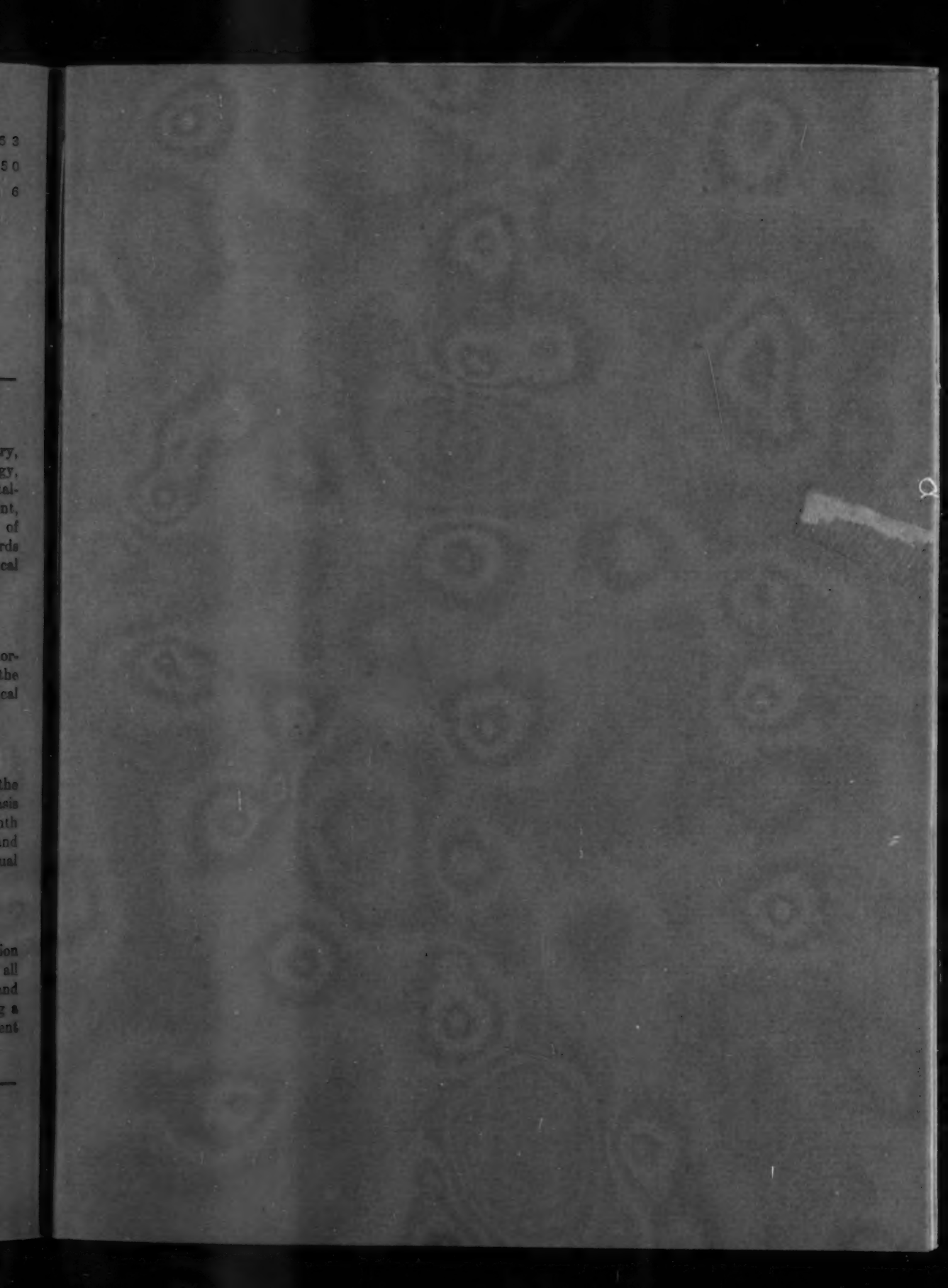

UNITED STATES
GOVERNMENT PRINTING OFFICE
DIVISION OF PUBLIC DOCUMENTS
WASHINGTON 25, D. C.

OFFICIAL BUSINESS

PENALTY FOR PRIVATE USE TO AVOID PAYMENT OF POSTAGE, $300 (GPO)

Journal of Research of the National Bureau of Standards Vol. 50, No. 6 June 1953

# Contents

| | | Page |
|---|---|---|
| Electron microscopy of synthetic elastomer latices. Robert R. Stromberg, Max Swerdlow, and John Mandel. | RP2419 | 299 |
| Second-order transitions of rubbers at high pressures. Charles E. Weir. | RP2420 | 311 |
| Thermodynamics of the rubber-sulfur system at high pressures. Charles E. Weir. | RP2421 | 321 |
| Laboratory measurement of the corrosion of ferrous metals in soils. W. J. Schwerdtfeger. | RP2422 | 329 |
| Effect of temperature on the electrical resistance and voltage departures (errors) of glass electrodes, and upon the hygroscopicity of glass. Donald Hubbard. | RP2423 | 337 |
| On the numerical solution of parabolic partial differential equations. Gertrude Blanch. | RP2424 | 343 |
| Thermal properties of some butadiene-styrene copolymers. George T. Furukawa, Robert E. McCoskey, and Gerard J. King. | RP2425 | 357 |
| Index to volume 50 (January to June 1953, Research Papers RP2380 to RP2425). | | 367 |

Single copies of the above Research Papers are not available for sale, but the Superintendent of Documents, U. S. Government Printing Office, Washington 25, D. C., will reprint 100 or more copies, and request for the purchase price should be mailed promptly to that Office.

For sale by the Superintendent of Documents, U. S. Government Printing Office, Washington 25, D. C. Price 60 cents (single copy). Subscription Price: $3.50 a year; $1.25 additional for foreign mailing. Single copies vary in price.

UNITED STATES GOVERNMENT PRINTING OFFICE, WASHINGTON : 1953